Summer 7-21-2010

Preparation of Coated Microtools for Electrochemical Machining Applications

Ajaya k. Swain
IMSE, University of Nebraska-Lincoln, ajayswain2007@gmail.com

PREPARATION OF COATED MICROTOOLS FOR ELECTROCHEMICAL MACHINING APPLICATIONS

By

Ajaya K. Swain

A THESIS

Presented to the Faculty of

The Graduate College at the University of Nebraska

In Partial Fulfillment of Requirements

For the Degree of Master of Science

Major: Industrial and Management Systems Engineering

Under the supervision of Professor K.P.Rajurkar

Lincoln, Nebraska

August, 2010

PREPARATION OF COATED MICROTOOLS FOR ELECTROCHEMICAL MACHINING APPLICATIONS

Ajaya K. Swain, M.S.
University of Nebraska, 2010

Advisor: K.P. Rajurkar

Coated tools have improved the performance of both traditional and nontraditional machining processes and have resulted in higher material removal, better surface finish, and increased wear resistance. However, a study on the performance of coated tools in micromachining has not yet been adequately conducted. One possible reason is the difficulties associated with the preparation of coated microtools. Besides the technical requirement, economic and environmental aspects of the material and the coating technique used also play a significant role in coating microtools. This, in fact, restricts the range of coating materials and the type of coating process. Handling is another major issue in case of microtools purely because of their miniature size. This research focuses on the preparation of coated microtools for pulse electrochemical machining by electrodeposition.

The motivation of this research is derived from the fact that although there were reports of improved machining by using insulating coatings on ECM tools, particularly in ECM drilling operations, not much literature was found relating to use of metallic coating materials in other ECM process types. An ideal ECM tool should be good thermal and electrical conductor, corrosion resistant, electrochemically stable, and stiff enough to withstand electrolyte pressure. Tungsten has almost all the properties desired in an ECM

tool material except being electrochemically unstable. Tungsten can be oxidized during machining resulting in poor machining quality. Electrochemical stability of a tungsten ECM tool can be improved by electroplating it with nickel which has superior electrochemical resistance. Moreover, a tungsten tool can be coated *in situ* reducing the tool handling and breakage frequency.

The tungsten microtool was electroplated with nickel with direct and pulse current. The effect of the various input parameters on the coating characteristics was studied and performance of the coated microtool was evaluated in pulse ECM. The coated tool removed more material (about 28%) than the uncoated tool under similar conditions and was more electrochemical stable. It was concluded that nickel coated tungsten microtool can improve the pulse ECM performance.

ACKNOWLEDGEMENTS

I am forever grateful to all those people who have contributed to this work.

First and foremost, I wish to express my sincere gratitude to my adviser, Dr. Kamlakar P. Rajurkar for his invaluable guidance, support, and encouragement. Certainly, this thesis would have not taken place had he not afforded me this opportunity. It is only appropriate that I convey my deepest appreciation to him here.

I wish to thank Dr. Murali M. Sundaram, who introduced me to the topic and Dr. Lin Gu who had always time for discussing with me and guiding me through my difficult times during this work.

1 would like to thank Dr. Michel Riley and Dr. Marc J. Schniederjans for their valuable comments and suggestions and having agreed to serve on my thesis committee.

My special thanks go to all the fellow graduate students in the Center for Nontraditional Manufacturing Research (CNMR). I want to thank them for all their support, interest, and helpful inputs and making me feel like being part of the CNMR family.

I am indebted to my parents for guiding me in defining and achieving my goals in every step of my life. I thank my parents in law for their affection and moral support. I owe my deepest gratitude and appreciation to my family, especially my elder sister ‘Sipra’, for her love and generosity and inspiring throughout my life for what I am today.

Perhaps, I cannot thank enough my wife, Sharmistha, for her continuous encouragement and being proud of me for every little progress I made in life.

Finally, I dedicate this thesis to our loving son ‘Ainesh’, who had to stay with his grant parents back in India, while his parents continued their studies here. We thank him for everything.

TABLE OF CONTENTS

TITLE AND ABSTRACT ……..……..…i-iii

ACKNOWLEDGEMENTS ……..……..…iv

TABLE OF CONTENTS ……..…v-viii

LIST OF FIGURES …….. ……ix-xi

LIST OF TABLES …….xii-xiii

CHAPTER 1: INTRODUCTION

1.1 ELECTROCHEMICAL MACHINING ……..…….2

1.1.1 MICRO ELECTROCHEMICAL MACHINING ……..……4

1.1.2 FACTORS INFLUENCING ECM AND RESEARCH ISSUES ……...4

1.2 MOTIVATION OF THIS RESEARCH …….6

1.3 THESIS ORGANIZATION ……9

CHAPTER 2: LITERATURE REVIEW

2.1 INTRODUCTION ……...….10

2.2 TOOLS IN MICROMACHINING....……....10

2.3 ISSUES IN ECM TOOLING ……12

2.3.1 ECM TOOL MATERIALS …….13

2.3.2 STRENGTH, RIGIDITY, AND STABILITY ……15

2.3.3 EFFECT OF ELECTROLYTE ON TOOL CONSTRUCTION …….16

2.4 ECM AND CORROSION ……17

2.5 COATING ON TOOLS ……17

2.6 COATINGS ……...21

2.7 COATED TOOLS IN ELECTROCHEMICAL MACHINING ……...23

2.8 MICROTOOL COATING ISSUES ……..26

2.9 COATING METHODS …….26

2.10 ELECTROCHEMICAL COATING PROCESSES ……28

2.11 ELECTROPLATING ……..28

2.11.1 PRINCIPLES OF ELECTROPLATING ……...29

2.11.2 PULSE ELECTROPLATING ……...33

2.11.2.1 PULSEPLATING CHARACTERISTICS ……...35
2.11.2.2 ADVANTAGES OF PULSE PLATING ……35
2.11.2.3 NANOSTRUCTURED COATINGS BY PULSE ELECTRODEPOSITION ……..……36
2.12 NICKEL ELECTROPLATING ……..40
2.13 SUMMARY ……40

CHAPTER 3: RESEARCH METHODOLOGY

3.1 INTRODUCTION ……41
3.2 PURPOSE OF THIS RESEARCH ……...41
3.3 EXPERIMENTAL APPROACH ……..……42
3.4 OBJECTIVES OF THIS WORK ……..43
3.5 SELECTING MAJOR FACTORS ……44
3.6 SELECTING FACTOR LEVELS ……48
3.7 FINDINGS OF THE PRELIMINARY TRIALS ……..……49
3.8 SYSTEM SET UP ……..……51
3.8.1 ELECTROCHEMICAL CELL ……52
3.8.2 ANODE AND CATHODE ……..54
3.8.3 CATHODE HANDLING AND MOVEMENT MECHANISM ……55
3.8.4 POWER SUPPLY ……55
3.9 EXPERIMENTAL PROCEDURE ……...57
3.10 COATING CHARACTERIZATIONS ……...61

CHAPTER 4: COATING CHARACTERIZATION

4.1 INTRODUCTION ……62
4.2 PULSEPLATING PARAMETERS ……..62
4.3 COATING THICKNESS AND DISTRIBUTION ……...63
4.3.1 COATING THICKNESS IN DC PLATED SAMPLES ……64
4.3.2 COATING THICKNESS IN PULSEPLATED SAMPLES ……...66

4.4 SURFACE ROUGHNESS OF DEPOSIT ……71

4.4.1 SURFACE ROUGHNESS IN DC PLATING …….72

4.4.2 SURFACE ROUGHNESS IN PULSEPLATED SAMPLES ……..77

4.5 COMPOSITION OF COATING ……..80

4.6 GRAIN SIZE OF DEPOSITS ……...86

4.6.1 EFFECT OF CURRENT DENSITY ON GRAIN SIZE IN DC PLATING ……...87

4.6.2 GRAIN SIZE IN PULSEPLATING ……90

4.6.3 EFFECT OF PULSE ON-TIME ……..91

4.6.4 EFFECT OF PULSE OFF-TIME ……92

4.6.5 EFFECT OF CURRENT DENSITY ……...94

4.7 COMPARISON OF PULSE AND CONTINUOUS CURRENT (DC) PLATING ……..96

4.8 SUMMARY……..97-98

CHAPTER 5: PERFORMANCE EVALUATION OF COATED MICROTOOLS

5.1 INTRODUCTION …….99

5.2 EXPERIMENTAL SYSTEM ……...99

5.3 ELECTROLYTE …….....100

5.4 WORKPIECE AND TOOL ……101

5.5 CONTROLLING INTERELECTRODE GAP ……...102

5.6 EXPERIMENTAL CONDITIONS …….105

5.7 RESULTS AND DISCUSSION …….105

5.7.1 MATERIAL REMOVAL RATE (MRR) ……..106

5.7.2 SIDE MACHINING GAP OR OVERCUT ……...108

5.7.3 SURFACE ROUGHNESS ….. ….……111

5.7.4 CORROSION TEST ……..111

5.8 DIFFICULTIES ...…….…..113

5.9 CONCLUSION ……...114

CHAPTER 6: SUMMARY, FINDINGS, AND RECOMMENDATIONS

6.1 SUMMARY OF THIS WORK ……...115

6.2 FINDINGS ……..116

6.3 CONCLUSIONS …….118

6.3 RECOMMENDATIONS ……..……118-120

REFERENCE……...121-127

LIST OF FIGURES

Fig. 1 Major factors affecting ECM performance

Fig. 2.1 Microtools fabricated by precision grinding

Fig. 2.2 Side-insulated electrode

Fig. 2.3 Comparison of geometric shape of the gas film

Fig. 2.4 Sectional images of coated tool electrode

Fig. 2.5 Scheme of a copper electroplating unit

Fig. 2.6 Distribution of voltage and current in the electrolyte bulk

Fig. 2.7 Equilibrium potential and Overpotential

Fig. 2.8 Schematic summary of DC and Pulse electrodeposition

Fig. 3.1 Power supply and the experimental set up

Fig. 3.2 The electrochemical cell for preliminary trials

Fig. 3.3 SEM image of the uniform nickel coating on copper rod.

Fig. 3.4 Non-uniform coating in patches on tungsten microelectrode

Fig. 3.5 The experimental setup

Fig. 3.6 Pulse Function generator

Fig. 3.7 Scheme of experimental approach

Fig. 4.1 Coating thickness variation in DC samples

Fig. 4.2 DC plated sample at 2.5 A/dm^2 and 5 minutes

Fig. 4.3 Smooth coating at 5 A/dm^2 and 10 minutes

Fig. 4.4 Rough sample at 10 A/dm^2 DC plated for 5 minutes

Fig. 4.5 Nodular deposits at 10 A/dm^2 and 10 minutes

Fig. 4.6 Coating thickness variation in Pulseplated samples at different Duty Factors

Fig. 4.7 (a, b, and c) Pulse plated samples at current density of 5 A/dm^2 and different Duty factors and Pulse frequencies

Fig. 4.8 Samples plated at 2.5 A/dm^2 and at different pulse on-times

Fig. 4.9 Rough and burnt deposit at 10 A/dm^2, 80 %, and 10 Hz

Fig. 4.10 Non uniform coating in some samples

Fig. 4.11 Variations of surface roughness with DC plating parameters

Fig. 4.12 Cracks on the sample surface at 2.5 A/dm^2 and 10 minutes

Fig. 4.13 (a) AFM statistics of the sample surface at 2.5 A/dm^2 and 10 minutes

Fig. 4.13 (b) AFM images of the sample surface at 2.5 A/dm^2 and 10 minutes

Fig. 4.14 DC plated sample at 5 A/dm^2 for 5 minutes and 10 minutes and AFM image corresponding to top right SEM image

Fig. 4.14 (a, b, & c) Variation of deposit roughness with current densities and pulse frequencies at Duty Factors a) 20%, b) 50%, and c) 80%

Fig. 4.15 (a, b, & c) Hydrogen cavities on coating surface with increasing pulse on-times

Fig. 4.15 (d) Coated surface of pulse and DC plated specimen at comparable plating conditions

Fig. 4.15 (e) Etched and the electroplated surface

Fig. 4.16 Coating composition at different DC plating conditions

Fig. 4.17 Non uniform coating on some DC plated specimen

Fig. 4.18 Coating composition at different pulse parameter combinations

Fig. 4.19 EDS micrograph for pulseplated sample at 5 A/dm^2, 50%, and 50 Hz

Fig. 4.20 Effect of mean current density on grain size of DC plated samples

Fig. 4.21 (a) SEM picture and (b) AFM micrograph of DC plated sample at 5 A/dm^2 and 7 minutes

Fig. 4.22 Grain size variation at different pulse parameters

Fig. 4.23 Grain size variation with different pulse on-times at 5 A/dm^2

Fig. 4.24 Change in grain size with pulse off-times at 2.5 A/dm^2

Fig. 4.25 Grain structure in plated samples with DF 20% and PF 50 Hz at different current densities

Fig. 4.26 Grain structure in plated samples with DF 50% and PF 50 Hz at different current densities

Fig. 4.27 Grain structure in plated samples with DF 80% and PF 50 Hz at different current densities

Fig. 4.28 Pulseplated sample (a) and (b), and DC plated sample (c) and (d)

Fig. 5.1 Experimental set up for micro ECM experiments

Fig. 5.2 The Scheme of Experiment and Gap Control strategy

Fig. 5.3 Material Removal Rate (MRR) Vs Applied Voltage

Fig. 5.4 Surface of the uncoated tool before (left) and after machining (right) at different magnifications

Fig. 5.5 Surface of the coated tool before (left) and after machining (right)

Fig. 5.6 Supply voltage Vs. Side machining gap

Fig. 5.7 Tool feed rate Vs. Side machining gap

Fig. 5.8 SEM pictures of the machined surfaces using both types of tools

Fig. 5.9 Surface generated by Ni coated tungsten and by uncoated tool

Fig. 5.10 (a) Surface of the uncoated tungsten microtool after the corrosion test

Fig. 5.10 (b) Surface of the nickel coated tungsten microtool after the corrosion test

LIST OF TABLES

Table 2.1 Materials used as ECM tools

Table 2.2 Comparison of characteristics of commonly used ECM tool materials

Table 2.3 Improvement in process output by use of coated tool in traditional machining

Table 2.4 Coated tool performance in nontraditional micromachining

Table 2.5 Comparison of surface coating processes

Table 2.6 Equilibrium potentials in different electrode reactions

Table 2.7 Few previous works in DC and Pulse electrodepostion

Table 3.1 Potential Factors and ranges

Table 3.2 Specification of the power supply

Table 3.3 Electrodeposition conditions and plating parameters

Table 3.4 Major factors and levels

Table 3.5 Watt's Bath composition range

Table 3.6 Watt's bath ingredients

Table 3.7 Specifications of the translation stages

Table 3.8 Specifications of the power supply

Table 3.9 Coefficient of thermal expansion

Table 3.10 Scheme of substrate preparation

Table 3.11 Composition of Wood's Bath

Table 4.1 Pulse on-time and Pulse off-time values at different DF and PF

Table 4.2 Coating thickness in DC plated samples

Table 4.3 Coating thickness in Pulseplated samples

Table 4.4 AFM settings

Table 4.5 Surface roughness results for continuous current (DC) plating experiments

Table 4.6 Surface roughness results for pulseplating experiments

Table 4.7 Percentage of Ni deposits in DC plated samples

Table 4.8 Percentage of Ni deposits in Pulseplated Samples

Table 5.1 Workpiece composition

Table 5.2 Experimental Conditions

CHAPTER 1

INTRODUCTION

Recent advances in science and engineering has led to unusual demands on the metal working industry. These demands on products and production processes have been the driving factors behind developments in today's cutting technologies. The advent of metals with high strength-to-weight ratios and alloys with improved properties such as greater corrosion resistance, high temperature strength, and increased stiffness to serve specific purposes, have called for higher emphasis on suitable, effective, and efficient machining processes. With the miniaturization of products and product components in sub-micron and nanometer level becoming the trend, the manufacturing engineering community has been developing new, improved, and rapid manufacturing processes aimed at making those products or components economically feasible.

During the 1980’s various lithography based micromechanical systems such as wet and dry etching, photolithography were developed for microns and sub-micron level machining. But those processes had the inherent limitation of range of work materials and the type of features that could be generated by them. Moreover, the processes required specialized installations with clean ambience and were expensive. Although some conventional cutting techniques have been successfully downscaled to the microlevel, further downsizing is limited because of the associated problems of size effects, various stresses that develop in the machined surface, amount of material that can be added/ removed/ formed per cycle, and achievable precision.

Nontraditional machining processes, comparatively newer methods of metal cutting and forming, are emerging as possible alternatives. These processes are applicable to most metals and their alloys because of their mechanical, electrical, thermal, and chemical material removal actions. These processes differ from traditional machining in their effects on surface properties and often can be compared favorably in terms of surface roughness, heat-affected zone, hardness alteration, cracks, and residual stress. Nontraditional machining processes such as electrical micromachining, abrasive micromachining, and laser micromachining have the distinction of producing high aspect ratio (depth to diameter ratio) micro components and products.

1.1 ELECTROCHEMICAL MACHINING (ECM)

ECM, an electrolytic process governed by Faraday's laws of electrolysis, uses electrical energy to remove material. Material removal is achieved by electrochemical dissolution of an anodically polarized workpiece which is one part of an electrolytic cell. An electrolytic cell is created in an electrolyte medium, with the tool as the cathode and the workpiece as the anode. The schematic diagram of an ECM system is given in Fig. 1. The tool is positioned very close to the workpiece for maximum amount of dissolution and minimum ohmic voltage drop between the two electrodes. A high-amperage (30~200A/cm^2), low-voltage (10~20V) current is generally used to dissolve and remove material from the electrically conductive workpiece. The metal ions removed from the workpiece are taken away by the vigorously flowing electrolyte through the inter electrode gap and are separated from the electrolyte solution in form of metal hydroxides by suitable methods. Both the electrolyte and the metal sludge can then be recycled. ECM

has a wide range of mode of applications such as electrochemical grinding, electrochemical honing, electrochemical milling, electrochemical drilling, electrochemical deburring, and electrochemical turning. The process finds its application in the manufacturing of aircraft, aerospace components, automobile products, forging dies, and computer and semiconductor components.

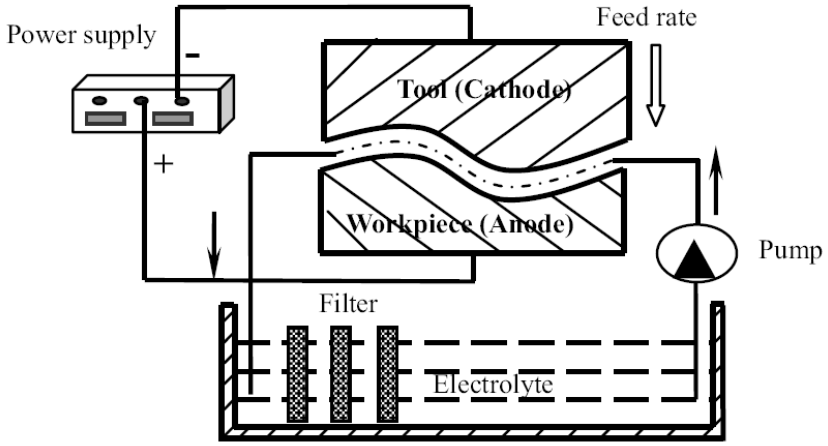

Fig.1 Schematic diagram of an ECM system [101]

Unlike in traditional cutting techniques, workpiece hardness is not a factor because of the non-contact nature of the machining process, making ECM suitable for advanced difficult-to-machine materials. ECM can have higher material removal rate than that of other traditional or nontraditional machining methods. Also it has a unique advantage of machining features with shapes of complicated geometry and can generate smooth undamaged surface with lower roughness, no burrs, and without any metallurgical alterations. The main advantage of electrochemical machining lies in its long tool life; there is no tool wear. Limitations of ECM include factors such as high

specific energy consumption, need for special disposal of the electrochemical reaction products and used electrolyte, and its complicated process control.

1.1.1 MICRO ELECTROCHEMICAL MACHINING (MicroECM)

The electrochemical machining process, when applied to the micro-machining range of applications associated with machining ultraprecision shapes with complicated geometry, is termed as micro electrochemical machining. MicroECM uses microtools that are in micron level dimensions. This micromachining technology because of its distinct advantages such as high material removal rate (MRR), better precision and control, short machining time, reliability, process flexibility, and environmental acceptability is capable of machining chemically resistant materials such as titanium, copper alloys and stainless steel, that are widely used in biomedical, electronic and other micro mechanical machining applications [1]. In microECM—the principle of material removal is same as the conventional ECM that is by controlled anodic dissolution—the tool never touches the workpiece, nor is it consumed in the process. As a result, micro ECM offers an accurate, highly repeatable process with rapid machining times that produce final surface and edge. The continuous and uniform replacement of electrolyte in the gap and localization of anodic dissolution in the process of course poses some difficulties in drilling a microhole and machining 3D complex cavities that and that needs to be suitably addressed [2].

1.1.2 FACTORS INFLUENCING ECM AND RESEARCH ISSUES

Effectiveness and efficiency of an ECM process is critically dependent on certain factors. These factors not only have a significant influence on the machining performance, but also control the process behavior. Fig. 2 shows various major factors influencing the process output. The type of electrolyte, its concentration, temperature, and the rate of flow through the electrode gap affect the current density and in turn have great impact on the material removal rate, surface finish and dimensional accuracy. The influence of current density, current distribution, anodic reactions and mass transport effects on material removal and accuracy are important considerations in ECM. These parameters can affect the machining performance and their range of values should be properly selected to achieve the desired output.

For effective utilization of ECM in micromachining applications, extensive research efforts have been made to address the important issues associated with the process. Continual improvements are taking place in the field of design and development of microtool, monitoring and control of the inter electrode gap (IEG), control of material removal and accuracy, developing power supply, elimination of microsparks generation in IEG, limiting stray current, and selection of electrolyte. However, to enhance the application of this micromachining technology in modern industries it is imperative to understand the inherent uncertainties of the process to address the key issues mentioned above.

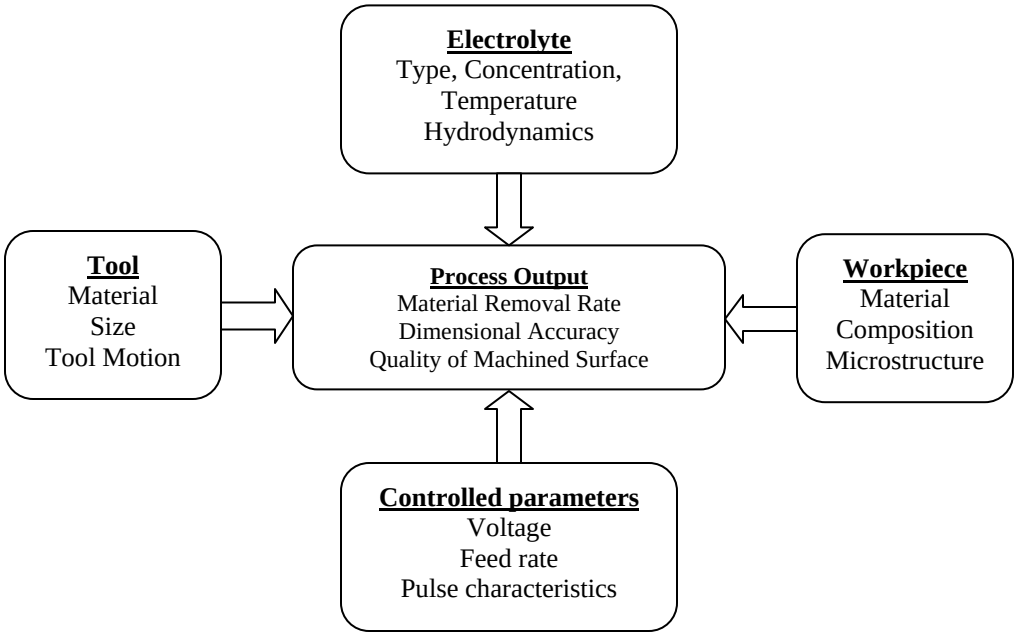

Fig. 2 Major factors affecting ECM performance

1.2 MOTIVATION OF THIS RESEARCH

Innovations such as the application of advanced work materials, together with needs for non-pollutant machining processes, increased flexibility and improved cost-effectiveness trigger the application *of* high performance processes, imposing higher emphasis on tools and their performance. This often reveals the desired characteristics in conventional tool materials such as high wear and corrosion resistance, strength and rigidity, and other tribological properties. Coating technology is one means of achieving a crucial enhancement in tool performance. Ample experimental evidence of the increase in tool life of coated tools has been presented by many researchers. Increases in tool life in coated tools ranging from two to 40 times that of uncoated tools have been reported for certain drilling and turning operations [3]. One of the major recent innovations in cutting tool technology has been the introduction of thin, hard, vapor-deposited surface coatings

on various cutting tool materials. The coating has resulted in reduction in the forces and power due to reduced friction at the tool-chip interface, reduction in the tool temperatures and tool wear that led to an increase in tool life, and improvement in surface finish due to reduction in tool-chip friction and associated build-up-edge formation [3].

Also in nontraditional machining processes like electrochemical machining (ECM), electrical discharge machining (EDM), and ultrasonic machining (USM) tool coating has been noticed to have led to increased material removal rate, better surface finish, and higher wear resistance. However, a study on the performance of coated tools in micromachining has not been adequately conducted so far.

Tooling is one area in ECM and microECM that has been of major concern for scientists and researchers. It has been concluded that a practical tool design solution should provide not only the cathode dimensions but also a suitable electrolyte path and an appropriate insulating pattern to prevent undesired overcut. There is currently no such standardized method available for perfect prediction of tool shape, especially in the area of micro-ECM. Therefore, in-depth research combining theory and supporting experimental investigation is still needed in the area of microtool design and development [1].

Platinum, Tungsten and Copper are the most commonly used electrode materials in microECM with platinum and copper being chemically stable and lower strength. Tungsten is the predominant tool material for microECM. Tungsten has higher strength but is chemically instable (oxidization) during machining process [4]. The chemical instability of tungsten can be addressed by coating it with a chemically stable material such as nickel. Nickel (Ni) is widely used as corrosion and wear resistant plating material

for its high yield strength, hardness, and other mechanical properties. Research on the properties of Ni-based electrodeposited composite coatings developed by co-deposition of particles such as oxides, carbides or nitrides enhance properties in terms of wear, corrosion and oxidation resistance [5-8].

Nickel electroplating is an appropriate technique even for extreme resolution applications because of the nanometer level grain size of the coated nickel. It was shown that as small as 20 nm lines could be deposited in a resist mold [9]. Electroplating in general has been reported to have better properties. For example, in an investigation of mechanical properties of nanocrystalline nickel films deposited by pulse plating, it has been reported that nanostructured nickel coatings exhibited high hardness and improved tribological properties [10]. In an another study the influence of pulse plating conditions on the structure and properties of pure and composite nickel nanocrystalline coatings have been studied and it was concluded that the mechanical properties of pure nickel and nickel composite coatings can be improved by proper control of the parameters [11]. Similar studies have also been carried out on the influence of pulse parameters on the microstructure and microhardness of nickel electrodeposits [12]. The study has revealed that the microhardness of the nickel deposits is related to the grain size and can be altered by controlling the grain size. Hence, in this study pulse plating has been selected to coat nickel on tungsten microelectrodes.

1.3 THESIS ORGANIZATION

Chapter One introduced the nontraditional machining processes in general and electrochemical machining in particular. The major factors influencing ECM and relevant research issues were outlined and motivation of this research was discussed along with the thesis organization statement.

Chapter Two makes a review of literature on tooling issues in ECM, and microtool coating issues in general, various types of coatings and coating technologies, and performances of coating on tools in different machining processes. A review of electroplating and nickelplating is also presented.

Chapter Three describes the in house built experimental setup in detail, research methodology, and the experimental investigation procedure.

Chapter Four illustrates the results of the preliminary experiment results and discusses the outcomes of the coating experiments. The parametric relations for the coated electrode in terms of surface quality and coating thickness are also investigated. This chapter also presents the characterization results of the coating surface and optimizes the parameters for the best coating.

Chapter Five presents the comparative results of the coated tool performance in micro electrochemical machining experiments.

Chapter Six, the concluding one, summarizes the findings of this work along with some recommendations for future research.

CHAPER 2

LITERATURE REVIEW

2.1 INTRODUCTION

This chapter reviews literature on basic principles of electrochemical machining, tooling issues in this process, and use of coated tools in micromachining applications. The microtool coating issues and comparison of various surface coating methods are summarized. Also presented here is a review of theory of electroplating and nickelplating.

2.2 TOOLS IN MICROMACHINING

Tooling has been one of the major challenges in micromanufacturing. It has three main aspects namely, selecting the appropriate tool material that is application dependent, tool design that deals with determination of accurate tool geometry, and finally, developing the microtool for actual machining. In case of nontraditional manufacturing, the tooling issue also plays a significant role in overall process performance and cost economics. Take the case of electrodischarge machining (EDM). Since the mode of material removal in EDM is by thermal erosion or vaporization, it provides a distinct advantage for manufacturing mold, die, automotive, aerospace and surgical components. In die and mold production, shaping or machining of electrode is typically 25-40 per cent of the tool-room lead time and that can account for about 50 per cent of the total machining cost [13]. Complex features and profiles in dies and molds need multiple cavities that require electrodes of specific geometry to be run in sequence. Any delay during mold making process increases the total tool-room lead time that subsequently gives rise to a higher total cost. Since major cost and time element of EDM is electrode

production, an accurate method of manufacturing one-piece electrodes quickly with minimum manual intervention is of great interest to the researchers. In this work, we will discuss in detail, the tooling issues in electrochemical machining.

Electrochemical machining (ECM) is a set of complex processes that impart, by means of anodic dissolution, an intended shape to the machined surface or workpiece; drill holes (through or blind) of variable cross section; remove from it a defective surface layer; improve surface finish by polishing or deburring [14]. The shape of the tool is almost reproduced on the machined surface by high rate anodic dissolution in this process. During the dissolution process, the tool is progressively advanced towards the workpiece at a rate sufficient to balance the rate of dissolution, and thus maintaining an optimum working gap, typically in the order of one or several tenth of a millimeter. Since extremely high current densities, up to 100 A/cm^2 or more, are applied to achieve high machining rates, it is essential to have an electrolyte flow rate of several meters per second in the inter-electrode gap in order to sweep away the electrochemical reaction products and prevent boiling by Joule heating [15]. As the machined surface in ECM is almost a negative mirror image of the tool used, the tool shape completely defines the shape of the workpiece; and the dimensional accuracy of the produced surface is linked with the shape and geometry of the tool along with other parameters such as tool feed rate, interelectrode gap, gap voltage, and electrolyte pressure.

2.3 ISSUES IN ECM TOOLING

The main challenge in ECM is to establish a relation between the workpiece surface and the surface of the tool electrode and its trajectory under specified conditions [14]. Prediction of the tool shape is a formidable inverse boundary problem involving Laplace equations [16]. The iterative procedure of tool design is time consuming, resulting in costly machine downtime and long lead times [17]. Many investigations have been carried out into the development of tool design procedures using simple and complex variable techniques, and various numerical techniques [18-20]. Besides tool design, development of the microtool is also vital for electrochemical machining. Microtools can be fabricated by electrochemical etching or wire electro-discharge grinding (WEDG) where an accurate tool profile is accomplished by controlling the current density and voltage [21]. Even micropins and microspindles fabricated by microECM can also be used as tool electrodes for electrochemical micromachining [19]. For minimizing the stray current effect, the tool should be properly insulated or coated so that current flows only through the front face [22]. A proper insulation of the tool is a must for achieving high machining accuracy especially in micro and nano level. An insulating cover of SiC/Si_3N_4 may be coated onto the cathode tool by means of chemical vapor deposition (CVD), which can increase the accuracy and surface finish. Microtools can be manufactured by applying small-hall ECM and electrochemical broaching, alternately changing the polarity of the machining current in such a way that dissolution takes place from the tool [1]. Microtools in the range of 15–20 μm diameters can be produced by special precision grinding machines (Fig 2.1).

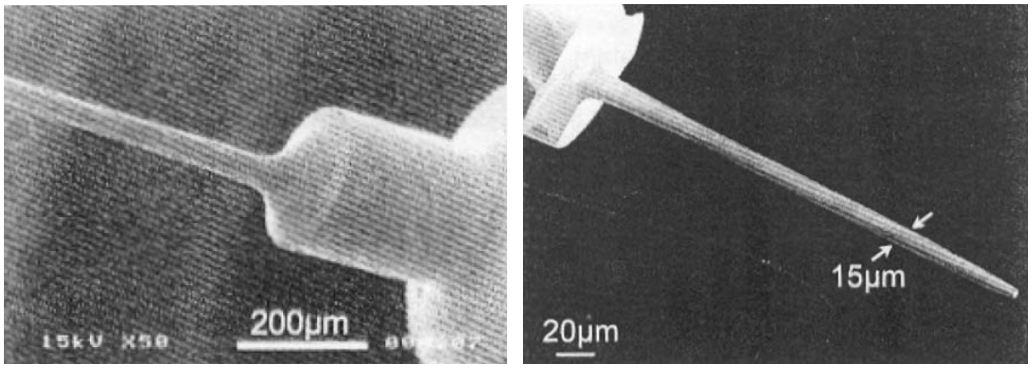

Fig. 2.1 Microtools fabricated by precision grinding [23]

A dual pole tool also can increase the machining accuracy in which the insulated negative charged tool is covered by a positive charged insoluble metal bush that reduces the chances of over cut due to the flow of stray current flux in the precise machining area [1]. Use of multiple electrodes and disk-type electrodes can increase accuracy and productivity.

2.3.1 ECM TOOL MATERIALS

The material for microtools in microECM, in general, should consist of a chemically inert material with good thermal and electrical conductivity, corrosion resistance, stiffness to withstand electrolyte pressure without vibration and good machinability. A highly electrically conductive material with high melting point and heat resistant characteristics can be an option for tool material in ECM. The diameter of the tool in the order of 150-200 microns gives the tool a high current density that is desired in ECM [24]. Metals, used mostly, include platinum, tungsten, titanium, molybdenum, and copper alloys. Table 2.1 lists some of the other materials that can be used in making of ECM tools.

Table 2.1 Materials used as ECM tools

Aluminum	Copper-manganese
Brass	Copper-nickel
Bronze	Copper-tungsten
Copper	Stainless steel
Carbon	Titanium (99%pure)

There are a number of factors that determine ECM tool materials; the most important one is resistance to chemical corrosion. Since an ECM environment could contain corrosive electrolytes such as sodium chloride, sodium nitrate, sodium bromide, and occasionally sodium fluoride above 100deg C, high corrosion resistance requirement restricts the number of materials for tool and tool fixtures. The small operating gaps, high electrolyte flow rates, and pressure used in electrochemical machining also require maximum stiffness and rigidity in the construction of tools and their holding attachments. Table 2.2 compares the characteristics of some commonly used tool materials in ECM.

Table 2.2 Comparison of characteristics of commonly used ECM tool materials

	Platinum	Tungsten	Copper
Strength, Stiffness, and Hardness	Very low; can be easily deformed by small physical contact	• High strength; about twice as strong as platinum. • High stiffness and hardness	• Moderate strength • High ductility and malleability
Machinability	Good	Poor	Good
Thermal conductivity	Moderate (71.6 W m-1 K-1)	High (174 W m-1 K-1)	Very High (401 W m-1 K-1)
Electrical conductivity	Moderate (9.4 x 106 S m-1)	High (18.2 x 106 S m-1)	Very High (59.6×106 S m-1)
Electrochemical stability	High	Low; can be dissolved or oxidized during machining	Moderate
Corrosion resistance	Moderate	Low	Low
Availability	Extremely rare metal	Moderate	Abundant
Cost	Expensive	Less costly compared to Platinum	Least expensive

2.3.2 STRENGTH, RIGIDITY, AND STABILITY

In ECM, even though the tool does not make contact with the workpiece, at times the machining forces involved especially the electrolytic pressure, within the small working gap, exerts forces of several tons, and tools and fixtures must be of adequate strength and rigidity to withstand those forces. There are certain configurations of electrodes in which the electrolyte, traveling at high speed, creates a negative pressure because of its high kinetic energy in the interelectrode gap and makes the tool to be drawn on to the workpiece. In that case, tool must posses enough strength to limit deflections to small dimensions. Considering static forces, the sudden movement of the

tool may initiate self excited vibrations in ECM and to avoid this effect known as ‘water hammer’, there is a need for rigidity in the tool and fixtures. Usually these vibrations are excited by forces acting in the direction of the tool feed, but transverse forces can cause the same effect. Water hammer is the major reason for building strength and rigidity into the tooling [25]. However, other factors, such as high magnetic forces between parts carrying heavy electrical currents and external vibrations of the machine structure, also require strong and rigid tools. Material stability is important in obtaining repeatable accuracy in an ECM process. For that reason the chosen tool material for ECM must posses chemical stability and desirably chemically inertness qualities besides other properties.

2.3.3 EFFECT OF ELECTROLYTE ON TOOL CONSTRUCTION

The flow of electrolyte between the tool and workpiece facilitates the ECM action. As the length of flow path across the tool increases, as in case of a longer and wider worksurface, the flow must be increased to sweep away the products of the machining action. Enough dilutions of the gases are required; otherwise gases will reduce the conductivity of the electrolyte towards the exit from the tool, causing a reduction in machining gap size [25]. This effect can be countered by using high flow rates, instead of compensating for it in the shape of the tool. While operating at smaller tool working gaps in order to achieve greater accuracy, a higher pressure for the same electrolyte flow is required. To have higher tool feed rates, a proportionate increase in flow will be required with a corresponding increase in pressure. A rise in pressure again will call for suitable stronger and rigid tools.

2.4 ECM AND CORROSION

ECM is an anodic dissolution process and so is corrosion. The associated electrochemical reactions depend on the electrodes and the electrolyte, particularly on its pH. In majority of applications low or neutral pH is preferred. Barring the acid/base consideration, the dissolution kinetics also depends on the possible existence of aggressive anions, such as halides in the electrolyte, which may modify the nature of protective films [26]. Chloride is one of the most aggressive halide anions commonly associated with corrosion and pitting. Sulfate, perchlorate, and nitrate ions are also known to cause pitting under certain conditions. The aggressive nature of the chloride ion in the presence of most metals and alloys has made its use very effective as an ECM electrolyte. As it is also not expensive in the form of sodium chloride (NaCl), it has become a commonly used electrolyte particularly when machining iron, steels, nickel, and nickel based alloys. However, in case of Nb, Ta, V, and Ti, bromides and iodides are more effective than chlorides as electrolytes [27]. In general, chloride ions are aggressive for most metals. The critical concentration of chloride ions required for pitting in uninhibited sodium chloride (NaCl) was reported to be about 0.002 to 0.02 M NaCl [28]. This value increases with increase in pH of the solution.

2.5 COATING ON TOOLS

The need for an improved productivity, meeting the higher production demands at lower costs, has put a serious emphasis on development of the cutting tools. Over the years, researchers have tried to improve the tool characteristics in terms of tool wear, surface finish of the machined surface, and tool life by providing coating on tools. Wear

resistance, being one of the most wanted properties in conventional machining processes; has been enhanced by suitable coatings described earlier. For over half a century, hard coatings, such as TiN, TiC, Al_2O_3 have been applied on cutting tools to increase tool life [29]. Various other coating materials and their combinations with advanced coating systems have been used by the tool industries to tailor superior quality tools to meet the requirement of the dry, hard, high speed, and precision machining processes. The tool making trend today is shifting away from the standard conventional tools towards production of more and more specific high quality tools and tool manufacturers are emphasizing on configuring individual coatings and coated tools [30]. The Tables 2.3 and 2.4 list a few of the micromachining processes where the tool coating has improved the quality of the machined surface and resulted in enhanced tool life.

Table 2.3 Improvement in process output by using coated tool in traditional machining

Parameters	Process and conditions	Work Piece	Tool	Coating		Performance		Ref.
				Material/ Process	Thickness	Coated	Uncoated	
Main cutting forces	End milling	6061-T6 Aluminum	Tungsten carbide (WC)	Fine grained diamond/ Hot Filament CVD	0.5-1 µm	0.49N (+/- 0.09N)	2.14N (+/- 0.85N)	[40]
Thrust forces						0.34N (+/- 0.04N)	4.40N (+/- 0.44N)	
Main cutting forces				Nano-crystalline diamond/ HFCVD	200 nm	0.18N (+/- 0.07N)	2.14N (+/- 0.85N)	
Thrust forces						0.17N (+/- 0.02N)	4.40N (+/- 0.44N)	
Type of surface generated						Highly patterned, Uniform bottomed	Sporadic finish	
Feed Force	Lateral milling	Co-Cr-Mo alloy	?	Diamond/CVD	15 (+/-2) µm	20 N (+/-10N)	35 +/- 15N)	[93]
Tool Life	Drilling	Titanium alloy Ti-6Al4V	WC-Co	TiAlN/PVD	?	7.8 mins	Less than 1 minute	[3]
	Turning	Plain carbon steel	Cemented carbide	TiC/CVD	2-3 µm	7 mins	3 minutes	[94]
				TiC, Ti(C,N) and TiN/CVD	5 µm	30 mins		
Cutting speed	Milling	Heat resistant steel casting	Cemented carbide (K20)	TiC/CVD	1.5 µm	190 m/min	120 m/min	
				TiC and TiN/CVD	1.5-2 µm	280 m/min		
M/C components per edge	Milling	Alloyed gray cast iron (GG25)	Hard metal	Sr17 [TiC+TiCN+ Ceramic based on Al_2O_3] /CVD	15 +/-5 µm	200	100	

Table 2.3 Continued

Life time	Facing	Steel 42 CrMo4	HS steel	TiN/CVD	5 µm	120 components	40 components	
		100Cr6	HS Steel (M35)	TiN/CVD	5 µm	1500 components	Up to 300 components	
Surface roughness	Dry turning	Tool steel AISI D2	Carbide (K313)	Coating (KC9125) [TiN+Al_2O_3+TiCN] /CVD	?	0.3-1.51 µm	0.36-4.05 µm	[95]
Surface topography						Smoother	Not so smooth	
Micro hardness						300-380 HV	260-350HV	
Surface roughness	CNC Turning [300m/min, 0.25mm/rev, 2mm]	AISI 1030 steel	Cemented carbide WC-Co	TiN/CVD		2.16 µm	3.39 µm	[96]
				TiAlN/PVD		2.3 µm		
				AlTiN/PVD		2.46 µm		
	Turning on universal lathe [05-50 m/min, Feed rate 0.24-0.32mm/rev]	AISI 1015 steel	Cemented carbide WC-Co (P20)	AlTiN (P20)/PVD		3.74 µm	4.25 µm	[97]
				TiAlN (P20)/PVD		3.46 µm		
				TiN (3 layer coating Al_2O_3+TiC+TiN) (P10)/CVD		2.77 µm		
Surface roughness	Micro milling	H13 tool steel	2-flute flat micro end mills	AlCrTiN /PVD	1.37 µm	0.34 µm	1.56 µm	[98]
					1.85 µm	0.47 µm		
Surface roughness	Micro grinding [60,000 rpm, 1 mm/min]		Carbide shanks	Nickel-embedded diamond grains/ Electroplating	?	10 nm	?	[99]

Table 2.4 Coated tool performance in nontraditional micromachining

Parameters	Process and conditions	Work Piece	Tool	Coating		Performance		Reference
				Material/ Process	Thickness	Coated	Uncoated	
Hole diameter	ECDM drilling [35Volt continuous DC]	Borosilicate glass	WC (200 µm)	Ceramic tube	?	328 µm	426 µm	[100]
Machining depth						550 µm	320 µm	
Roundness error						16%	22%	
Hole diameter	ECDM drilling [35Volt DC rectangular pulse]					327 µm	361 µm	

2.6 COATINGS

A coating can be defined as an overlay or film of a determined material which is deposited on the surface of another material to improve or alter its mechanical, chemical, or electrical and optical characteristics. Surface coatings convert the substrate surface either partially or wholly into a new material of certain desirable properties or impart desirable properties. Coatings increase the endurance of the base material by protecting it from thermal or corrosive degradation, impart wear resistance and hardness to the surface while retaining the toughness and ductility of the original component, and also can enhance the aesthetic and decorative appeal. The modified surfaces permit to amend chemical characteristics such as permeation, temperature insulation, biocompatibility, wettablity, electrical properties like conductivity, and provide special optical properties in terms of transmission, reflection, absorption, color of the coated material [31]. The selection of coating process depends on several factors such as operating conditions,

material compatibility issues, nature and surface preparation of substrate, time or speed of application, cost, safety, environmental effects, coating properties, and structural design. Now, that the technology is matured enough to coat substrates of almost all material compositions by a large number of materials, selecting the right coating for a particular application is often a process of elimination rather than selection.

Coatings can be classified in terms of thickness and composition of the coating material. The boundary limit for thick and thin coatings is not very well defined and is somewhat arbitrary [31]. Generally coating thickness in millimeters is considered thick; micrometric thicknesses are considered thin. A thickness of 1 μm is often accepted as the boundary between thin and thick films. Again a coating can be considered thin and thick depending on whether it exhibits surface-like or bulk-like properties [32]. Chemical and electrochemical processes have the ability of giving a substrate a thick coating by depositing molecules or ions on the surface. For example, diamonds can be grown on steel by chemical reactions to provide a wear protection coat and chrome oxide could be deposited for corrosion protection on stainless steel. Nickel, because of its strong bonding characteristics and growth pattern, can be coated by galvanic means to provide a corrosion resistant surface. For electronic applications, evaporation, ablation, and sputtering of sources can yield thin layers on a clean substrate.

Coatings can be also categorized by the expected added property to the base material (substrate) such as corrosion resistance, wear, and thermal resistance. The suitability of a coating for a particular application depends on various mechanical and chemical properties of the surface to be coated and also on the adherence of coating material to the substrate, which is linked to its chemical composition. There are many

coating material combinations and coating methods available, but for this work we will focus our attention on wear and corrosion resistant coatings.

2.7 COATED TOOLS IN ELECTROCHEMICAL MACHINING

In general, size and shape of machined microstructures get affected by tool size, shape and also by the machining gap. For the fabrication of microstructures by ECM it is crucial to have a small inter electrode or working gap. This is achieved on the machine side by using the techniques of oscillating tool-electrodes [33] or ultra short voltage pulses [34]. Machining accuracy increases by providing an electrically isolating layer or insulated coating on the electrode on those areas where current passage is undesirable and for high accuracy requirements, this insulating layer or coating must be as thin as possible, e.g. 10 μm or less. Many types of insulating materials have already been proposed by researchers over the years. The metal core of the electrode is covered by isolating polymer layers or compounds of inorganic compound networks [35].

Stray machining is one issue in ECM that needs to be controlled to achieve the desired machined surface. Stray machining usually occurs at the surface adjacent to the machining area which is exposed to the electrolyte flow and electric field. Controlling this effect involves development of an appropriate tool structure and electrolytes which enable more localized dissolution. Over the years this issue has been dealt with by using masked tool; coating a certain portion of tool by some insulating material so that the current is discharged from the desired point in the tool. Tool insulation has been proposed for several electrical and chemical micromachining techniques, for example, ECM and EDM, to enhance the accuracy and machinability [36]. Tool insulation

improves the machining accuracy and efficiency of electrochemical or electrical discharge drilling processes by preventing undesirable machining at the side of the tool. Studies show that the use of a side insulated tool (Fig.2.2) can improve the discharge current uniformity of the ECDM process by reducing the stray electrolysis and minimizing the fluctuation of the current peak value [37]. They reported that the geometric accuracy of the channel, created by the side insulated tool, improved and the surface roughness of the milled surface area bettered from 3.64 to 1.72 μm.

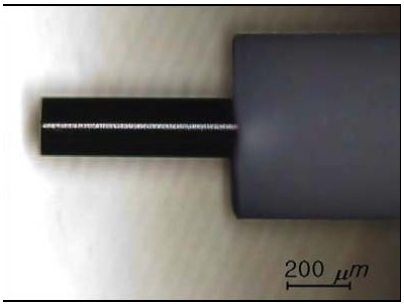

Fig. 2.2 Side-insulated electrode [37]

The authors in this work observed that the side-insulated tool provides new possibilities for describing the exact geometry of a gas film by inducing single bubble formations (see Fig. 2.3).

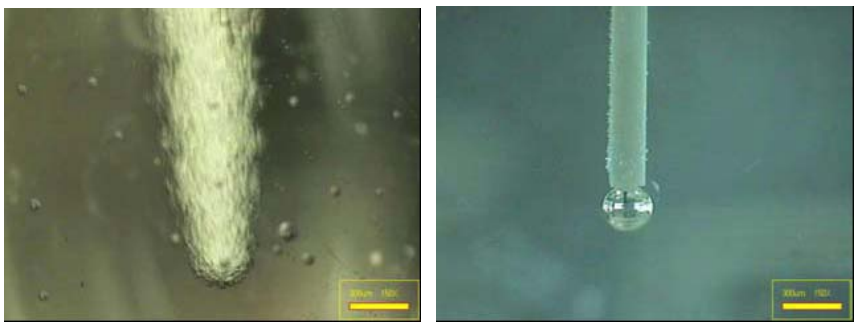

Fig.2.3 Comparison of geometric shape of the gas film [37]

(Left) conventional electrode, (right) side-insulated electrode (single bubble formation)

In ECM drilling, with the tool electrode moving downward, the area of the electrode–electrolyte interface increases. As the immersion area increases, the rising time of the double layer increases, and the dissolution rate (that is, the machining rate) gradually decreases. The dissolution time at the entrance to the hole is much longer than that at the exit and since dissolution occurs not only on the bottom of the tool, but on the side of the tool as well, using a cylindrical tool electrode, a microhole with a taper shape is obtained [38]. When the side of the tool electrode is coated with an insulator, potential is charged only in the double layer of the tool bottom (uninsulated area). Therefore, dissolution does not occur along the tool's side, and tapering is thereby prevented. Moreover, since dissolution is restricted only to the bottom of the tool, the dissolution rate is not affected by the immersion depth of the tool, while the machining rate is kept constant [39]. The insulating or coating material should adhere to the tool electrode typically made of metals, and must be resistant to the acid electrolyte. Polystyrene as an adhesive and a tetrahydrofuran (THF) as a solvent are used for these requirements and a pigment can be added to improve visualization. Figure 2.4 shows section of an electrode of insulation thickness about 3 μm.

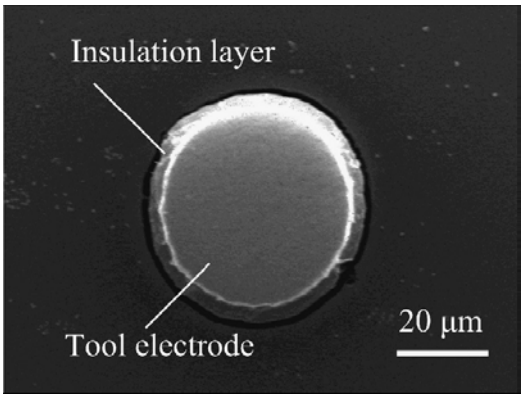

Fig. 2.4 Sectional images of coated tool electrode [39]

2.8 MICROTOOL COATING ISSUES

Coating the microtool involves technical challenges such as choosing the appropriate coating material or its combination thereof for a particular application, adherence to the substrate that is dependent on the substrate physical and chemical properties, uniformity of the coating which affects the finish of the machined surface, and of course, the coating thickness, that decides the coating strength, porosity, and corrosion resistance. Besides the technical requirement, economic and environmental aspects of the material and the coating technique used also play a significant role in coating microtools by restricting the range of coating material and the type of coating process to be selected. Handling is another major issue incase of microtools purely because of their miniature size. Handling involves at least three main stages such as removing from the machine tool, transferring to the coating location, and fitting back the coated tool. Experts in industry suggested that this handling issue can be better resolved if the microtool manufacturers had their coating equipment of their own [40]. It has been observed that most of the tool manufacturers don't have their captive coating system and get the tools coated by external agencies and have to bear with extremely high tool damage rate and it estimated that "about 95 percent of microscale cutting tools remain uncoated" for these reasons [40].

2.9 COATING METHODS

The coating methods not only decide characteristics and quality but also determine the material, thickness, durability, and performance of the coating. The ability of a particular coating method to wear sufficiently is the criterion for its selection [41].

The surface coating methods can be categorized into three main groups: mechanical, thermal, and chemical coatings, based on how the coating is prepared and applied. The comparison of the three mentioned processes is given in Table 2.5.

Table 2.5 Comparison of surface coating processes

Surface coating processes				
	Mechanical coating Processes	**Thermal coating processes**		**Chemical coating processes**
		Flame spraying	**Vaporized metal**	
Bonding forces	Primarily adhesive	Adhesive	Chemical	Adhesive
Coating material	Metallic or non-metallic	Metals (Zn, Al, W) and ceramics	Most metals, metal alloys, and metal compounds	Metallic (pure metals, alloys, or metals with dispersed particles of other substances such as oxides and Teflon
Workpiece material	Metallic or non-metallic	Steels, Al alloys, and Nickel	Mostly metals, occasionally plastic, glass, and paper	Brass, Nickel, Ni alloys, Al, steel, Nonmetals and certain plastics
Methods of application of coating	Dipping, spraying, electrostatic forces, or other mechanical means like mechanical plating	Coating material is melted by flame, arc, or plasma and applied with a jet of compressed air	Vaporization of coating material and deposition on workpiece	Chemical deposition, oxidation, and electrolysis followed by rinsing, drying, curing etc.

2.10 ELECTROCHEMICAL COATING PROCESSES

The electrolytic deposition of metals has been in extensive commercial use in a variety of applications. Electrodeposition is generally understood as electroplating, in which a relatively thin film of metal is electrodeposited onto a supporting substrate. Electroforming, on the other hand, refers to an electrodeposition process, in which a somewhat thicker film of metal is deposited electrochemically onto a substrate which is subsequently removed leaving a self-supporting hollow metal article [42].

2.11 ELECTROPLATING

Electroplating is a finishing process widely used in the automotive, aerospace, electronics, and other engineering applications to deposit a metallic coating on a substrate to prevent corrosion, to provide wear resistance and to add to product aesthetics. In most cases, the plating metal is a single metallic element; however, some metal alloys can also be plated. Chrome plating on steel parts on automobiles and motorcycles, hand tools, crank and cam shafts, zinc coated nuts, bolts, and washers are common applications of electroplating.

Electroplating can be defined as electrolytic deposition of a very thin layer of metal to a base metal or substrate to enhance or change its physical appearance and/or properties. Theoretically, electroplating is probably one of the most complex unit operations because of the large number of critical elementary processing steps that control the overall process [43]. Electroplating has an interdisciplinary nature that involves electrochemistry, electrochemical engineering, surface science, solid state physics, metallurgy and materials science, and electronics.

2.11.1 PRINCIPLES OF ELECTROPLATING

Schematically, an electroplating system consists of a tank, electrodes, electrolyte and a power supply (Fig. 2.5). The electrolyte contains metal ions and some additive species, such as a brightener, a leveler, and an accelerator. The plating bath or the electrolyte serves as a conductive medium and completes the electrical circuit for electrochemical reactions, called electrolysis, to occur. When a current flows through the electrolyte, the cations and anions move toward the cathode and anode, respectively. A charge transfer reaction occurs in the electrodes, and therefore deposition occurs. As replenishment for these deposited ions, the metal from the anode is dissolved and goes into the solution and balances the ionic potential. In an ideal process, the amount of metal deposited on the cathode is equal to the amount of metal dissolved at the anode. It is comparatively easy to control the deposition area, in the electrolyte, as the electrical resistance of the cathode surface area determines the amount of available electrons for deposition [44].

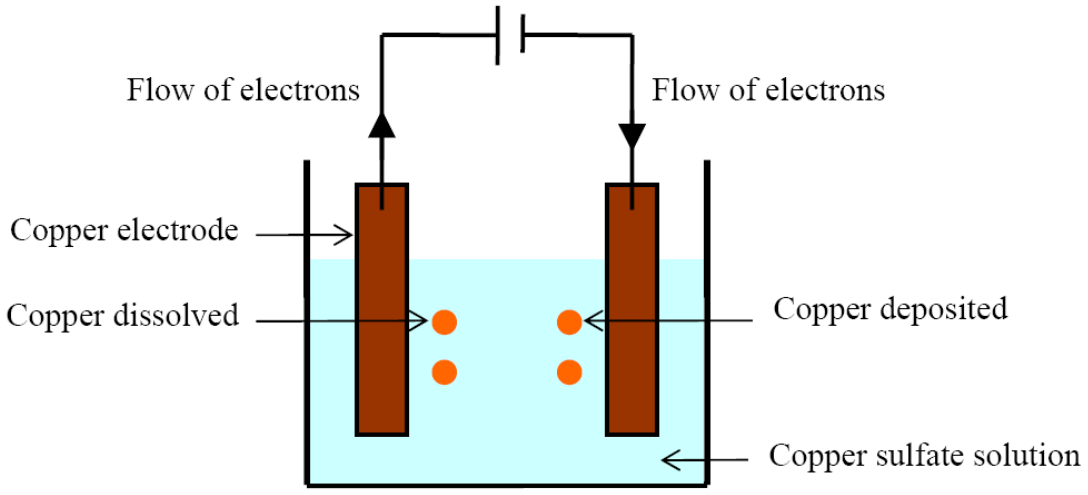

Figure 2.5 Scheme of a copper electroplating unit [15]

Because electroplating is an effect of the electrolysis process, the distribution of both potential and current density play important roles in the processing and most of the potential drops within 1000 angstroms near the surface of the electrodes. The distribution of voltage in the bath is shown in Fig. 2.6. The feature geometry and arrangement of electrodes do not influence the current distribution as much as they influence potential distribution. The current distribution tends to concentrate at edges and points. Because uniformity is desired in most electroplating applications, obtaining a uniform current distribution is fairly important. Theoretically, the thickness of the electroplated layer deposited on the object is determined by the time of plating, and the amount of available metal ions in the bath relative to current density. Metal objects with sharp corners and edges will tend to have thicker plated deposits on the outside corners and thinner deposits in the recessed areas as the current flow is denser around the outer edges than the less accessible recessed areas.

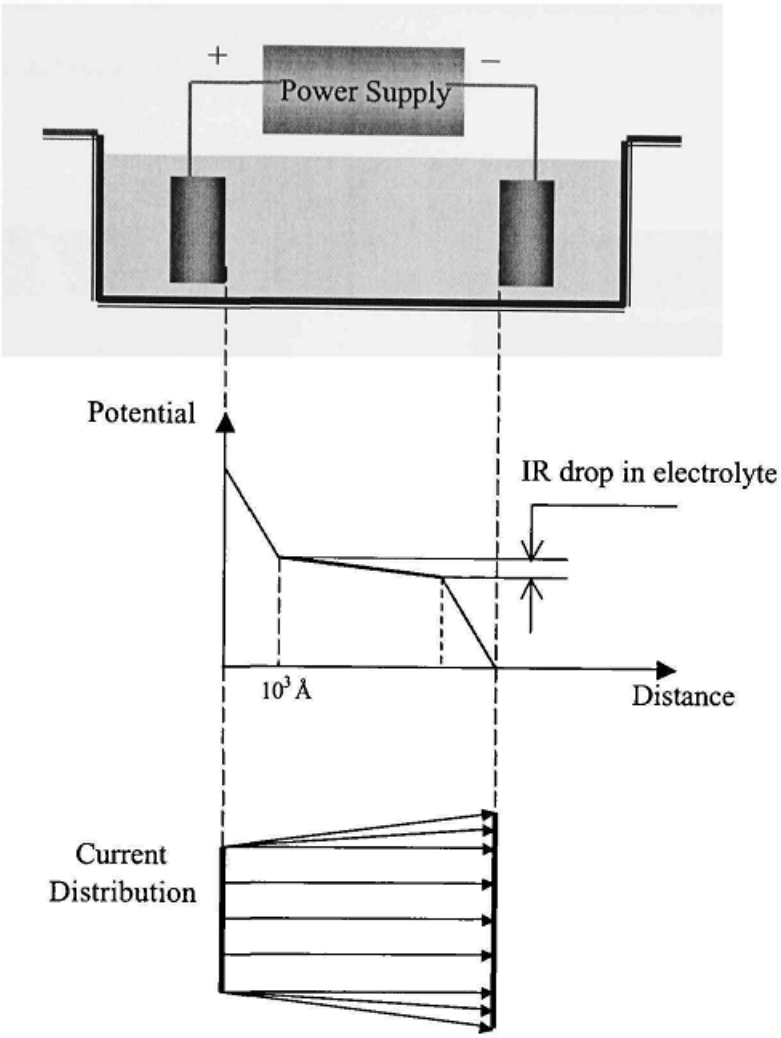

Fig. 2.6 Distribution of voltage and current in the electrolyte bulk [45]

In electroplating systems, overpotential, the potential difference that drives the current of electroplating, is a significant factor. Even if the power supply is cut off in an electroplating system, the electric field at the interface does not disappear and the remaining potential is termed as equilibrium potential. Overpotential is the difference of the potential drops between the two conditions; when the external power supply is on and when it is off. So the external supply potential must be higher than equilibrium potential in order to initiate a current flow in the plating bath. Fig. 2.7 shows the concepts of

overpotential and equilibrium potential. Equilibrium potential for a reaction in a given solvent system is constant at a constant temperature. Equilibrium potential values for some reactions are listed in Table 2.6.

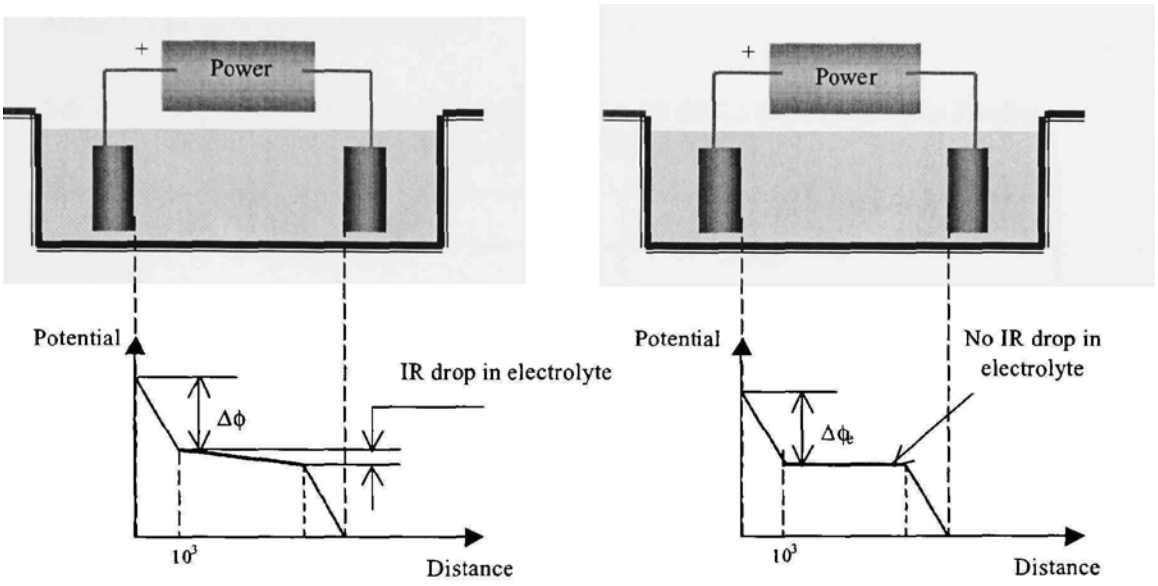

Figure 2.7 Equilibrium potential and overpotential [45]

Table 2.6 Equilibrium potentials in different electrode reactions [46]

Electrode Reaction	**Equilibrium Potential (V)**
$Fe^{2}+ + 2e \rightarrow Fe$	-0.440
$Ni^{2}+ + 2e \rightarrow Ni$	-0.250
$Sn^{2}+ + 2e \rightarrow Sn$	-0.136
$Cu^{2+} + e \rightarrow Cu^{+}$	0.153
Cu+ + e → CU	0.52
Ag+ + e → Ag	0.7991
$Pb^{2}+ + 2e \rightarrow Pb$	0.83
$Au^{3}+ +3e \rightarrow Au$	1.42
Au+ + e →Au	1.70

2.11.2 PULSE ELECTROPLATING

Conventional pulse current plating usually termed as ‘pulseplating’ or ‘pulse electrodeposition’ can be simply defined as metal deposition by pulsed electrolysis [47]. Direct Current (DC) plating, the conventional method of electrodeposition, is modified in this case and interrupted direct current is used for electroplating. The process uses a series of pulses of direct current, of equal amplitude and duration in the same direction, separated by periods of no current. During the period when the current is on, the metal ions next to the cathode are depleted and a layer rich in water molecules is left. During the portion of the cycle when the current is off, the metal ions from the bulk of the plating solution diffuse into the layer next to the cathode forming deposits. Two different modes of operation are used: constant current and constant voltage, in pulseplating operations. The method has been adopted in a number of metal finishing industries, especially the electronics industry. Metals generally deposited using pulsed current include gold and gold alloys, nickel, silver, chromium, tin-lead alloys, and palladium.

Pulseplating provides an opportunity to change the properties of the deposit, just like the addition of organic compounds. In addition to the usual independent variables in electrodeposition such as pH, temperature, current density, bath composition, and agitation, there are further degrees of freedom such as pulse duration, current density, current on and off-time, polarity, and pulse height. The only variable in the conventional continuous current plating or DC plating is the mean current density (J_m) applied by the power source. On the other hand, pulse electrodepostion or pulse plating, because of its pulsating current supply has two main additional parameters: pulse ontime and pulse offtime. Pulse time, t_{on}, is the amount of time during which the current is supplied and t_{off}

is the pulse offtime when the power is off. On a current density versus time diagram, PED typically exhibits a periodic square wave function, when the DC plating is described by a straight line. Following are few frequently used electrodeposition parameters.

Pulse Frequency = $1 / (t_{on} + t_{off})$,

Duty Factor = $t_{on} / (t_{on} + t_{off})$, and

Peak Current Density = Mean current density / Duty Factor.

The pulse electrodeposition deposition process includes six steps; namely ion diffusion in front of substrate, charge transfer reaction, adatom formation, surface diffusion, growth, and stress and ion relief during pulse off-time [48].

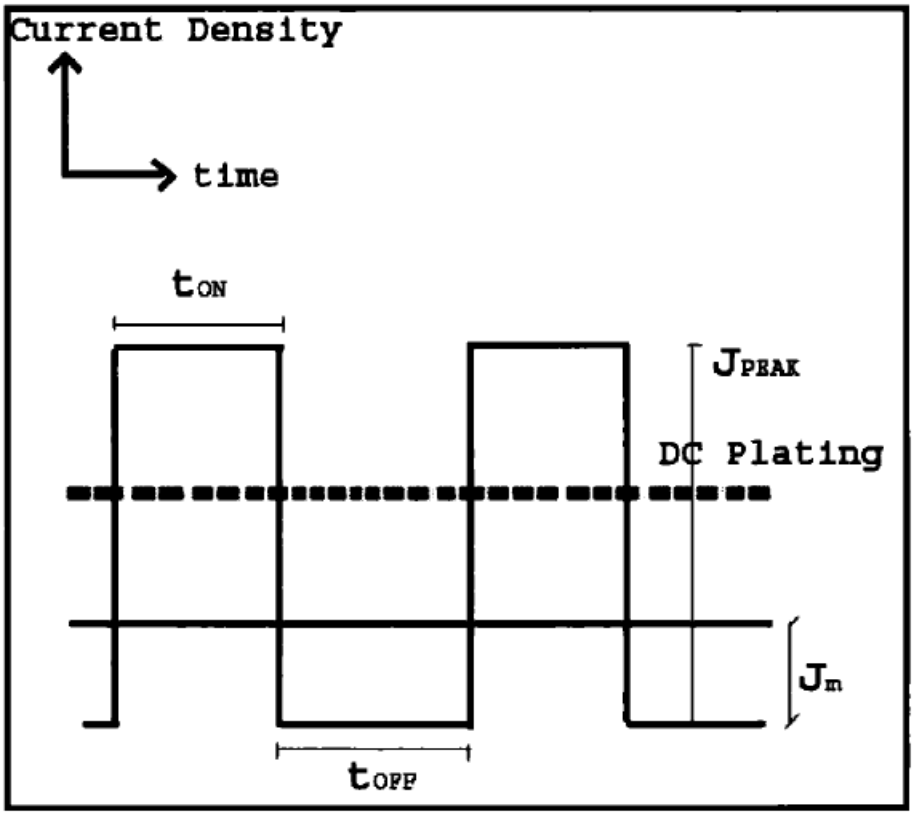

Fig. 2.8 Schematic summary of DC and Pulse electrodeposition [48]

2.11.2.1 PULSEPLATING CHARACTERISTICS

The following is a list of pulseplating characteristics.

- Decreased porosity and increased density due to reduction in grain size.
- Improved adhesion since the peak voltage can be several times greater than DC voltage.
- Improved deposit distribution since localized high current density “burning” associated with DC is significantly reduced.
- Reduced stress in the electrodeposits since the lattice imperfection, impurities, voids and nodules usually found with DC plating are generally reduced with pulse plating.
- Although the cathodic current is applied for less than half the total plating time, the overall metal deposition rate can be greater than that obtained with DC alone.

2.11.2.2 ADVANTAGES OF PULSE PLATING

The advantages of pulseplating are listed here.

- High current density at the beginning of a pulse creates a more strongly reducing environment at the cathode surface and thereby enhances the cleaning action, apparently by cathodic desorption. This in turn increases the number of sites where metal deposition can occur and improves adhesion of the deposited metal.
- The increased current density increases the free energy of the charge carriers, thereby increasing the number of nucleation processes. Pulsed current deposits hence tend to be more fine-grained and denser (less porous) and better adhering than their DC deposited analogues.

- During plating, other metallic or non-metallic materials are simultaneously formed that can be deposited as coatings. During the off time, they diffuse into the bulk electrolyte, because of this, the probability of such co-evolved products being incorporated into the deposited metal, is reduced and pulse-deposited metals are thus usually of higher purity than the DC-deposited ones.
- The co-evolution of hydrogen during electrolysis leads to a pH increase in the near-electrode layer, and this can strongly affect the composition of the deposit. In case of pulse plating, this effect is less marked, since hydrogen ions can diffuse/ desorb during the off-time.

The disadvantages of pulseplating are: a pulsed-current rectifier is typically costs more than a conventional DC unit, optimization of results requires thorough planning and experimentation, and there is always a demand for redesigning or upgradation of the plating equipment.

2.11.2.3 NANOSTRUCTURED COATINGS BY PULSE ELECTRODEPOSITION

Varieties of methods have been developed to synthesize nanoparticles such as severe plastic deformation, chemical vapor deposition (CVD), metal alloying, inert gas condensation, and electrodeposition. Electrodeposition stands out among all the methods as an inexpensive process and offers a simple and viable alternative to the complex and costly high temperature and vacuum deposition processes. Pulse electrodeposition is a powerful means for controlling the electrocrystalization process and producing deposits with unique structure and properties. Many nanocrystalline materials have been produced by pulse electrodeposition successfully [49]. Some of them have been adopted for

industrial and/or commercial applications such as production of copper foil for printed circuit boards, repair of heat exchangers, production of water resistant coatings, and electrodes for the catalysis of oxidation and evolution reaction [50]. The deposition of nanostructured coatings by pulse electrodeposition is dependent on two main processes namely nucleation and growth of grains [51]. During the deposition, these two processes are in competition with each other and are influenced by many factors. Ultrafine-grained deposits can be achieved when the deposited ions are discharged to form new nuclei rather than incorporated into existing crystals. Therefore, factors causing a high nucleation rate and slow grain growth are responsible for the formation of nanograined deposits. Table 2.8 lists some of the previous works in DC and pulse electrodeposition.

Table 2.7 Few previous works in DC and pulse electrodeposition

Reference	Coating Material	Substrate	Bath Composition	Temp.	Method	Findings
[52]	Co Al_2O_3	Brass	310 g/L CoSO4 .7H2O 41 g/L CoCl2 .6H2O 25 g/L H3BO3 pH 2.0 No additive	40^0C	Pulse plating 0-800 mA/cm^2 Rotating disk electrode	High current pulse increased the strength. Mechanical properties of Co-Al2O3 improved by pulse current plating
[53]	Ni	TiN	300 g/L $NiSO_4$ .7H_2O 5 g/L $NiCl_2$ .6H_2O 45 g/L Boric acid pH (2 and 4.5) Additive: Saccharin	60-65^0 C	Pulse plating ton=2.5, 5 ms toff=15 and 45 1.6 and 1.9 A/cm^2	Average grain size 11 +/- 1 nm
[54]	Pd	Steel/Ti	112 mmol/L $PdCl_2$ 378 mmol / L $(NH_4)_2SO_4$ pH = 6-7 Additive: Citric acid, tartratic acid, organic amines, and NH4OH	40^0C	Pulse plating t_{on} = 1 and 4 ms t_{off} = 5 and 50 ms i_c = 0.1 and 1.25 A/cm^2 t = 5, 15, 30, and 90 min	Grain size varies 17 to 27 nm
[55]	NI Al	Ni	400 g/L Ni(NH_2)SO_3 30 g/L boric acid pH 4.0 5 g/L $NiCl_2$ Al particles 1.25 μm 150, 225 g/L Al powder Additive: sodium laurel sulphate & coumarin	50^0 C	DCt plating 100 A/cm^2 1.5 h Rotaing disk electrode	• 8-2 volume % Al in coating • Microhardness decreases with increasing Al volume %

Table 2.7 Continued

[59]	Cu Al_2O_3	Cu	0.25 M $CuSO_4$ H_2SO_4 12.5 g/L γ-alumina pH 4.0 Additive: $C_6H_5Na^3O_7.2H_2O$	25^0 C	DC plating (RCE) 10 mA/cm^2 Pulse-reverse plating 5 mA/cm^2	Pulse-reverse plating increased the particle concentration in metal matrix
[57]	Cu	Si (100) Cu Seed TiN	0.4 M $CuSO_4$ 1.53 M H_2SO_4 No additive	35^0 C	DC plating Rotating disk electrode 10 - 60 mA/cm^2 30 sec	Grain size 35-45 nm at 30-60 mA/cm^2
			0.8 M $CuSO_4$ 0.75 M H_2SO_4 No additive			
[56]	Cu Al_2O_3	Steel	0.1 M $CuSO_4$ 1.2 M H_2SO_4 39, 120, 158 g/L Al_2O_3 No additive	Room	Rotating cylinder electrode (RCE) 5 to 25 mA/cm2	Size and density differences of alumina powders have little effect on codeposition.
[59]	Ni Al_2O_3	Cu/Steel with 1μm Au coating	$NiSO4.6H_2O$ 0.3 M $Na_3C_6H_5O_7.2H_2O$ 25 g/L γ-Al_2O_3 pH 4.0 Additive free	Room	DC Plating (RCE) 13.3 - 92.8 mA/cm^2 Pulse-reverse plating 26.5 to - 26.5 mA/cm^2	0 - 1.01 wt% γ-Al2O3

2.12 NICKEL ELECTROPLATING

Electroplated nickel coatings reduce mechanical wear, corrosion, fretting, and scaling, and are extensively used in electroforming of tools, molds, and dies. Nickel plate is often applied over copper and under chrome to obtain a decorative finish. In addition, nickel tends to gall when rubbed against some metals even when lubricated, which requires chromium to be used as an overlay. The original process of electroplating of nickel was patented by Watts in 1916 (known as Watts' bath). These baths use solutions of nickel sulfate, nickel chloride, and boric acid. The major source of nickel in the bath is nickel sulfate and the minor source is nickel chloride. The chloride ions in the bath increase the electrical conductivity of the electroplating bath. Agitation and heat increase ionic diffusion and plating rate. Wetting agents are added to bath to prevent sticking of hydrogen gas that forms during plating to the workpiece, which could lead to surface imperfections such as pits. The bath is cleaned by circulation over activated carbon to trap impurities. Periodic cleaning is necessary because the adhesion of nickel coatings is impaired by contaminants such as copper, lead, zinc, and cadmium.

2.13 SUMMARY

A review of literature on coating on tools, issues involved, and comparative analysis of different coating methods is presented. Electrodeposition because of its superior coating properties is found to be appropriate coating technique for this work. A brief overview of theory of electroplating has been given for understanding of the process and electrochemistry responsible for deposition.

CHAPTER 3

RESEARCH METHODOLOGY

3.1 INTRODUCTION

This chapter describes the purpose of the current work and the key objectives. The experimental approach is illustrated here along with the equipment set up. The experimental design and selection of important parameters for the process have also been detailed.

3.2 PURPOSE OF THIS RESEARCH

Literature review in the earlier section suggests that electrochemical machining has many advantages over other finishing methods such as no tool wear, low heat generation during machining, and stressfree machined surfaces. The process is also quite fast and unlike electrodischarge machining (EDM), a copper electrode can be used to machine titanium and other high performance alloys. Tooling is considered to be one of the most important challenges in ECM and there is no standardized method to produce, or predict the tool shape in this process. However, literature on the use of coated tool in ECM was found to be limited and inadequate. Again as has been emphasized in the literature review section, the microtool coating issues are significant and there is always an endeavor to make the microtool and its subsequent processing right near the machine where it will be used. In EDM, generally the microtool is prepared by wire electric discharge grinding machine attached to the EDM machine. That makes the tool handling, repair, and replacement more simple, convenient, and

easy. However, similar method of making the ECM tool near the ECM setup has not been sufficiently explored. Pulse electroplating has shown enough promise to be an alternate method of coating to the conventional PVD and CVD processes. Moreover, the vapor deposition technologies need specialized arrangements and are expensive. These methods have limitations of coating a round microtool because of their process restrictions. Electroplating on the other hand can use the setup used for ECM and can coat the microtool of any shape with precision being inexpensive. Tungsten has almost all the desired properties of an ECM tool material besides its low electrochemical stability which leads to corrosion. This property can be improved by coating the tungsten microtool with a material of higher corrosion and oxidation resistance such as nickel. Developing microtool for ECM applications in the form of nickel coated tungsten microelectrode by electroplating using the set up for ECM is the foundation of this research proposal.

3.3 EXPERIMENTAL APPROACH

The goal of this research is to prepare coated microtool by electroplating using the equipments that are in an ECM set up. In this work, coating was attempted by conventional continuous current and also by pulseplating technology. Tungsten and nickel are of particular interest because these were the two materials used in the plating process in all the experiments. The parameters and their range were carefully chosen after a lot of screening or preliminary experiments. A full factorial experimental design was used for both the plating processes. This work optimized the experimental process

with an optimal set of potential parameters. A concise summary of experimental approach in this work is given in fig. 3.7.

3.4 OBJECTIVES AND SPECIFIC TASKS FOR THIS WORK

The objectives of this work and the related tasks are listed below.

Objective 1

To prepare nickelcoated tungsten microtool by electrodeposition for electrochemical machining applications

Tasks for objective 1

- Develop an in-house electroplating apparatus for coating microelectrodes.
- Conduct preliminary plating trials for selection of factors and levels.
- Design and conduct a 3x3 for DC and 3^3 randomized experiments for pulseplating experiments.
- Characterize the coating in terms of thickness, surface roughness, grain size, and microstructure, and optimize the parameters for best coating.

Objective 2

To evaluate the performance of coated microtool in pulse electrochemical machining (PECM)

Tasks for objective 2

- Design and develop the in-house PECM setup
- Machine the SS303 workpiece by coated and uncoated micro electrode
- Compare the performance of two type of tools

Thickness of the coating produced by an electrodeposition process is one of the most important considerations. If only a single test is carried out for determining the quality of coating, it would be a thickness determination [60]. In the thickness test, often a mean value of the deposit thickness is required, but sometimes the value at a particular location is of significance. Depending on the applications of the coated product, which requires accurate determination of the thickness, it is always attempted to make as many measurements as possible, not only over the surface of the component, but also more than once at each location. Since the shape and profile of the tool is exactly reflected on the workpiece, and accuracy and tolerance capabilities are dependent upon tool part geometry in an ECM operation, roughness is also another important characteristic of the tool profile. Again, considering the fact that we are planning to develop a tool with enhanced corrosion resistance, density and uniformity of coating can not be overlooked. So this work focused on several responses: coating thickness, coating uniformity, microstructure and roughness of the coated surface. The combination of process parameters that gave the optimal result was determined.

3.5 SELECTING MAJOR FACTORS

A comprehensive list of factors and their ranges that have significant influence on the outcome of the plating process were determined either by the preliminary experiments or from the literature. Table 3.1 lists some of the major potential factors and their ranges.

Table 3.1 Potential factors and ranges

FACTORS/ PARAMETERS	RANGE/ TYPE
Voltage	5-15 V
Current density	1-500 A/cm^2
Pulse Frequency	10-1000 KHz
Duty Factor	20-80%
Electrolyte Bath	Sulfate or Sulfamate
Plating Time	1-20 minutes
Temperature	70-130 ^0F

For the preliminary plating trials, copper electrodes of diameter 3.15mm were arbitrarily chosen. The average current density decided the total current to be supplied in the process. The power supply used for the preliminary trials had the provision for adjusting the voltage and current by internal resistance control. A power supply (model PPTAA100020) developed by Rapid Power Technologies Inc., was used for the experiments. The specification of the power supply is given in Table 3.2.

Table 3.2 Specification of the power supply

Rated Dc Output	100 Amps (Average) and 200 Amps (Peak); 20 Volts Square Wave Pulses
Control	Transistorized
Time ranges (in milli sec)	On-time 1-99; Off-time 1-99
Ripple	0.5% RMS (conventional DC)
Protection	Short circuit proof
Meters (average)	DC ammeter & DC voltmeter

Substrates underwent a variety of pretreatment in order to remove dirt and contaminants. Deposition was carried out in a 150 ml electrolytic cell with parallel electrodes in a standard Watt's bath. The electrodeposition conditions were as shown in Table 3.3. A 50 cm^2 area nickel rod was used as an anode and copper electrode of 3.15 mm diameter as cathode. Duty factors of 30-62.5% and current densities of 2.5-5 A/ cm^2 were used with different plating time for pulseplating of pure nickel in these set of experiments. The pH was controlled by adding dilute 5% sulfuric acid or by adding nickel carbonate. The set up used for these trials is shown in Fig 3.1and 3.2.

All experiments were conducted at room temperature and in the sulfate bath. This left five factors to be varied in the experiments. Those factors were voltage, current density, frequency, duty cycle, and plating time.

Table 3.3 Electrodeposition conditions and plating parameters

PH	4-5
Temperature	20ºC
Substrate (Cathode)	Copper (ϕ 3.15mm)
Anode	Pure Nickel (ϕ 6.3mm)
Peak current density	2.5-5 A/ cm^2
Duty cycle	50-62.5 %
Plating time	2-5 minutes

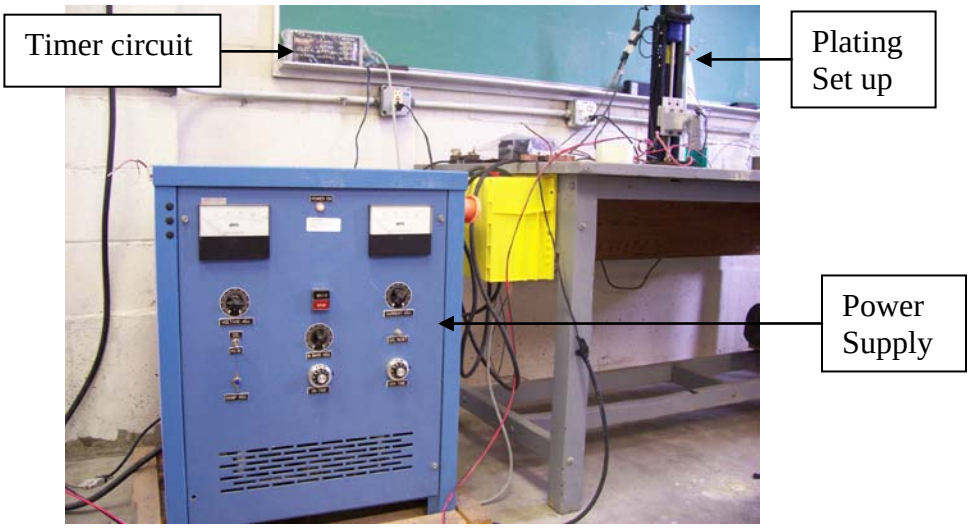

Fig. 3.1 Power supply and the experimental set up

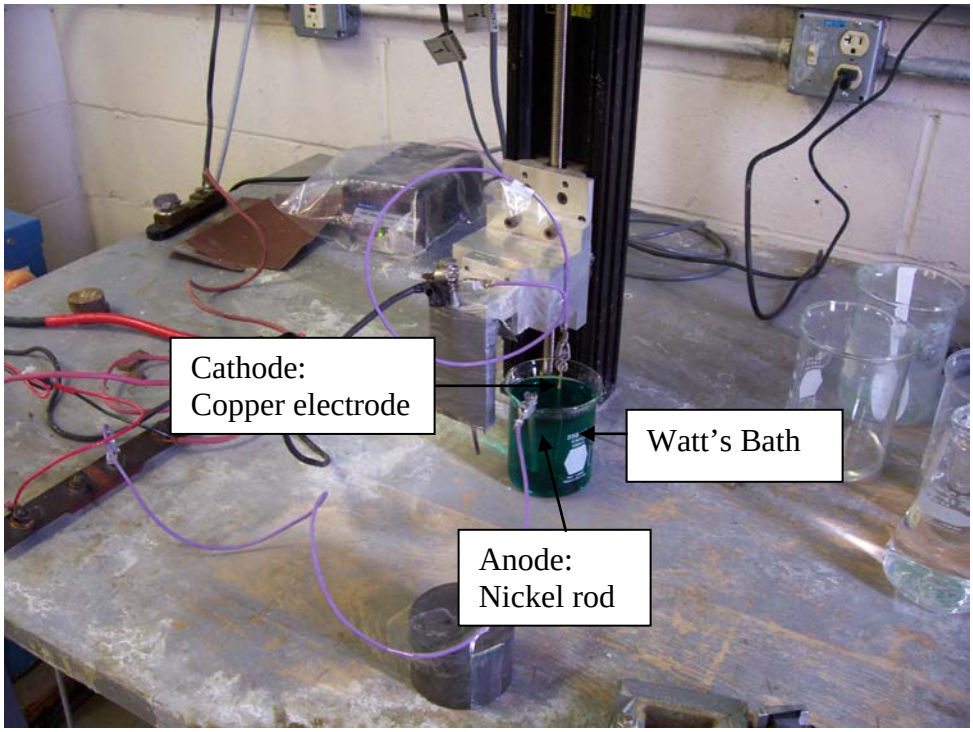

Fig. 3.2 The electrochemical cell for preliminary trials

3.6 SELECTING FACTOR LEVELS

The trial started with screening experiments involving all factors at two levels to determine the effect of each factor, if any, on plating performance. The screening experiments were conducted using copper electrodes. The screening experiments involved four factors with two levels each as shown in Table 3.4.

Table 3.4 Major factors and levels

FACTORS	LEVELS (LOW-HIGH)
Voltage	10-15 Volts
Current Density	2.5-5 A/cm^2
Frequency	100Hz-1000Hz
Duty Factor	50-62.5%
Plating Time	5-15 minutes

3.7 FINDINGS OF THE PRELIMINARY TRIALS

The coated samples were observed under a Nikon measuring microscope (Model MM-40) that captured the image and measured the dimensions of the electrode. The diameter of the microelectrode was measured before and after the plating to find the thickness of the coating. A smooth coating was noticed to have taken place on the copper substrate. Then the specimens were analyzed by a scanning electron microscope to determine the surface topography. Images shown in Fig.3.3 indicate the uniformity of the coating thickness and smoothness of the plated surface. However, when coating was attempted on micro electrode under similar experimental conditions, salt deposition, rather than coating was noticed in optical microscope observation (Fig. 3.4). This may have been due to change in cathode material and/or excessive current density during the process. As per calculations below, for an 8 mm long tungsten microrod of 300 μm diameter, 0.1903 A of current needs to be supplied, to ensure a peak current density of 2.5 A/ cm^2.

Area to be plated = Side area of the rod + End area of the rod exposed to the plating = (Cross sectional area of the microrod x Length of the rod dipped in the plating solution) + $(\pi/4)$ (rod diameter)^2 = [π (rod diameter) x Dipped rod length in the solution] + $(\pi/4)$ (0.03cm)^2 = [π (0.03 cm) x 0.8 cm] + $(\pi/4)$ (0.03cm)^2 = 0.075428 + 0.000707 = 0.0761 cm^2

For a current density of 2.5 A/cm^2, Current to be supplied = Current density x Area exposed to plating = 2.5 A/cm^2 x 0.0761 cm^2 = 0.1903 A

Because of the hardware limitations of preliminary experimental setup, current densities of 100, 150, and 200 A/ cm^2 were used. This resulted in defects such as cracks and salt deposition. Hence, another experimental set-up having a pulse rectifier of lower peak current supply range was used for the subsequent experiments on tungsten micro electrodes. The next section describes in detail the experimental set up used for the final set of plating experiments.

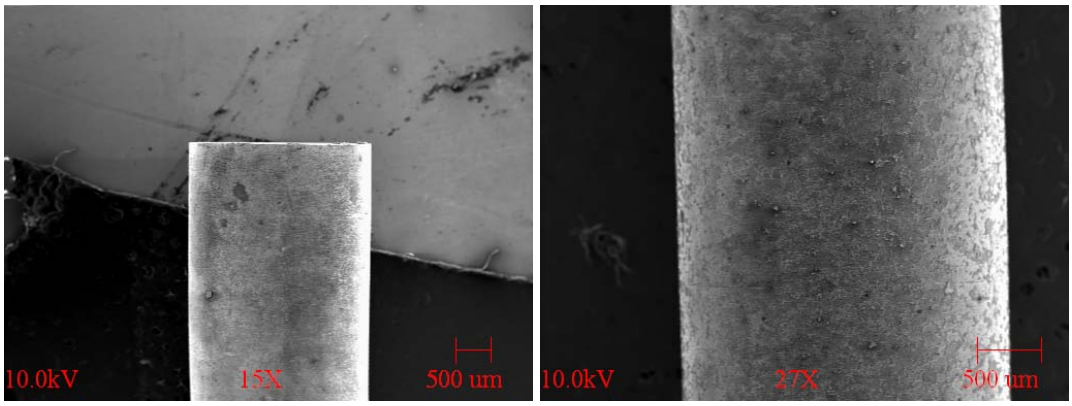

Fig. 3.3 SEM image of the uniform nickel coating on copper rod

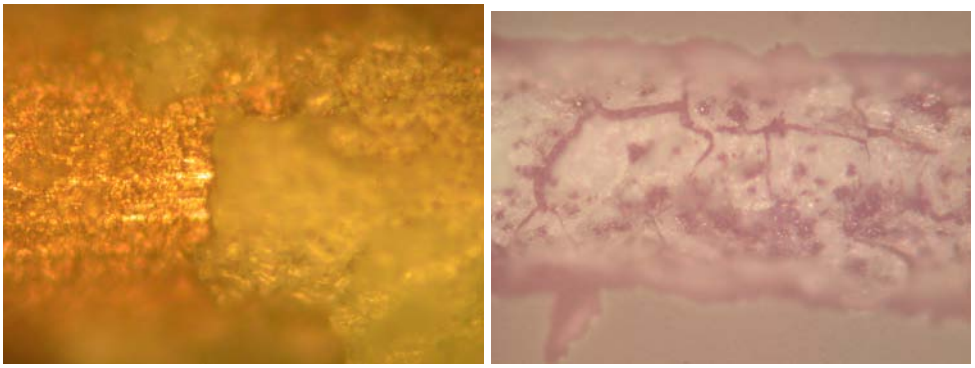

Fig. 3.4 Non-uniform coating in patches on tungsten microelectrode

3.8 SYSTEM SET UP

The in-house developed system comprised of mainly three basic units; the electrochemical cell, the tool holding and motion mechanism, and the power supply unit with accessories (Fig. 3.5). Each key component of the individual section is described in detail along with its functions in the following sections.

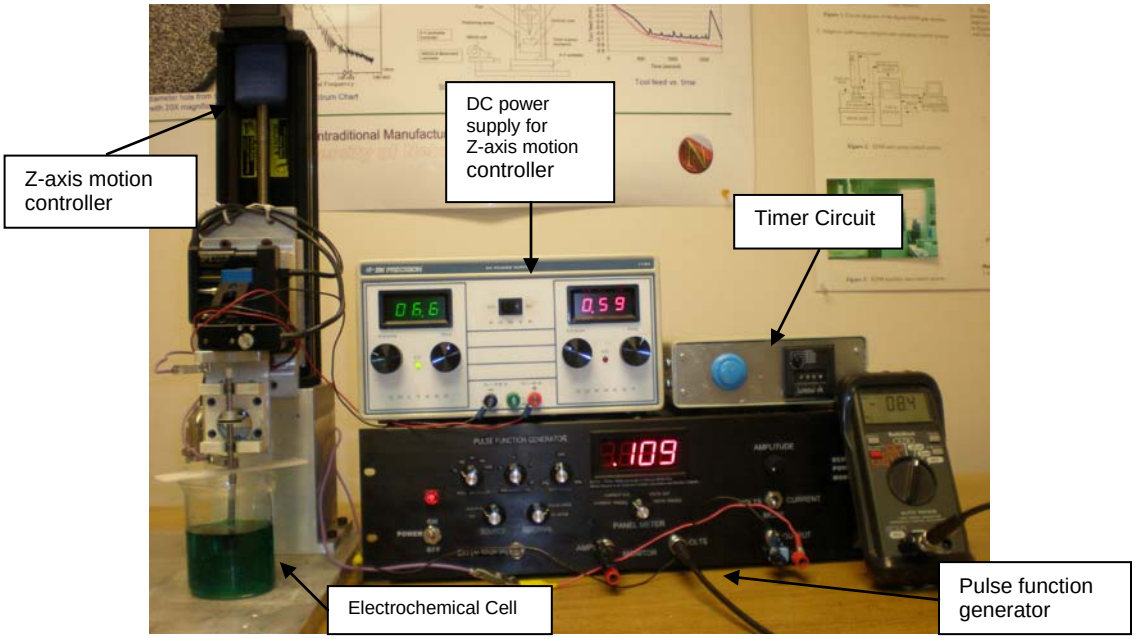

Fig. 3.5 The experimental setup

3.8.1 ELECTROCHEMICAL CELL

The most important component in the electrochemical cell is the electrolyte bath. Most commercial nickel plating solutions/ bath are based on the one named after Watts who first introduced it. The Watt solution is a low demanding formulation that generally offers good result such as uniform coating thickness and adhesion, low pitting. The immanent problem with Watt solution is the presence of high level of tensile stress in the deposited layers. The term watts bath is used to cover a range of solutions whose compositions vary within the range shown in Table 3.5, the chloride ion sometimes being introduced in the form of sodium chloride.

Table 3.5 Watt's Bath composition range

INGREDIENTS	COMPOSITION RANGE
Nickel sulfate ($NiSo_4.7H_2O$)	150-400 g/l
Nickel chloride ($NiCl_2.6H_2O$) Or Sodium chloride (NaCl)	20-80 g/l 10-40 g/l
Boric acid (H_3BO_3)	15-50 g/l

Nickel sulfate, the principal ingredient of the bath, is the main source of nickel ions because it is readily soluble (570g/l at 50degC). In nickel plating solutions the activity of nickel ions is governed by the concentration of nickel salts in solution, their degree of dissociation and the nature and concentration of other components of the solution. If the concentration of Ni^{2+} available for deposition is low, burnt deposits will be produced at a relatively low current density, and in addition the limiting current density will be low. For these reasons the concentration of nickel sulfate must be high.

The presence of chloride has two main effects: it assists anode corrosion and increases the diffusion coefficient of nickel ions thus permitting a higher limiting current density. Researchers [61] have quoted values for the diffusion coefficients of nickel ions in sulfate and chloride solutions at specified conditions and showed that the limiting current density at a cathode in a chloride bath is approximately twice that in a sulfate bath, other factors being equal.

Boric acid is used as a buffering agent in Watts nickel solution to maintain the pH of the cathode at a predetermined value. Boric acid is a weak acid and exists in the solution as a mixture of borate ions and undissociated boric acid. When hydrogen ions are discharged in the presence of boric acid, some amount of boric acid dissociates to provide replacement of hydrogen ions that are lost and, thereby limiting the pH change of the bath. At the same time, formation of borate ions occur in the solution and the boric acid/borate ion buffer is able to maintain the solution pH relatively stable over a range of normal operation conditions. The concentration of boric acid remains constant in most cases and the optimal concentration of boric acid in the Ni-speed bath is 40 g/l with a range of 30–45 g/l [62]. Boric acid solutions of the strength used in Watts nickel solutions have a pH of about 4.0 due to nickel ions [63]. Boric acid is most suitable as a buffer at about pH 4, but it is satisfactory over the range of pH 3 to 5, probably due to the formation of complexes of boric acid and nickel. The buffer action of boric acid is particularly important in solutions of low pH (high activity of hydrogen ions), since hydrogen discharge occurs and consequently the pH increases in the cathode film with the possibility of co-deposition of nickel hydroxide. Boric acid can also act as a catalyst during high speed deposition [64].

A typical Watts, referred to as W2, of following composition was used to electrodeposit nickel on the tungsten microelectrode. De-ionized water was used to prepare all bath solutions and the bath was maintained at room temperature.

Table 3.6 Watt's bath ingredients

CHEMICAL	WEIGHT IN GRAMS PER LITER
Nickel Sulphate ($NiSO_4 .6H_2O$)	240
Nickel Chloride ($NiCl_2 .6H_2O$)	35
Boric Acid (H_3BO_3)	40

3.8.2 ANODE AND CATHODE

The purity of anode material is very important in plating; the nickel (plus cobalt) content should be at least 99% [65]. Impure anodes could lead to contamination of the solution and inferior physical properties of the deposit. Anodes should dissolve smoothly without undercutting of grains resulting in production of small nickel particles, which is not only wasteful but can also have detrimental effects on the cathode. For this work, a nickel rod of 6.3mm diameter of 99.9% purity was used as anode in the entire set of plating trials. In the electrochemical cell, tungsten rod of 300 microns diameter of 99.9% purity was used as cathode. Both cathode and anode material were purchased form Alfa Aesar®, Ward Hill, MA, USA. The tungsten rod was made to go through a series of surface preparation stage before it got plated.

3.8.3 CATHODE HANDLING AND MOVEMENT MECHANISM

The cathode holing and motion mechanism in this work was provided by Polytec PI Inc. ®, Tustin, CA. There are 3-axis stages to realize three-dimensional (X, Y, and Z) relative movements between cathode and anode and each stage has an individual motor to provide motion along its axis. A V-shape bearing is attached to the 3-axis stages that facilitates the holder rotation and movement and can be directly driven by the stages. The specifications of the translation stages listed in Table 3.7. The displacement and electrode holder motion are controlled by a controller with an embedded microtranslation motor. The cathode tool is fixed inside a mandrel and the tool mandrel rested on V-shape bearing is rotated by a DC motor.

Table 3.7 Specifications of the translation stages

DRIVE UNIT MODEL	M111.1DG
Motor Type	DC
Maximum Travel	15 mm
Resolution	7 nm
Maximum Velocity	1.4 mm/sec

3.8.4 POWER SUPPLY

The unit used for the experimental work was a customized power supply capable of providing microsecond pulse voltage (Fig. 3.6). The specifications of this power supply are listed in Table 3.8.

Fig. 3.6 Pulse Function generator

Table 3.8 Specifications of the power supply

Model	1cc – 10 Cv (Custom Design*) Pulsed Output Power Supply
Mode of operation	Pulse or DC
Current	0-2 A
Voltage	0-10V
Pulse Frequency	0-100KHz
Duty factor	20-100%

* Designed by QVR Designs LLC, San Diego, CA

The power supply discussed in Table 3.8 could operate in a constant voltage mode with maximum output up to 10V with compliance current of 1.5 A DC. The output voltage was adjustable by a front panel 10-turn potentiometer or from an external signal generator. Pulse frequency is programmable up to 100 kHz and Pulse duty-factor can be independently adjusted ranging from 20% to 80%. An external BNC connector was used for driving the power supply output. A Digital Volt Meter (DVM) on front panel of pulse generator displays preset output voltage and current level. For monitoring of output voltage and current, two BNC connectors were provided. Considering the practical operation, the pulse current is limited by power supply itself to avoid short-circuiting such as rapid heating of micro tool electrodes under high current and thereby damaging the tool. The power supply had a high resolution (0.01V) to set the voltage

output to the electrochemical cell. The DVM on the front panel of power supply provided reliable readout of the voltage (amplitude of the pulse).

3.9 EXPERIMENTAL PROCEDURE

The whole plating scheme is shown in fig. 3.7.

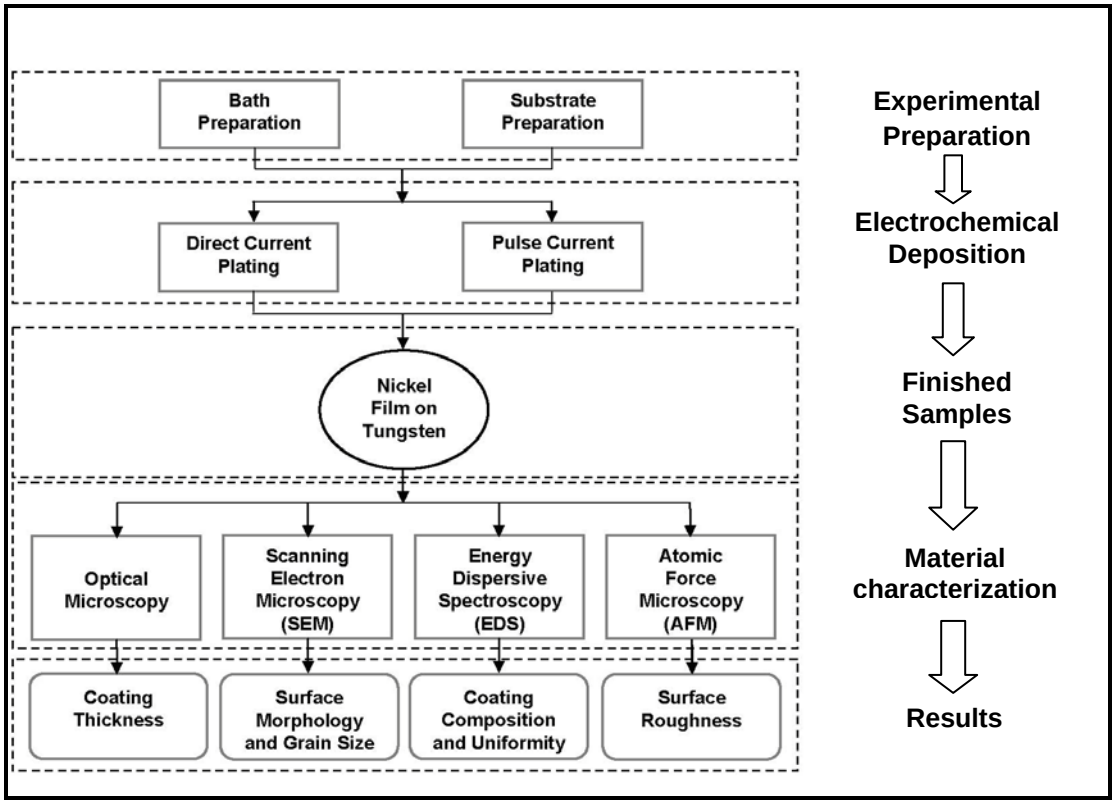

Fig. 3.7 The scheme of experimental approach

Tungsten is known to be a difficult metal to coat with adherent deposits because of a thin, tenacious, natural oxide film that forms on the metal surface. This film is very hard to remove and reforms quickly on the cleaned surface on exposure to air or water. So extensive surface preparation is required in case of plating any material on tungsten.

Strike baths have a vital role in getting adherent plating on metals, particularly where the metal to be plated has expansion characteristics differing considerably from tungsten. The coefficient of thermal expansion of some metals is listed in Table 3.9. It can be seen that nickel differs from tungsten considerably in terms of coefficient of thermal expansion and for that reason use of a strike bath before the actual plating is utmost essential to get an adherent coating.

Table 3.9 Coefficient of thermal expansion

METAL	COEFFICIENT OF THERMAL EXPANSION X 10^{-6} INCH/INCH/^{0}C
Tungsten	4.6
Chromium	6.2
Iron	11.4
Nickel	13.0
Gold	14.2
Copper	17.7

At first the substrates (tungsten rods) were cleaned free of any surface contaminants by degreasing with liquid detergent and washed with deionized water. Then they were again cleaned in an acetone ultrasonic bath followed by dipping in an acid mixture solution (hydrofluoric acid 37.5%, nitric acid 12.5%, and rest water) for 1 min, and finally rinsed with deionized water. The acid mixture removes the oxide film and also etches the metal surface. The substrates were etched again anodically in a sodium hydroxide (15% wt) solution for 2 minutes at a current density of 20 A/dm^{2} to remove any passive oxide surface that might have formed on the substrate surface. The

scheme of substrate preparation is given in Table 3.10. A Wood's strike bath with composition given in the Table 3.11 was used for striking at current density 10 A/dm^2 for 3 minutes.

Table 3.10 Scheme of substrate preparation

STAGE	OPERATING CONDITIONS	REACTANTS	DURATION	PURPOSE
Degreasing	Room temp.	Liquid detergent	1min	Removal of surface contaminants
	Ultrasonic bath, Room temperature	Acetone	3 mins	
Water Rinsing				
Acid dipping	Room temp.	37.5% by vol. concentrated HF (48%) + 12.5% by vol. Conc.HNO3 (70%) + 50% Water	1 min	Removal of the oxide film and Surface etching
Water Rinsing				
Alkali treatment (Anodizing)	Room temp. Cathode: Stainless steel Anode: Tungsten microtool Current: DC Current density: 20 A/dm^2	Sodium Hydroxide (NaOH) 15% solution	2 mins	Surface activation (removal of passive oxide film and to etch it further)
Water Rinsing				

Table 3.11 Composition of Wood's Bath

CHEMICAL	PROPORTIONS
Nickel Chloride ($NiCl_2.6H_2O$)	240g/l
Hydrochloric Acid (HCl)	85 ml/l

The pH of the plating bath greatly affects the coating properties. If pH is not maintained within a proper range, it could lead to a loss of throwing power of the electrolyte, low cathode efficiency, and also pitting, rough and brittle deposits [66]. So the pH of the bath was continuously monitored by a digital pH meter (VWR model SB20). Precise control over the pH of the bath over a long time was a difficult task since pH level increased with the progress of the deposition owing to the evolution of hydrogen gas on the cathode. The pH tended to increase at an inconsistent rate, and it was not possible to predict the exact rate of change to take necessary action for its control. However, the deviation was relatively small and during plating session of four hours was not more than +1.5. The pH was contained by addition of hydrochloric acid (10%) to the solution as and when required.

The nucleation rate and hence the grain size of the coating is heavily dependent on the mean current density. So, in this work, a variety of current densities was employed. The average current density for DC plating experiments was varied from 2.5 - 10 A/dm^2 and plating timings were 5, 7, and 10 minutes for each of the three current densities chosen. For the pulse plating, the average current densities were 2.5, 5, and 10 A/dm^2 at three duty factors of 20, 50, and 80%, and pulse frequencies of 10, 50, and 100

Hz. There were 9 (3x3) experiments for DC plating conditions and 27 (3^3) for pulseplating with full factorial design. All experiments were randomized and two replicates done for each experiment. To limit the scope of this work, pulse reverse plating was not considered. However, this can be considered for continuation of this research.

3.10 COATING CHARACTERIZATIONS

After the plating, the coated samples were rinsed with nitric acid solution (pH = 1), then with distilled water and acetone. The samples were allowed to dry in air thereafter before any characterization. A Nikon measuring microscope (Model MM-40) was used for imaging and dimensional measurements of the coated electrode. At least twelve test points were taken for each sample for determining the coating thickness and the average value was considered in this study. Using a scanning electron microscope (JEOL 840A), the morphology and the microstructure of the surface were examined. The attached Energy Dispersive Spectroscope (EDS) detector was used to determine the composition and uniformity of the coatings. The chemical analysis capability of EDS was adequate for determining the nickel and tungsten content in the coating. SPM analysis was conducted for determining the roughness value of the coated surface. An ex-situ atomic force microscopy (AFM, using Molecular Imaging model Pico SPMTM operated under contact mode) was used to analyze the surface roughness of the deposits at near-atomic resolution.

CHAPTER 4

COATING CHARACTERIZATION

4.1 INTRODUCTION

The reactions in an electrochemical process are very complex; more so when the process uses pulse current or voltage. The electrochemistry of the interactions between the electrodes and the electrolyte under different conditions has been studied extensively by researchers. In this study, plating experiments with continuous and pulse current were conducted to investigate the influence of various major potential parameters on the coating quality; mainly on coating thickness, uniformity and composition, grain size, and the surface roughness. Experimental results have been reported with regard to the effect of some predominant parameters such as current density, duty factor, pulse frequency, and the plating time on the process output in this chapter. Also presented here are the best parametric combinations for optimum process output characteristics.

4.2 PULSEPLATING PARAMETERS

The outcomes of pulseplating experiments reported by various researchers are very difficult to compare and as has been discussed, sometimes contradictory in nature. This is due to firstly, the complex nature of the electrodeposition process itself, secondly, large number of process variables involved, and lastly, absence of a standardized procedure in investigating the general effect of a particular pulseplating parameter [67]. In some cases the influences of duty cycle and pulse frequencies have been analyzed, where as pulse on-time and pulse off-time has been considered in many others. Similarly,

peak current densities and mean current densities (peak current density X duty factor) have been studied alternately by researchers.

In this work, the pulseplating parameters such as mean current densities, duty factors, and pulse frequencies have been altered to study their effects on the process outputs. Because the duty factor and the pulse frequencies are the extracted mathematical quantities from the original pulse parameters like pulse on-time and off-time and some argue that these extracted parameters do not clearly reflect the effects of the original parameters like pulse ontime and offtime, a conversion table is given below that shows the calculated pulse ontime and pulse offtime values for reference.

Table 4.1 Pulse ontime and pulse offtime values at different DF and PF

DUTY FACTOR (DF)	PULSE FREQUENCY (PF)		
	10 Hz	**50 Hz**	**100 Hz**
20%	20-80	4-16	2-8
50%	50-50	10-10	5-5
80%	80-20	16-4	8-2

The numbers show pulse on and off-time values in miliseconds

4.3 COATING THICKNESS AND DISTRIBUTION

Coating thickness distribution is a measurement of coating thickness at different locations across the sample cross-section. The samples were initially etched with hydrochloric acid and acetic acid mixture and then rinsed with water and the coating thickness was measured at various positions with an optical microscope (Nikon MM-40) located at Center of Nontraditional Manufacturing Research (CNMR), UNL. At least

twelve test points were taken for each sample for determining the coating thickness and the average value was considered in this study.

4.3.1 COATING THICKNESS IN DC PLATED SAMPLES

The thickness readings taken in case of continuous current plated samples are shown in Table 4.2 and the coating thickness changing trend observed in specimens is shown in Fig 4.1.

Table 4.2 Coating thickness in DC plated samples

PLATING TIME	MEAN CURRENT DENSITY		
	2.5 A/dm^2	**5 A/dm^2**	**10 A/dm^2**
5 minutes	2.6 microns	4.1	5.7
7 minutes	4.3	5.9	6.1
10 minutes	6.1	8.6	3.9

The thickness variation of nickel coating on tungsten substrate was analyzed as a function of the mean current density applied. The layer thickness showed an almost linearly increasing trend with plating time for current densities 2.5 and 5 A/dm^2 following Faraday's law. At low current density of 2.5 A/dm^2 and low plating time the thickness noticed was low, but at higher plating times the thickness improved (Fig. 4.2). The thickness was even higher when plating was conducted at 5 A/dm^2 with all three plating times and the coating appeared to be smooth and devoid of any major surface irregularities (Fig.4.3). Beyond that, with a further rise in current density, the rate of variation became very slow and as the curve tended to be flat and declining thereafter. A current density of 10 A/dm^2 at higher plating times neither produced higher thickness as

expected nor coatings of good quality. There were irregular localized deposition both on the sample walls and edges (Fig. 4.4). This could be attributed to the fact that the particular current density (10 A/dm^2) was beyond the limiting current density of the system that led to nodular deposits formed on the coating surface as shown in the SEM picture in Fig. 4.5. The best coating thickness achieved by the DC plating in this work was 8.6 microns and the corresponding parameter combinations were current density of 5 A/dm^2 and plating time of 10 minutes.

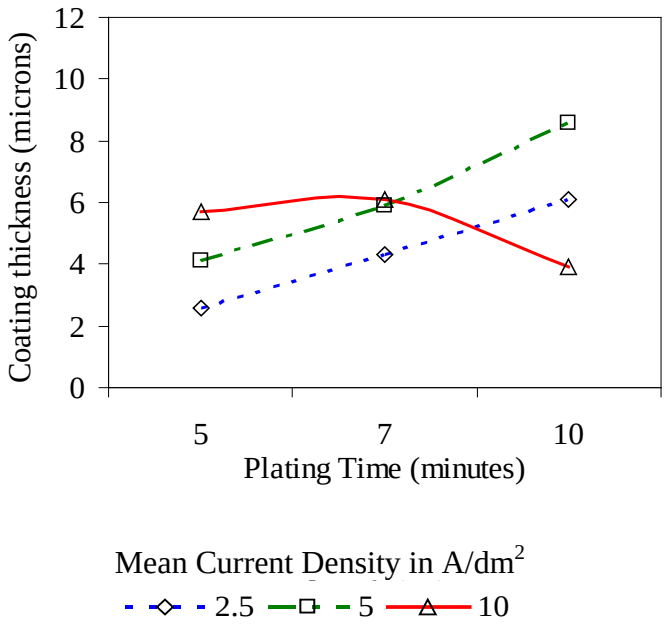

Fig. 4.1 Coating thickness variation in DC samples

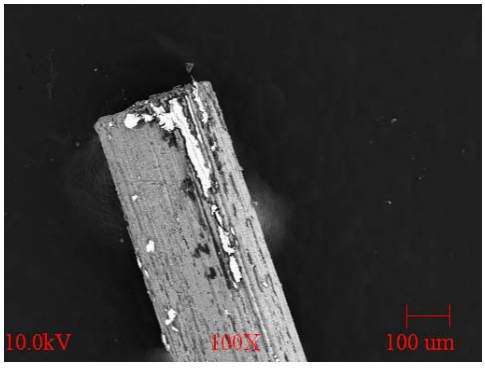

Fig. 4.2 DC plated sample at 2.5 A/dm^2 and 5 minutes

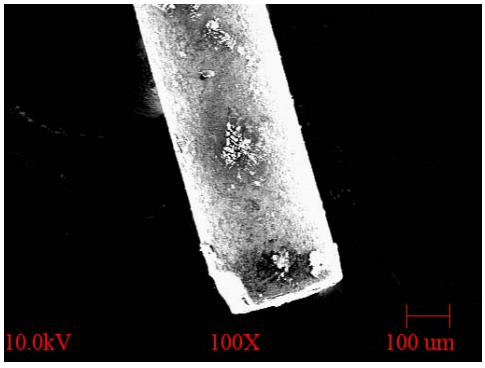

Fig. 4.3 Smooth coating at 5 A/dm^2 and 10 minutes

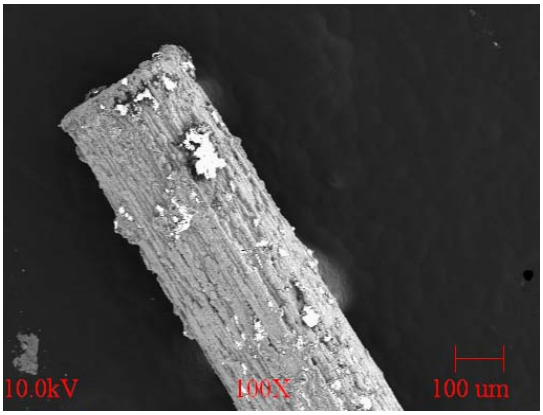

Fig. 4.4 Rough sample at 10 A/dm^2 DC plated for 5 minutes

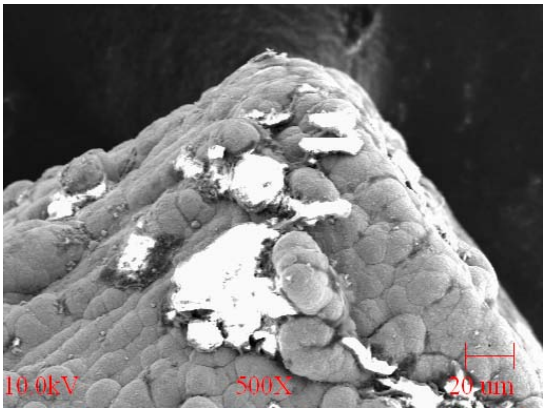

Fig. 4.5 Nodular deposits at 10 A/dm^2 and 10 minutes

4.3.2 COATING THICKNESS IN PULSEPLATED SAMPLES

In general, the pulseplated samples had higher coating thickness and the deposit surface appeared smooth even to the naked eye. Table 4.3 lists all the coating thickness readings and Fig. 4.6 (graphs) show the comparative coating thickness value achieved at different pulse parameter combinations. Coating thickness was noticed to be almost uniformly rising at a current density of 5 A/dm^2 at all combinations and showed a decreasing trend with a current density beyond that value. Coating thickness went on rising with increasing pulse on-time (high duty factor and high pulse frequency) at current density of 5 A/dm^2 (Fig. 4.6 a, b, and c). The coatings found to be smooth and uniform at almost all parameter combinations. See SEM image (fig. 4.7 a, b, and c).

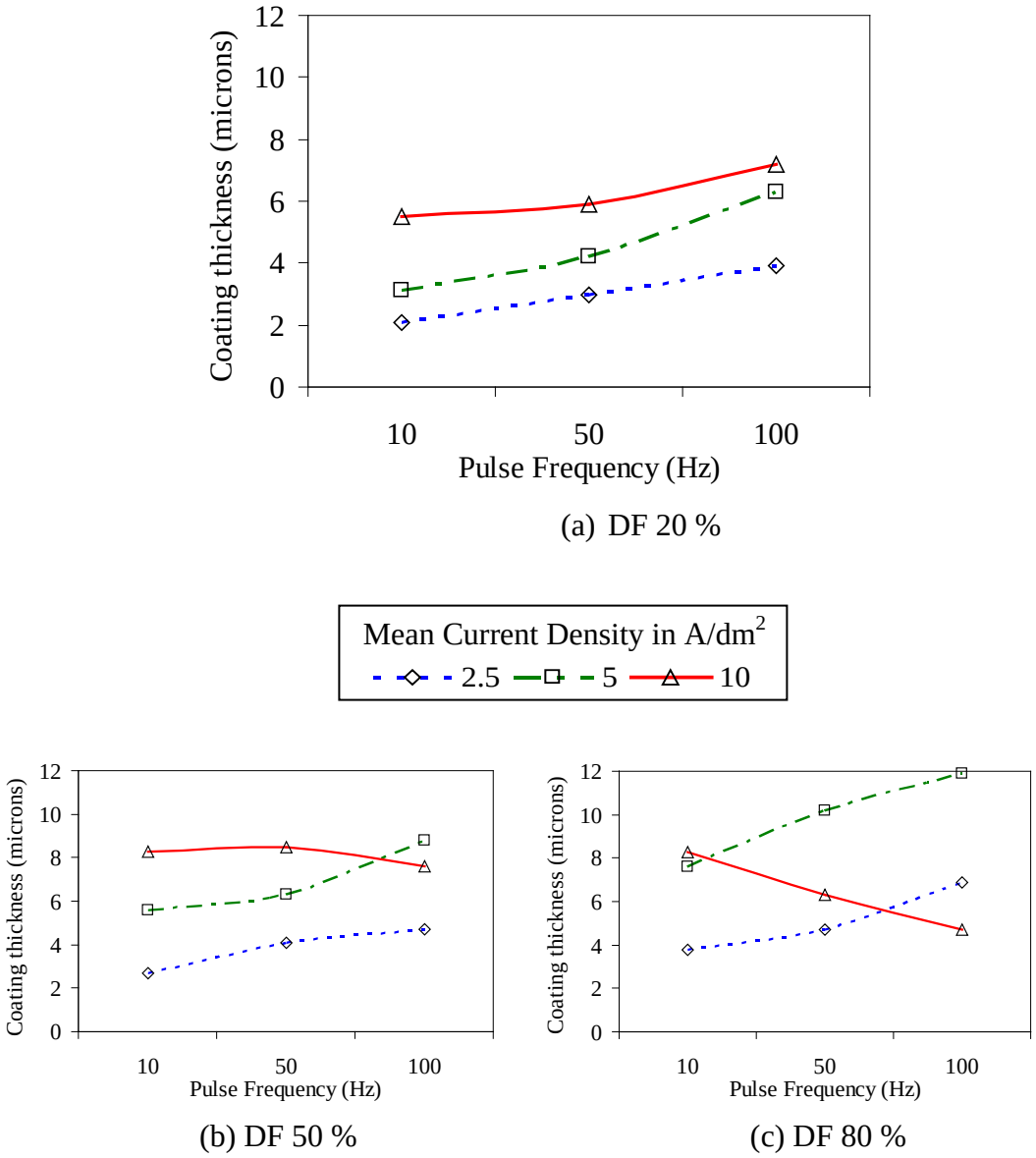

(a) DF 20 %

(b) DF 50 %

(c) DF 80 %

Fig. 4.6 Coating thickness variation in Pulseplated samples at different duty factors (a, b, & c)

Table 4.3 Coating thickness in pulse plated samples

DUTY FACTOR	PULSE FREQUENCY	MEAN CURRENT DENSITY		
		2.5 A/dm^2	**5 A/dm^2**	**10 A/dm^2**
20%	**10 Hz**	2.1 microns	3.1	5.5
	50 Hz	3	4.2	5.9
	100 Hz	3.9	6.3	7.2
50%	**10 Hz**	2.7	5.6	8.3
	50 Hz	4.1	6.3	8.5
	100 Hz	4.7	8.8	7.6
80%	**10 Hz**	3.8	7.6	8.3
	50 Hz	4.7	10.2	6.3
	100 Hz	6.9	11.9	4.7

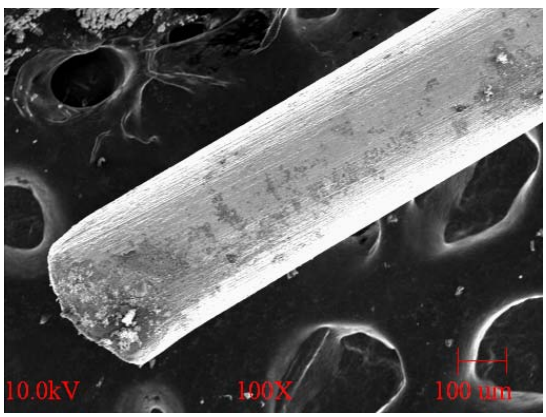

a) 5 A/dm^2, 20%, and 50 Hz

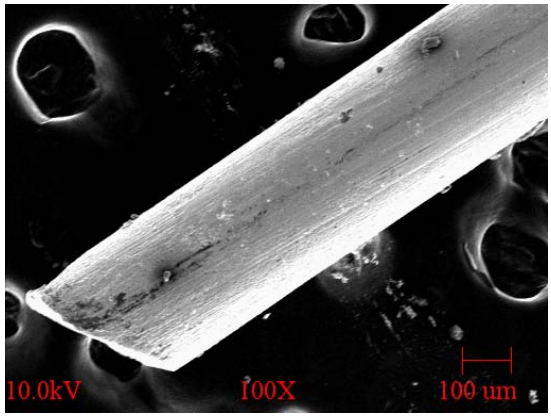

b) 5 A/dm^2, 50%, and 50 Hz

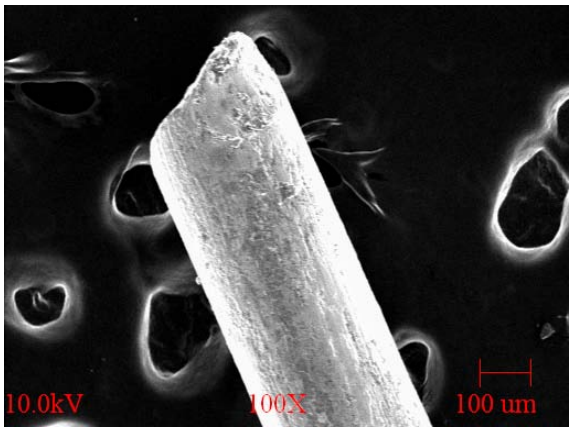

c) 5 A/dm^2, 80%, and 100 Hz

Fig. 4.7 (a, b, & c) Pulse plated samples at current density of 5 A/dm^2 and different duty factors and pulse frequencies respectively

Comparatively lower thickness was achieved at almost all duty factors and pulse frequencies with current density of 2.5 A/dm^2 (Fig 4.8 a, b, and c). This can be explained by the low current density itself. But the combination of duty factor 50% and a pulse frequency of 10Hz produced a smooth coating at this current density. There was no definite trend when samples were plated at current density of 10 A/dm^2. A reasonable coating thickness was obtained with lower pulse on-times (higher pulse frequencies of 100 Hz) but at almost other combinations the thickness tended to reduce. Current density

of 10 A/dm^2 with higher pulse on-time (duty factor 50%, frequency 50 Hz) resulted in burnt coating (Fig. 4.9). That was indicative of the fact that the system had reached a limiting current density and thus led to a reduction in deposition thickness. The coating thickness was not so uniform in some of the pulse plated samples with high coating thicknesses at the edges and the corners (Fig. 4.10). Thickness was low on the sample walls. This result was expected as the current density in the thicker deposition areas would be higher and led to higher thickness than those on the walls.

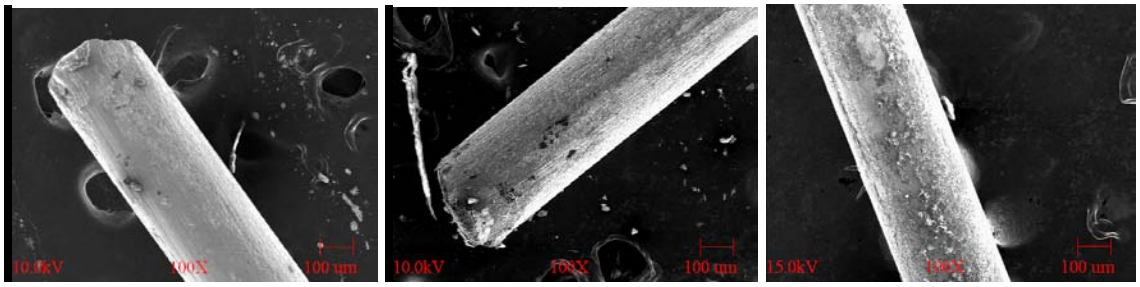

(a) DF - 50%, PF-10 Hz (b) DF - 50%, PF-50 Hz (c) DF - 50%, PF-100 Hz

Fig. 4.8 Samples plated at 2.5 A/dm^2 and at different pulse on-times

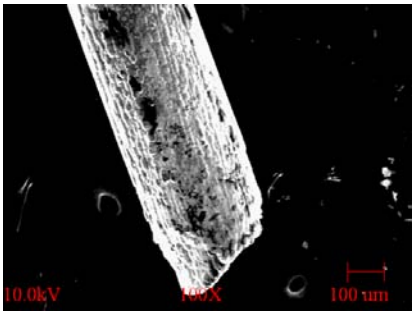

Fig. 4.9 Rough and burnt deposit at 10 A/dm^2, 50 %, and 50 Hz

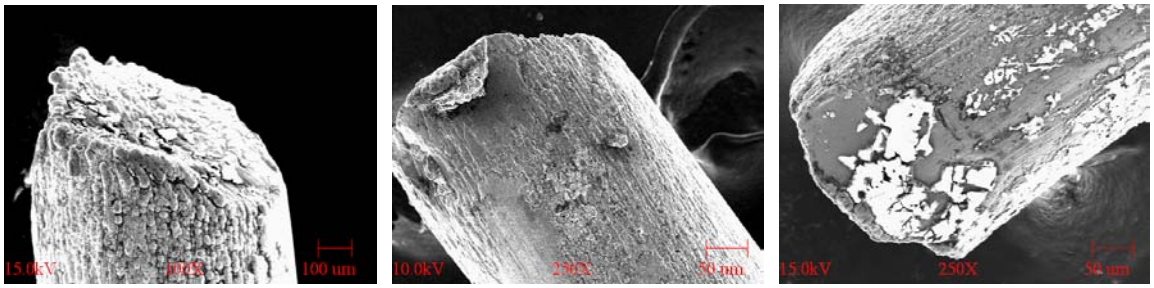

Fig. 4.10 Non uniform coating in some samples

A thickest coating of about 12 microns was obtained at a mean current density of 5 A/dm^2, duty factor 80% and pulse frequency of 100 Hz.

4.4 SURFACE ROUGHNESS OF DEPOSIT

In electrochemical machining the material removal is by anodic dissolution and a certain desired shape is imparted to the workpiece via the shaped tool. Since the machined surface is very nearly the negative mirror image of the tool involved, producing a low roughness surface starts from using a tool that has low surface roughness. So it is imperative to determine the roughness of the surface of the coated tool before considering its subsequent use in electrochemical machining.

The roughness measurement of the plated samples was carried out with DI Nanoscope IIIa Dimension 3100 SPM system in the Nebraska Center for Materials and Nanoscience (NCMN). The Digital Instruments Nanoscope IIIa Dimension 3100 SPM system is a multifunction scanning probe microscope for materials imaging and characterization. The DI 3100 SPM utilizes atomic force microscopy (AFM), magnetic force microscopy (MFM), lateral force microscopy (LFM), and scanning tunneling microscopy (STM) with the scanning tunneling spectroscopy (STS) techniques to measure surface characteristics for a large variety of materials, such as nanoparticles,

polymers, DNA, semiconductor thin films, magnetic media, optics and other advanced nanostructures. For this work, the AFM unit of the SPM system was used. The other specific settings for measurements are given in the table below.

Table 4.4 AFM settings

Probe	Silicon
Mode	Tapping
Scan Rate	1 Hz
Scan Size	400 μm^2

4.4.1 SURFACE ROUGHNESS IN DC PLATING

Fig 4.11shows the surface roughness value of the plated samples with continuous current (DC) as function of mean current density and plating time and the roughness measurement readings in nanometers of the deposit surface is listed in Table 4.5. The lowest roughness achieved in DC plated samples was about 41 nm and the maximum was 110 nm. The variation in roughness readings when the mean current density was 2.5 A/dm^2 was in the range of 14 nm; the deviation in observations was small. The best roughness in this set of readings was 71 nm. This indicated that perhaps the roughness of the coated surface did not depend significantly on the plating time at this current density. It showed a somewhat rising trend with an increase in plating time and quality of surface improved slightly as plating progressed. But the surface showed some cracks and cavities (Fig. 4.12). The AFM statistics and images are shown in Fig. 4.13 (a) and (b).

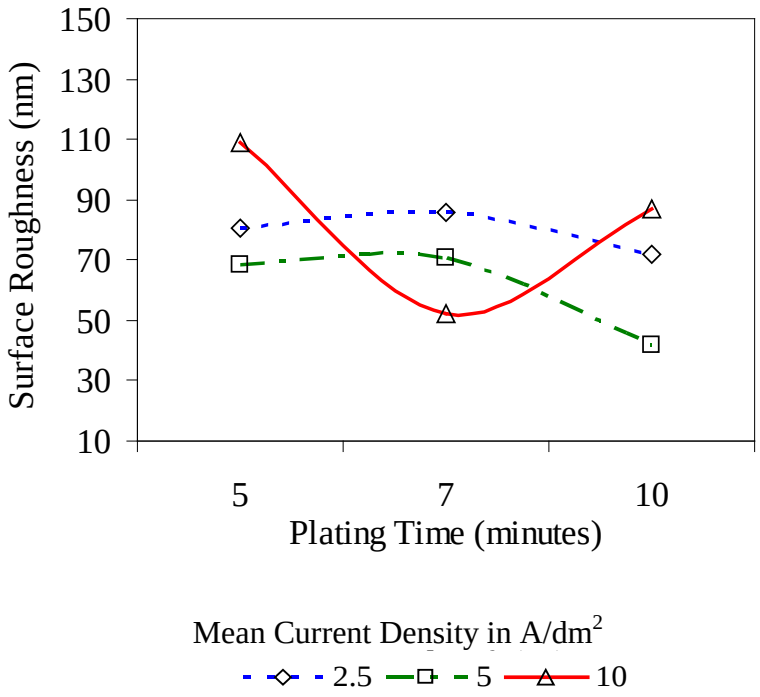

Fig. 4.11 Variations of surface roughness with DC plating parameters

Table 4.5 Surface roughness results for continuous current (DC) plating experiments

PLATING TIME	MEAN CURRENT DENSITY		
	2.5 A/dm^2	**5 A/dm^2**	**10 A/dm^2**
5 minutes	80.753 nm	68.717 nm	109.130 nm
7 minutes	85.676 nm	70.630 nm	52.066 nm
10 minutes	71.941 nm	41.603 nm	87.142 nm

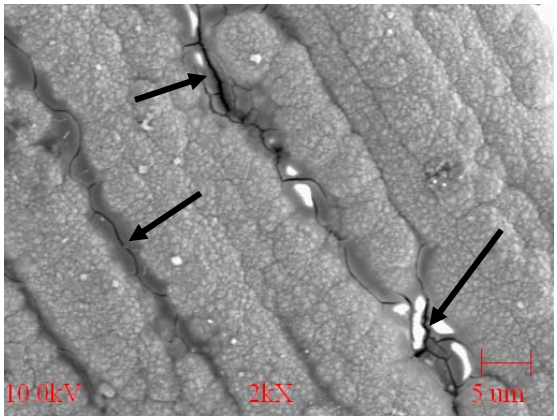

Fig. 4.12 Cracks on the sample surface at 2.5 A/dm^2 and 10 minutes

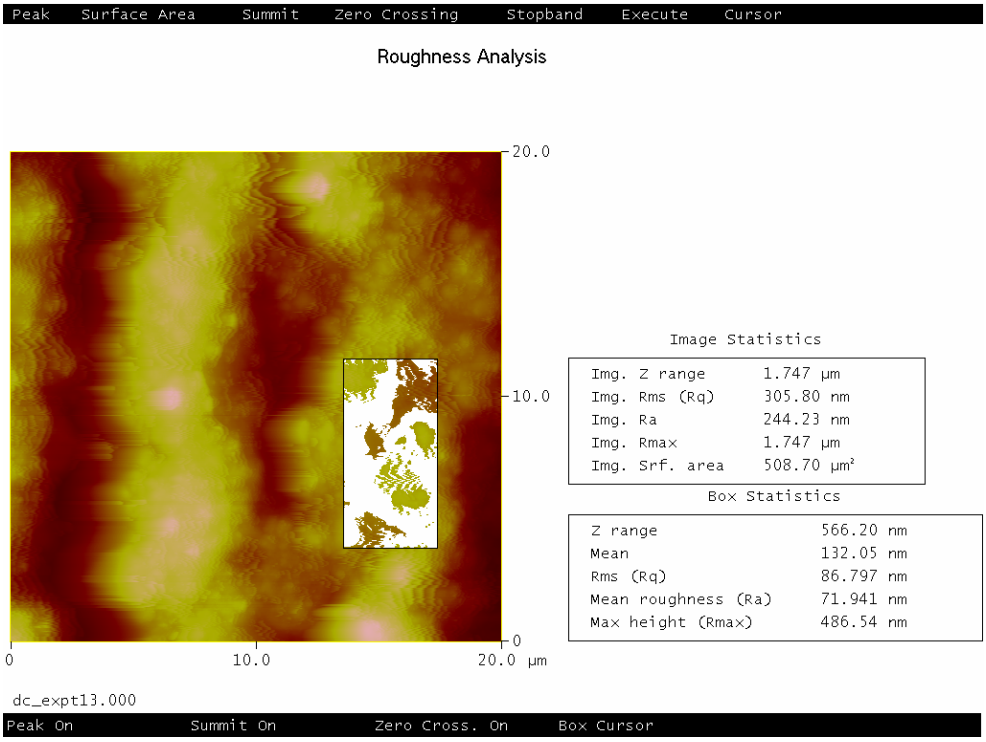

Fig. 4.13 (a) AFM statistics of the sample surface at 2.5 A/dm^2 and 10 minutes

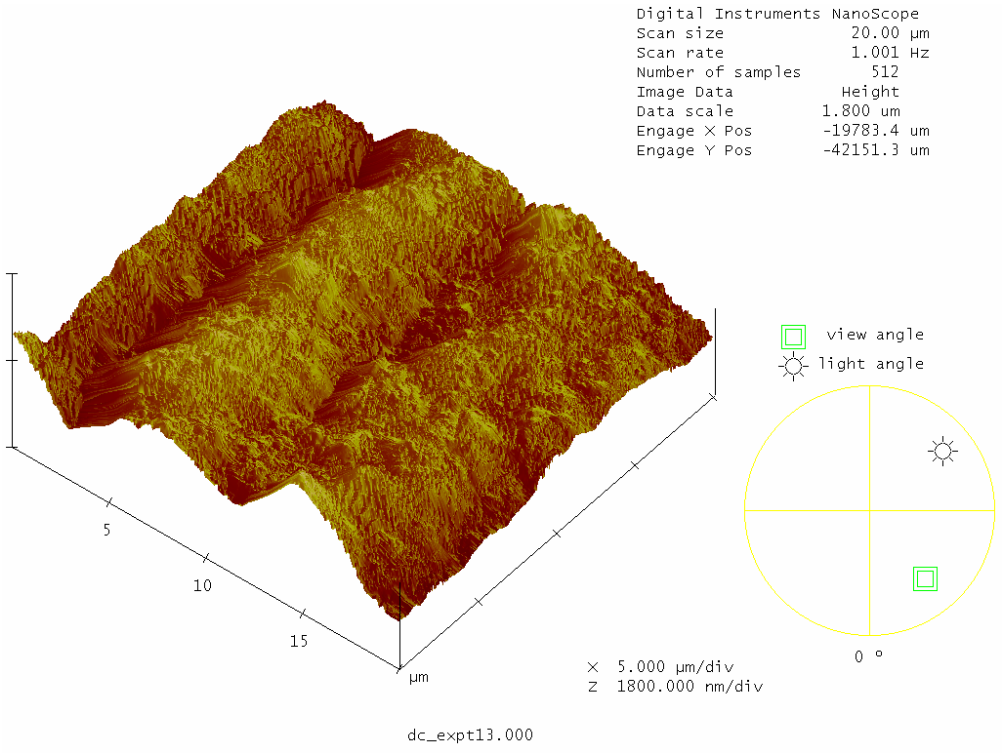

Fig. 4.13 (b) AFM images of the sample surface at 2.5 A/dm^2 and 10 minutes

The surface produced at a current density of 5 A/dm^2 was relatively smooth and it gradually improved in terms of roughness as plating time increased. Fig. 4.14 below shows SEM image of two samples at current density of 5 A/dm^2.The lowest roughness found here was 41 nm which in fact was the best result achieved in the entire set of DC plated samples.

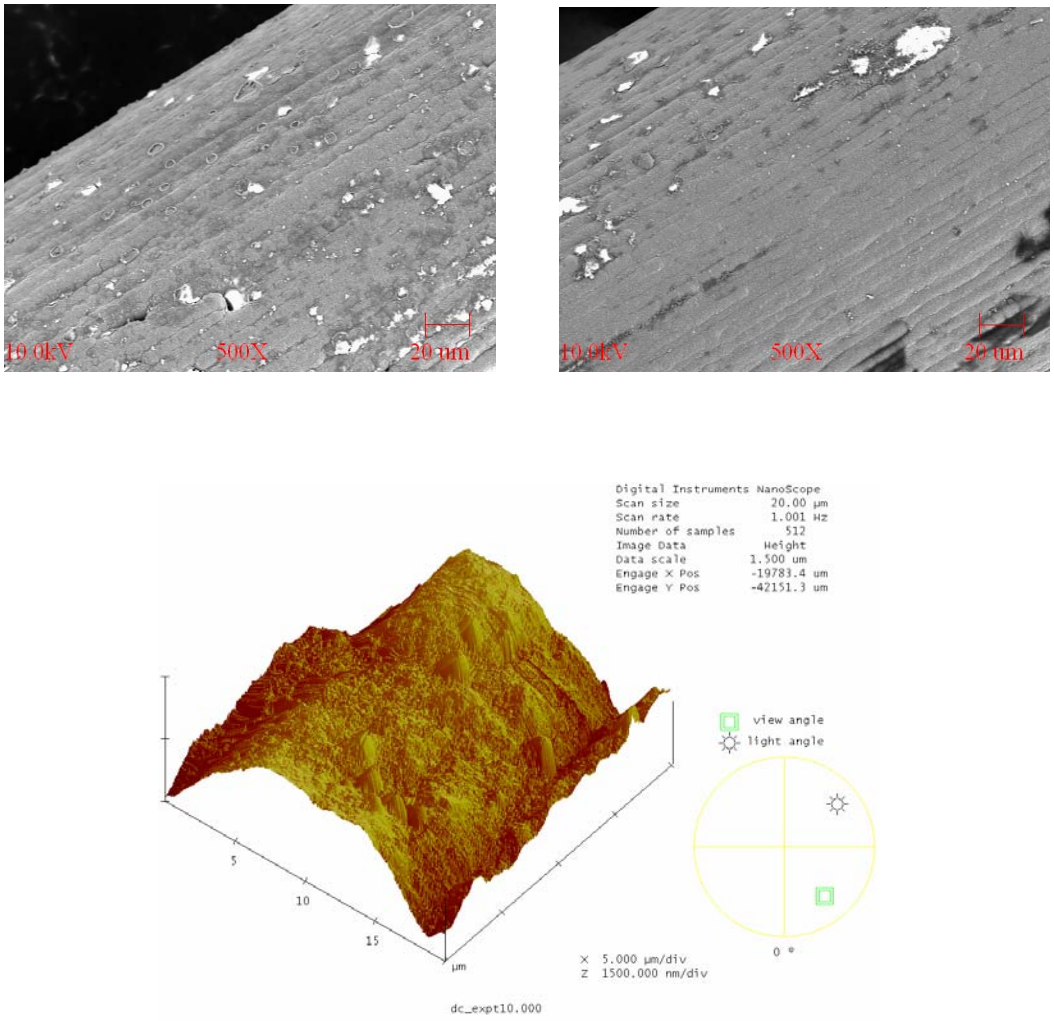

Fig. 4.14 DC plated sample at 5 A/dm^2 for 5 minutes (top left) and 10 minutes (top right) (Below) AFM image corresponding to top right SEM image

The trend noticed in case of the samples plated at current density of 10 A/dm^2 was erratic. The roughest coating was observed during this period at a plating time of 5 minutes and when the sample was plated for 10 minutes. However, a roughness of 52 nm was achieved in 5 minute plated sample. The lowest set of readings in terms of surface roughness was noted with a current density of 5 A/dm^2. The lowest reading was 41 nm and the variation range was about 27 nm with very little change in roughness between the samples plated for 5 and 7 minutes. The observations indicate that the other two mean

current densities used in the experiments were more toward limiting values. The combination of a current density of 5 A/dm^2 and a plating time of 10 minutes brought the lowest roughness result of 41 nm.

4.4.2 SURFACE ROUGHNESS IN PULSEPLATED SAMPLES

The surface roughness readings in nanometers in the tested pulseplated samples are listed in Table 4.6 and the variations of surface roughness with the pulse parameters are shown in Fig 4.14 a, b, and c.

Table 4.6 Surface roughness results for pulseplating experiments

DUTY FACTOR	PULSE FREQUENCY	MEAN CURRENT DENSITY		
		2.5 A/dm^2	**5 A/dm^2**	**10 A/dm^2**
20%	**10 Hz**	50.757 nm	39.787 nm	94.510 nm
	50 Hz	38.188 nm	36.257 nm	51.853 nm
	100 Hz	128.72 nm	34.999 nm	49.389 nm
50%	**10 Hz**	76.312 nm	38.172 nm	55.328 nm
	50 Hz	57.007 nm	43.272 nm	62.356 nm
	100 Hz	115.87 nm	33.408 nm	41.338 nm
80%	**10 Hz**	36.582 nm	24.355 nm	13.142 nm
	50 Hz	77.879 nm	110.80 nm	44.581 nm
	100 Hz	82.216 nm	36.686 nm	57.861 nm

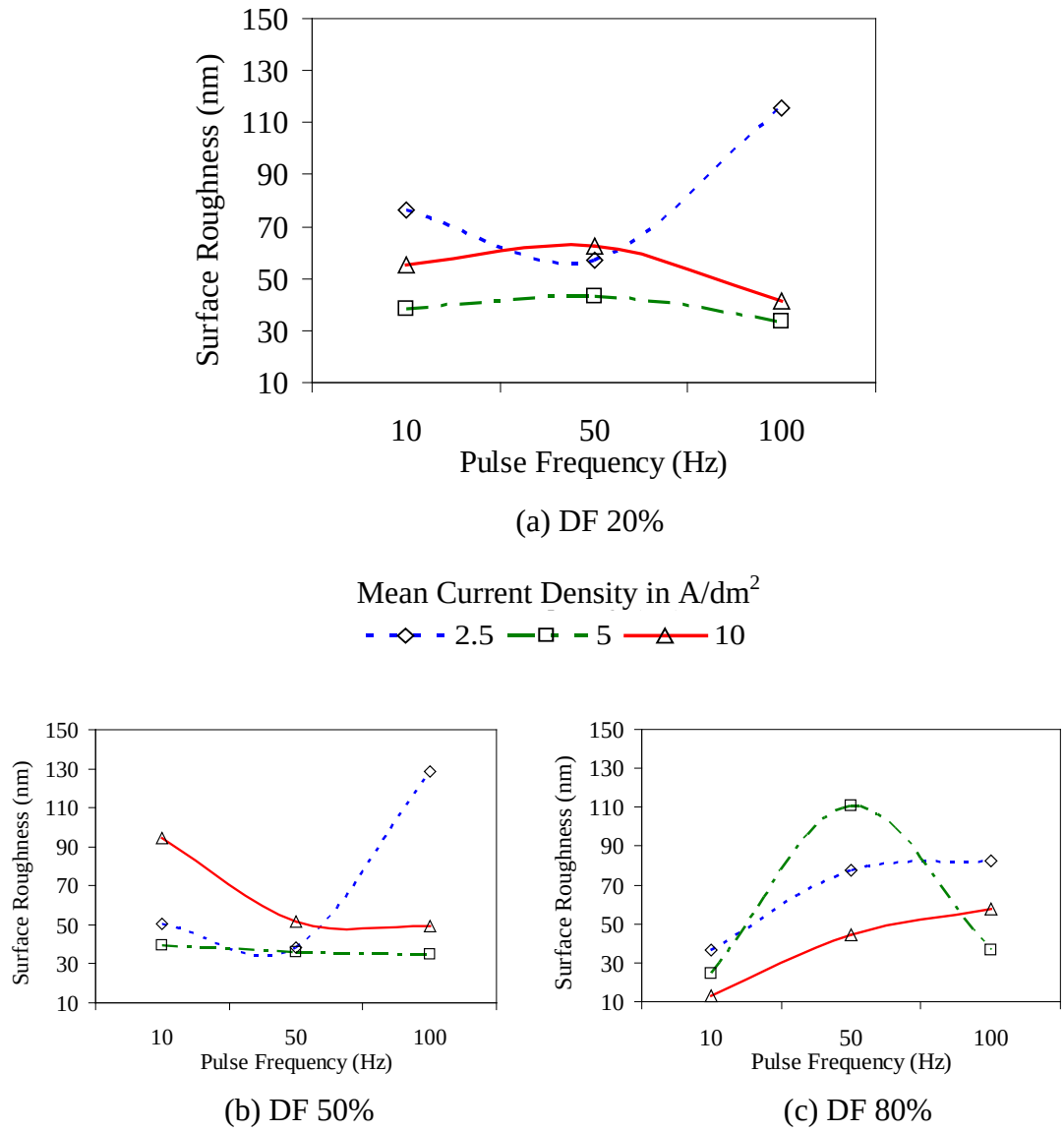

Fig. 4.14 Variation of deposit roughness with current densities and pulse frequencies at different duty factors a, b, & c

From the Fig. 4.14 it is evident that at the shortest pulse on-time (20% DF and PF 100 Hz), the best roughness value was in the range of 35 nm at a current density of 5 A/dm^2. The coating surface was smooth with no visible pores or pits. Increasing pulse on-time led to formation of a number of pits and got even bigger on the deposits with higher pulse on-time (Fig.4.15 a, b, & c). This could be due to the attached hydrogen gas

bubbles to the cathode surface for a longer period at higher on-times [68]. For nickel pulse electrodeposition, increasing densities of hydrogen gas bubbles at the cathode surface at longer on-times resulted from a more negative overpotential [69].

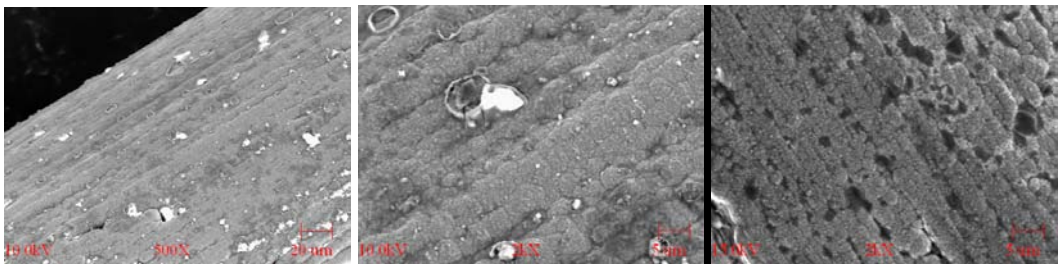

(a) (b) (c)

Fig. 4.15 a, b, & c
Hydrogen cavities on coating surface with increasing pulse on-times

Fig. 4.15 (d) showed the typical surface morphology of the coating surface at current density of 5 A/dm^2, DF 80%, and PF 10 Hz. This parameter combination is very close to the DC plating condition at 5 A/dm^2 and 5 minutes plating time. It can be seen that the deposited surface in case of pulseplating was very compact and virtually with no colony structures and differs completely from the ‘‘cauliflower-like’’ surface morphology of the DC plated one (Fig. 4.15 c).

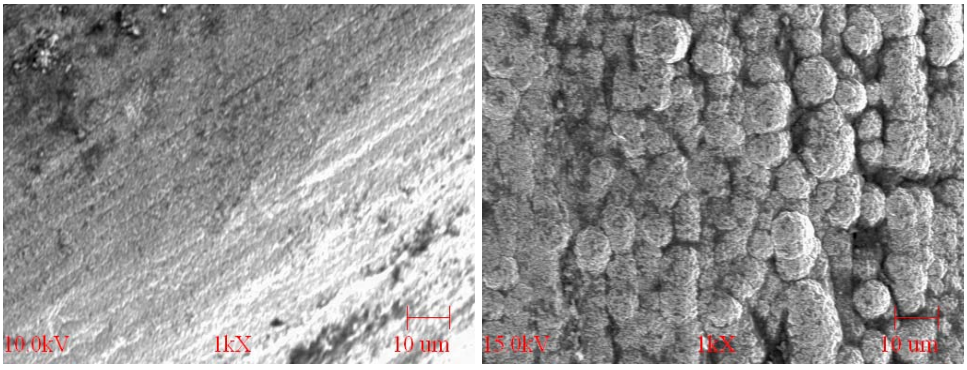

Fig. 4.15 (d) Coated surface of pulseplated (left) and DC plated specimen (right) at comparable plating conditions

The acid pickle pretreatment prior to electrodeposition etches the surface layer of the tungsten substrate and provides surface pits to act as sites for mechanical interlocking to improve adhesion. That can be seen in Fig. 4.15 (e).

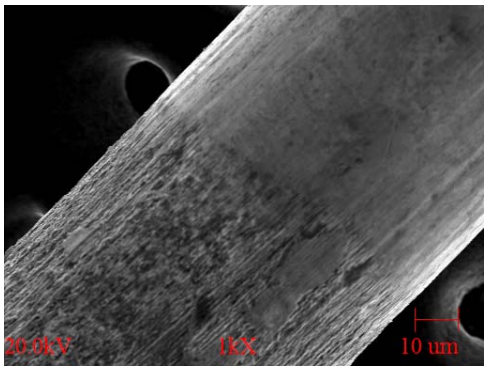

Fig. 4.15 (e) Etched surface (rough) and the electroplated surface (smooth)

Considering the findings in these experiments, the best parametric combinations were a short on time (PF 100 Hz at almost all DFs) and a current density of 5 A/dm^2. Comparing the coating achieved under this condition with that of a DC plated one, it was noticed that the pulseplated sample has lower roughness than its DC counterpart and grain size was also finer in the pulseplated one. Therefore the surface morphology of the coated samples is superior when coated with pulseplating.

4.5 COMPOSITION OF COATING

The desired properties in the coatings were the absence of macrostructural defects such as pores, dendrite formation, and localized deposition. Another important requirement was the stability of the coating composition under corrosive environments. A surface with few or no pores is considered to pose most resistance to the external corrosive environment. The samples were tested for the coating composition in terms of the atomic weight percentage of the material deposited. Since in this case pure nickel was

tried to be coated on the tungsten substrate, a 100% nickel deposition is the most desired outcome. The relative concentrations of different materials in the deposit were determined by Energy Dispersive Spectroscopy (EDS).

Energy Dispersive Spectroscopy is a technique based on the characteristic X-ray peaks that are generated when an energetic electron beam interacts with the specimen. Each element produces characteristic x-rays that may be used to identify the presence of that element in the region being examined. Comparison of the relative intensities of x-ray peaks may be used to determine the relative concentrations of each element in the specimen. Elements with an atomic number less than that of carbon are not generally detectable. The EDS equipment used for this study is attached to the JEOL 840A Scanning Electron Microscope (SEM) that belonged to the Nebraska Center for Materials and Nanoscience (NCMN), UNL. The specific settings for the equipment were KV: 20.0, Takeoff Angle: 13.2°, and the Elapsed Live-time: 100.0.

The relative composition of the plating deposits are tabulated in Tables 4.7 and 4.8 for continuous and pulse current coated samples respectively. A very high weight percentage of the material percentage would indicate a larger coverage area of that particular material. In this case, 100% nickel atomic weight percentage is most desirable in the deposit. The trends of variation of the composition concentrations are shown in Fig. 4.16. In the DC plated samples the best coating compositions (100% Ni) were achieved with current densities 5 A/dm^2 when the plating was done for 5 minutes and also for 10 minutes. Deposit concentrations were lower with the other current densities and the plating time combinations. With the reasonable high atomic weight percentage of tungsten (W) showing on the EDS result, the substrate appears to be not adequately

coated by the nickel layer and is an indication that the coating contains pores and not suitable for further applications (Fig. 4.17 a and b).

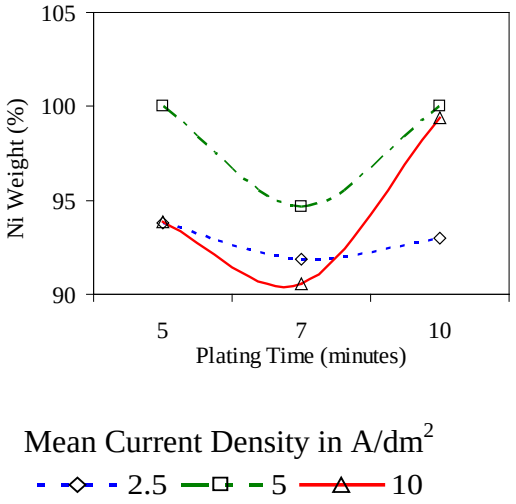

Fig. 4.16 Coating composition at different DC plating conditions

Table 4.7 Percentage of Ni deposits in DC plated samples

PLATING TIME	MEAN CURRENT DENSITY		
	2.5 A/dm^2	**5 A/dm^2**	**10 A/dm^2**
5 minutes	Ni (93.787) W (1.197)	Ni (100.000) W (0.000)	Ni (93.887) W (0.773)
7 minutes	Ni (91.876) W (0.994)	Ni (94.682) W (1.397)	Ni (90.581) W (0.810)
10 minutes	Ni (93.011) W (1.042)	Ni (100.000) W (0.000)	Ni (99.397) W (0.603)

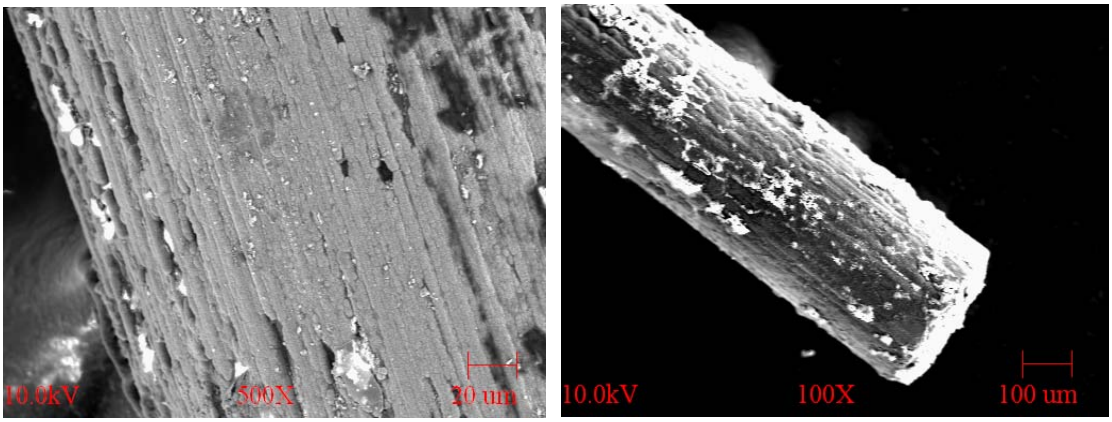

a) 2.5 A/dm^2 and 5 minutes b) 10 A/dm^2 and 7 minutes

Fig. 4.17 Non uniform coating on some DC plated specimen

The effect of pulse parameters such as mean current density, duty factor, and pulse frequency on the amount of nickel deposited in atomic weight percentage is shown in Fig. 4.18. An increase in current density and duty factor led to a rise in amount of nickel deposit, where as percentage of nickel deposition reduced with an increase in pulse frequency. Any change in pulse frequency did not have a great effect on deposit concentration of nickel when the current density was 5 A/dm^2. A desired concentration of nickel in the coating (100%) was noticed at various parameter combinations and in general, pulse plated samples showed very high percentage of nickel deposit compared to the DC plated ones. A sample EDS micrograph is shown in Fig. 4.19. However, it was very difficult to pin point one particular parameter combination for achieving the best coating composition.

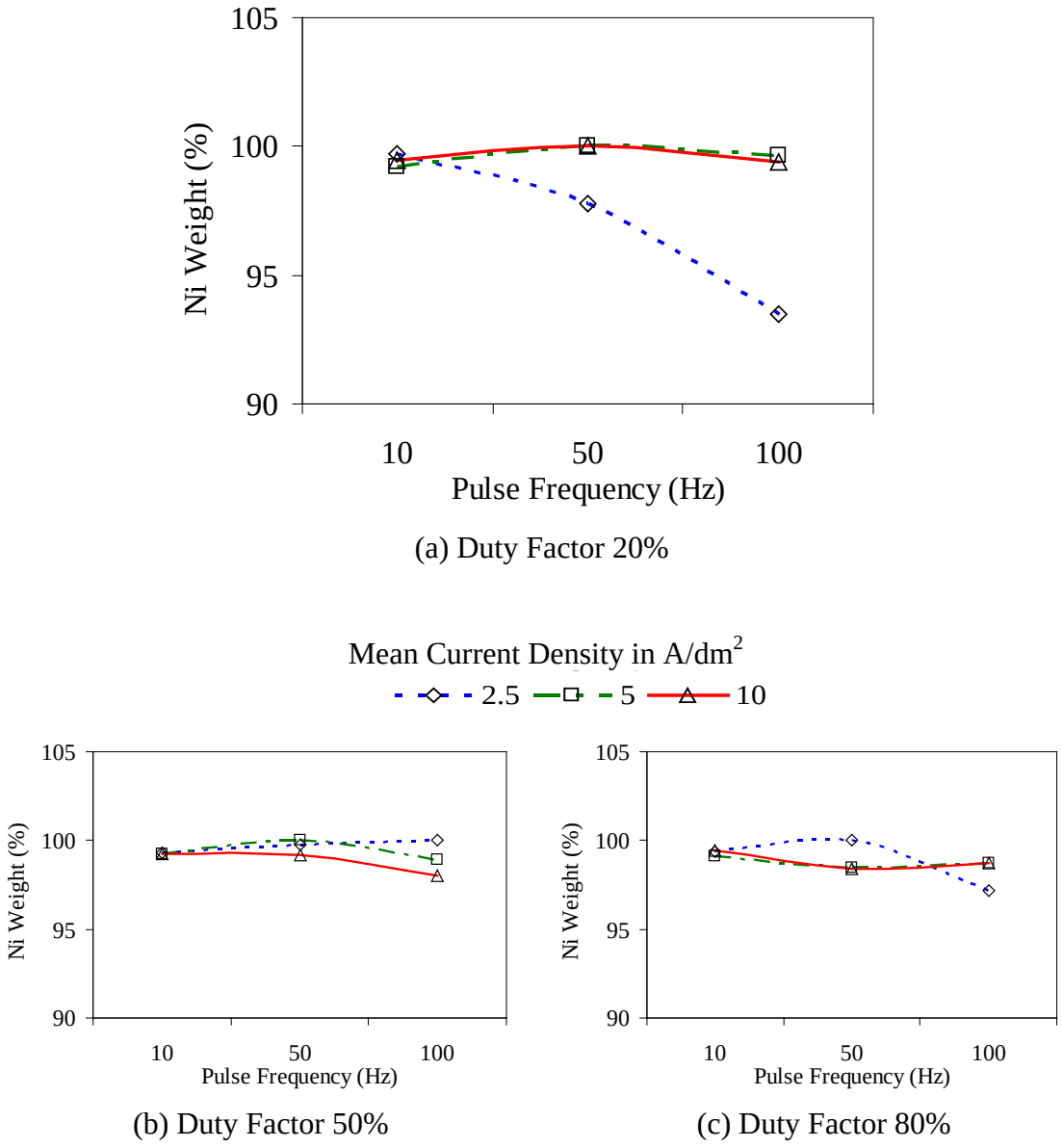

(a) Duty Factor 20%

(b) Duty Factor 50%

(c) Duty Factor 80%

Fig. 4.18 Coating composition at different pulse parameter combinations

Table 4.8 Percentage of nickel (Ni) and tungsten (W) deposits in pulseplated samples

DUTY FACTOR	PULSE FREQUENCY	MEAN CURRENT DENSITY		
		2.5 A/dm^2	**5 A/dm^2**	**10 A/dm^2**
20%	**10 Hz**	Ni (99.735) W (0.265)	Ni (99.209) W (0.791)	Ni (99.465) W (0.535)
	50 Hz	Ni (97.791) W (2.209)	Ni (100.00) W (0.000)	Ni (100.000) W (0.000)
	100 Hz	Ni (93.496) W (6.504)	Ni (99.651) W (0.349)	Ni (99.398) W (0.602)
50%	**10 Hz**	Ni (99.297) W (0.703)	Ni (99.229) W (0.771)	Ni (99.232) W (0.768)
	50 Hz	Ni (99.744) W (0.256)	Ni (100.00) W (0.000)	Ni (99.152) W (0.848)
	100 Hz	Ni (100.00) W (0.000)	Ni (98.915) W (1.085)	Ni (98.049) W (1.951)
80%	**10 Hz**	Ni (99.381) W (0.619)	Ni (99.103) W (0.897)	Ni (99.427) W (0.573)
	50 Hz	Ni (100.000) W (0.000)	Ni (98.470) W (1.530)	Ni (98.434) W (1.866)
	100 Hz	Ni (97.201) W (2.799)	Ni (98.710) W (1.290)	Ni (98.748) W (1.252)

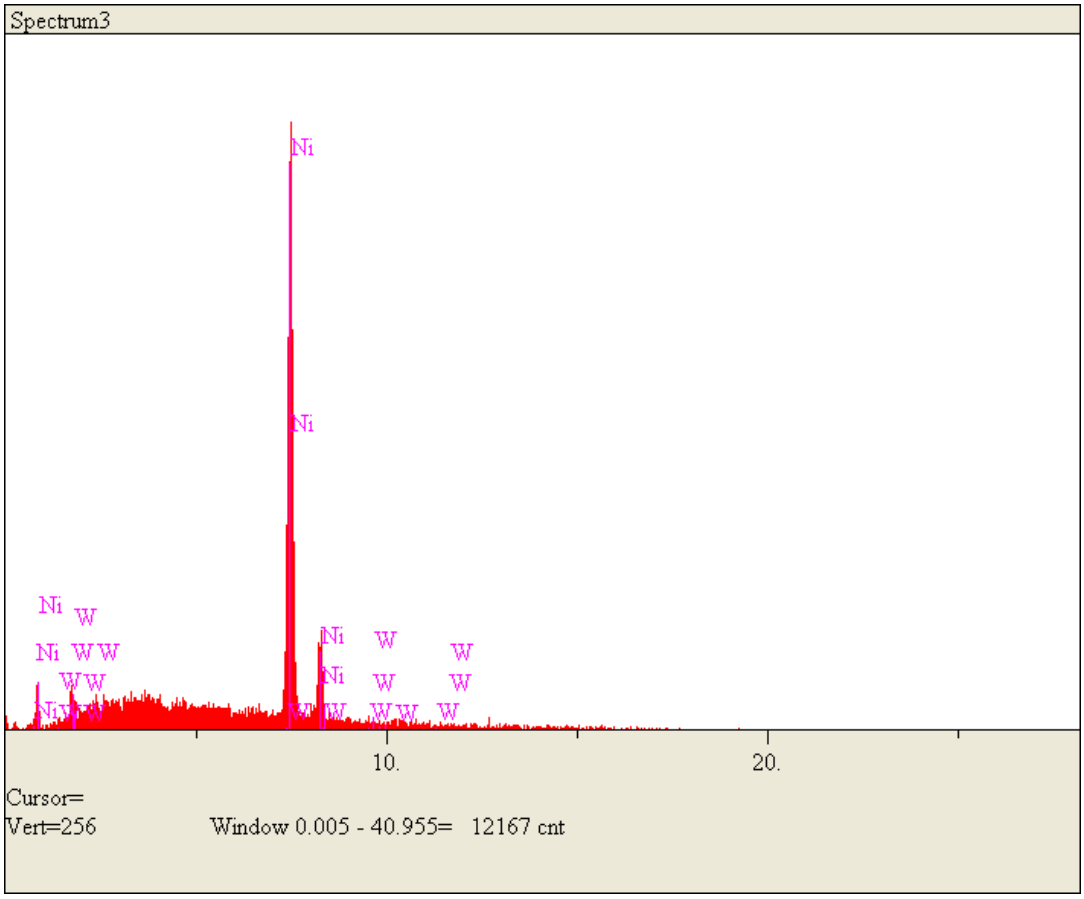

Elt.	Line	Intensity (c/s)	Error 2-sig	Atomic Wt %	Conc	Units	Z	A	F	
Ni	Ka	34.40	1.173	100.000	100.0	wt.%	1.0000	1.000	1.00	
W	La	0.00	0.000	0.000	0.000	wt.%	0.7312	0.8543	1.0	
				100.00	100.0	wt.%				Total

Fig. 4.19 EDS micrograph for pulseplated sample at 5 A/dm^2, 50%, and 50 Hz

4.6 GRAIN SIZE OF DEPOSITS

Certain properties of electrodeposits such as hardness, wear and corrosion resistance, and electrical resistivity are strongly affected by grain size. Properties such as thermal expansion, Young's modulus, and saturation magnetization show little grain size dependence. Normally, the electrodeposits have columnar grains, whose diameters increase with the deposit thickness [70]. In order to obtain equiaxed nanocrystals,

continuous nucleation of new grains should occur during the deposition. Many studies on these properties of the nanaocrystalline electrodeposits have been conducted in the recent past with contradicting or different observations. It was reported [71] that the grain size of nickel deposits reduced from 50 nm to about 20 nm by raising the current density from 50 to 100 mA/cm^2 and the effect of current density above 100 mA/cm^2 could be ignored. Contrary to these findings, a continuous rise in current density was found to have resulted in a steadily increasing grain size in direct current nickel electrodeposition [72, 73]. Also some researchers reported that the current density had no significant effect on grain size of nickel electrodeposits [74]. How grain size was affected by the change in current density in both DC and pulseplating of nickel on tungsten substrate was studied in the thesis.

4.6.1 EFFECT OF CURRENT DENSITY ON GRAIN SIZE IN DC PLATING

The grain size decreases with a rise in mean current density up to 5 A/dm^2as shown in the Fig. 4.20, and beyond that point, raising current density did not bring about further reduction in grain size but led to an increased deposit grain size. This observation is in agreement with the data found in the literature [71, 75]. Size of grain in the deposits decreases in general with a rise the current density, because a higher current density leads to a higher overpotential that increases the nucleation rate [43, 76]. Researchers have attributed this phenomenon to a decrease in concentration of Ni ions [77] and/or the codeposition of hydrogen at cathode-electrolyte interface [72]. The grain size of the nickel deposits did not substantially vary with current densities at plating time of 10 minutes. This could be due to co-deposition of hydrogen at cathode surface. The co-

deposition of hydrogen changes the surface energy [78] and the growth mechanism and also the distribution of applied currents between the reduction of Ni^{2+} and H^{+} ions [79]. During the reduction, pure current density available for nickel deposition did not increase considerably in spite of a rise in applied current density.

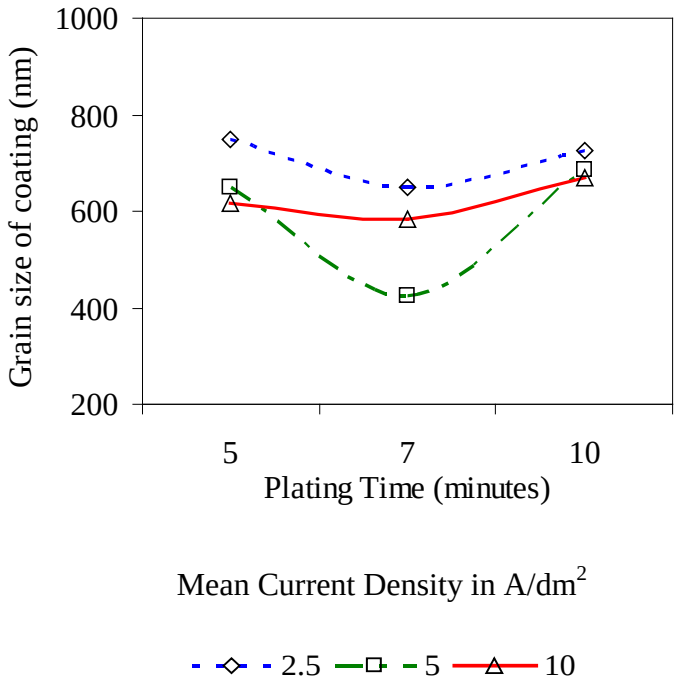

Fig. 4.20 Effect of mean current density on grain size of DC plated samples

The optimized condition in the experimentation for producing a nickel coating with lowest size grain by DC plating was a current density of 5 A/dm^2 and a plating time of 7 minutes. The SEM picture of the coated sample under the suggested optimum conditions is shown in the Fig. 4.21. The surface roughness analysis by AFM is also presented for reference.

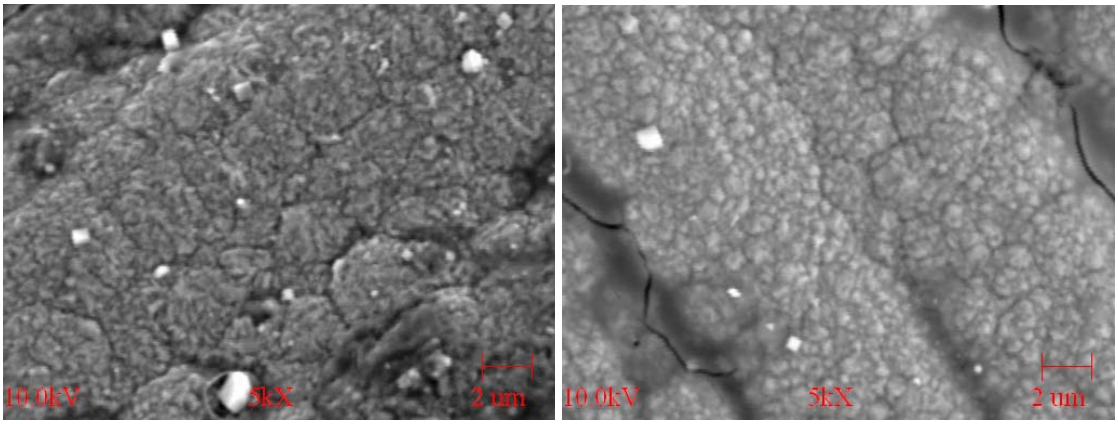

(a)

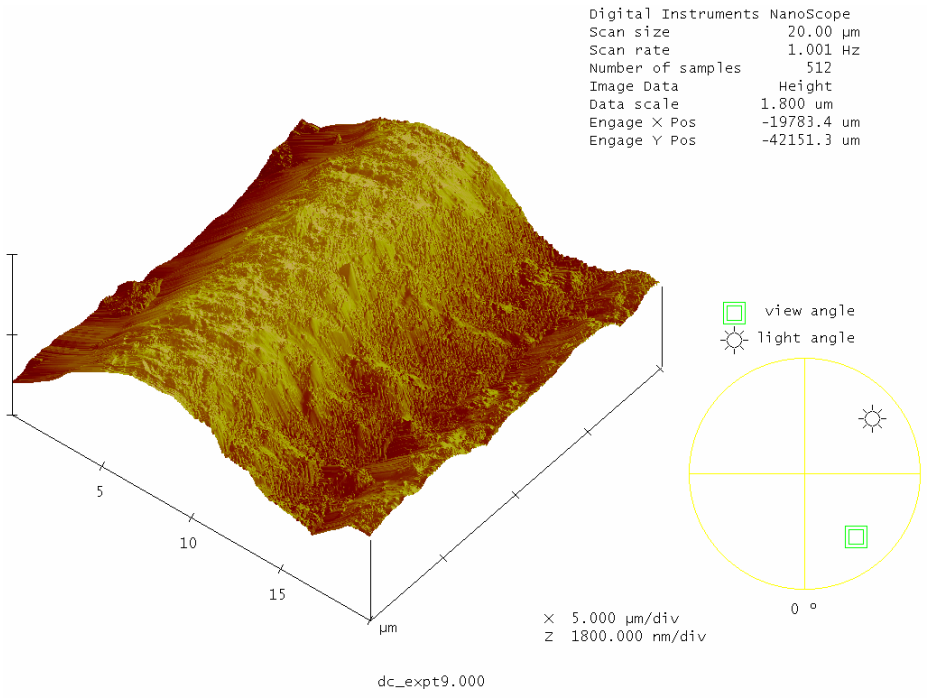

(b)

Fig. 4.21 (a) SEM picture and (b) AFM micrograph of DC plated sample at 5 A/dm^2 and 7 minutes

4.6.2 GRAIN SIZE IN PULSEPLATING

Pulseplating influences the composition of the nickel/electrolyte interface due to the imposed perturbation of the adsorption–desorption phenomena occurring at the interface [80]. Even small changes in the pulse parameters such as pulse on and off-time, and applied current density could result in dull deposits and bigger grain size. Again, the desorption of chemical species such as atomic hydrogen and nickel hydroxide that take place at medium alterations of pulse current could lead to large crystallites with a small number of crystalline defects. With increasing pulse on-time at constant duty cycle and peak current density, a reduction in grain size has been noticed by researchers [81]. Reduced grain size was attributed to an increased nucleation rate resulting from higher overpotential. An increase in overpotential has also been reported with increasing pulse duty cycle value during electrodeposition of palladium [82].

In this work, the grain size studies were carried out with an AFM by a DI Nanoscope IIIa Dimension 3100 scanning probe microscope at atmospheric pressure and room temperature in a contact mode. A Si_3N_4 cantilever with the force constant of 0.032 N m^{-1} was used and the obtained resolution of the images was 300 × 300 pixels. The grain size dimensions of the electrodeposited coatings were determined by means of SPM Lab software and from profile line analysis. The grain size study was also conducted from the SEM electron probe microanalysis with SEM JEOL 840A. The variation of grain size is shown in Fig 4.22 as a function of mean current density at different pulse on and off-times (various duty factors and pulse frequencies).

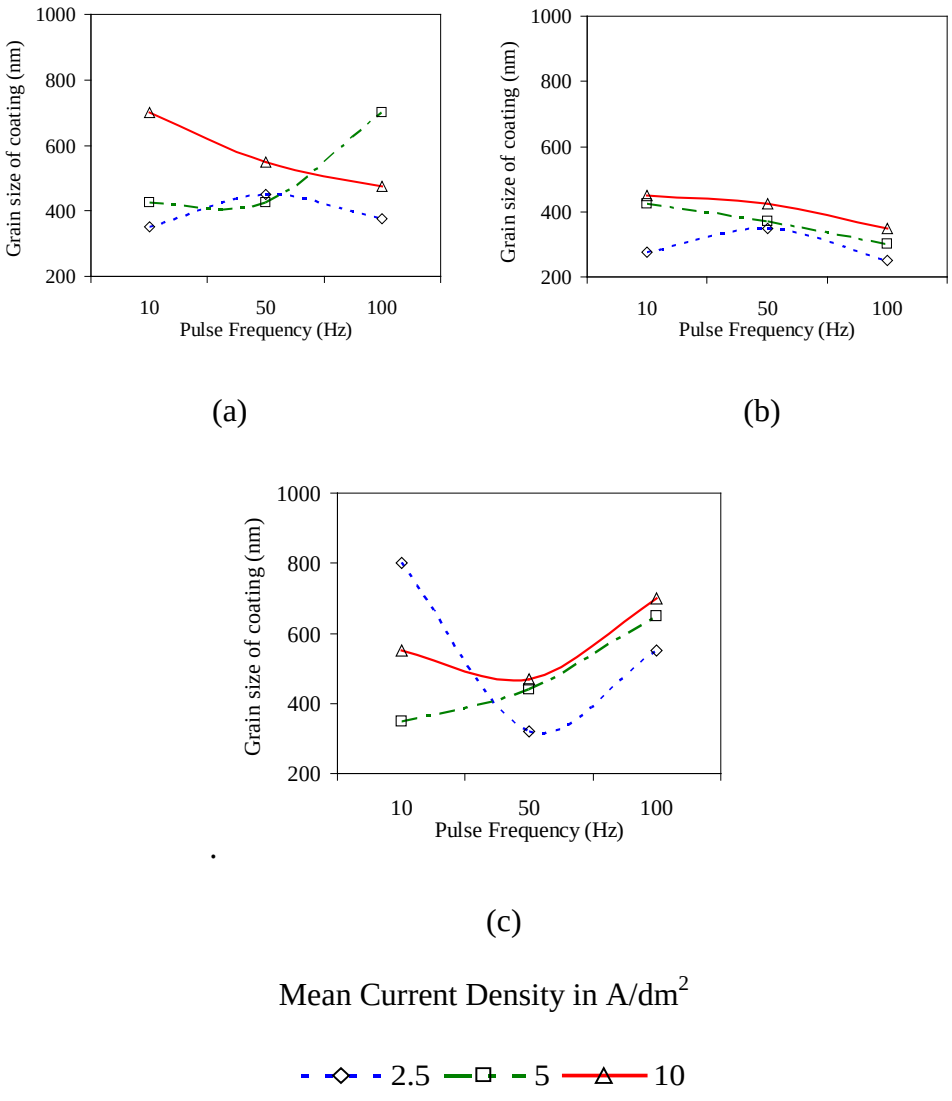

Fig. 4.22 Grain size variation at different pulse parameters

(a) DF 20%, (b) DF 50%, and (c) DF 80%

4.6.3 EFFECT OF PULSE ON-TIME

At the shortest pulse on-time (DF 20%, PF 100Hz), the coating surface was found to contain some large size grains surrounded by many finer grains (Fig. 4.23 a). Size of grains reduced with increasing pulse on-time (increasing duty factors) up to a DF of 50% and thereafter the grains went on appearing larger. The gradual change in grain size with

rise in pulse on-time towards refinement can be because of the increase in overpotential which helps deposit the finer size grains by increasing the number of nucleation sites [83]. At longer pulse on-times, a smaller portion of the on-time is used for charging the double layer which increases the Faradaic current and thus produces a more negative overpotential [69]. The refinement of grains could also have been because of the rise in the amount of hydrogen evolved associated with longer on-times that facilitate a growth-inhibiting effect resulting in formation of finer grains. At a very long pulse on-time (DF 80% and PF 10 Hz), a large portion of the applied current is consumed by the hydrogen ion reduction reaction which leads to lower deposition efficiency and coarser grains. A refinement in grain size could be achieved by pulses with 50% duty factors and higher frequencies (50 Hz). See Fig. 4.23 (b).

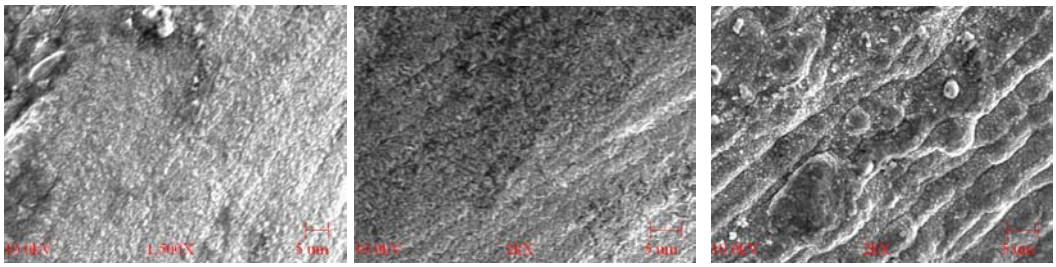

(a) **(b)** **(c)**

Fig. 4.23 Grain size variation with different pulse on-times at 5 A/dm^2

a) DF 50%, PF 100Hz, b) DF 50%, PF 50 Hz, and c) DF 50%, PF 10 Hz

4.6.4 EFFECT OF PULSE OFF-TIME

In the samples plated with the lowest pulse off-time (DF 80% and PF 100 Hz), hydrogen gas cavities are noticed in the coating surface (Fig. 4.24a.). This may be explained by the extremely short off-time itself which was not adequate for sufficient

replenishment on Ni^{2+} ions at the cathode. Because of the short off-time, there was a significant drop in the concentration of these ions at the diffusion layer which resulted in hydrogen evolution and led to formation of hydrogen gas cavities in the deposit. With an increase in the off-time, and subsequently an enhanced replenishment of $Ni2^{+}$ ions, the quality of the coating surface was noticed to have improved and was devoid of any hydrogen gas cavities (Fig. 4.24 b). At the increased off-time (DF 50%, 10 Hz), the coating surface was found to be consisting of very well facetted crystallites surrounded by smaller and finer grains. With any further rise in the pulse off-time (20%, 10 Hz), there was a gradual rise in the size of the crystallites. The longer off-times may have caused desorption that resulted in activation of growth centers and thereby coarser grains [80]. The nickel atoms may have had more time during longer off-times to migrate over the crystal surface before their incorporation to the deposit.

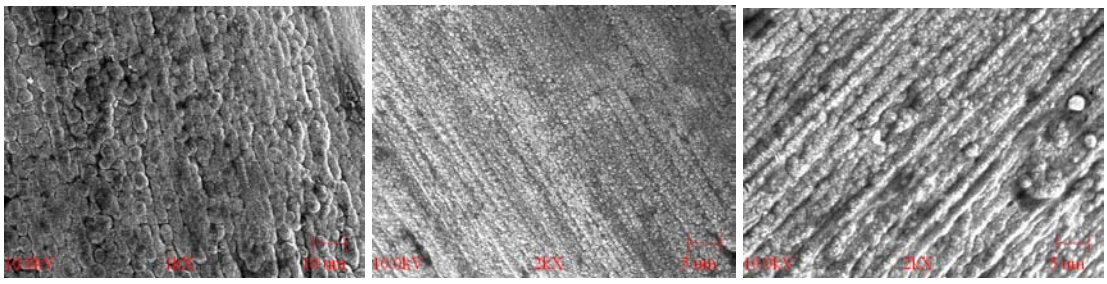

(a) (b) (c)

Fig. 4.24 Change in grain size with pulse off-times at 2.5 A/dm^2

a) 80%, 100Hz, b) 50%, 10 Hz, and c) 20%, 10 Hz

4.6.5 EFFECT OF CURRENT DENSITY

A high current density is expected to promote grain refinement. An increase in the current density is expected to result in a higher overpotential, which should increase the nucleation rate [84]. However, it has been reported elsewhere that increasing the current density from 100 to 500 mA/cm^2 using a sulfate-based solution resulted in an increase in the grain size of DC electroplated nickel. The increase in the grain size of the nickel deposited at relatively high current densities had been attributed to a decrease in the concentration of Ni ions at the deposit–electrolyte interface [85].

As seen in Fig. 4.22, it can be said that a rise in current density resulted in an increase in grain size of the nickel deposits in this work. As overpotential increased with increasing applied current density and the nucleation rate was enhanced. However, it has been reported that measured overpotential decreased with increasing current density from 18 to 25 mA/cm^2 and then increased when the current density was raised to 50 mA /cm^2 [72]. The researcher ascribed the behavior to the complex current–electrode potential relationship and could not correlate the grain size to the measured potential in their study. In our work, the electrode potential was not measured.

Progressive grain refinement was recorded with increased current density. The increased current density led to decreased nickel deposition efficiency and that was expressed as a reduction in the Ni ion concentration. With decreased deposition efficiency, more hydrogen formation took place at the cathode surface. Hydrogen decreases the surface energy of the crystallographic planes and encourages planar growth in nickel [78]. So, it is likely that the modification of the growth interface by hydrogen facilitates the formation of larger grains. With increased pulse on-time and simultaneous

increased electrode potential, the grain sizes were finer (Fig. 4.25, 4.26, and 4.27). The trend of decreasing grain size with increasing current-on time can best be explained by an increased number of nucleation sites caused by the higher overpotentials at longer current-on times. In pulse plating, there is no applied current during the pulse off-time, and fine-grained deposits were obtained during longer off-times as observed in Fig.4.25a.

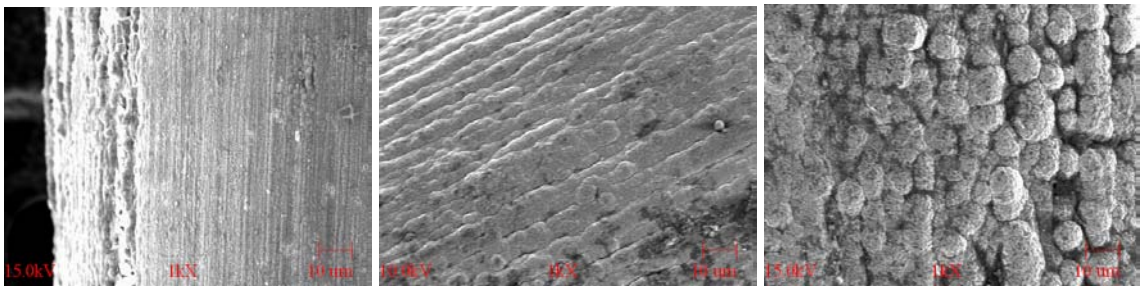

(a) 2.5 A/dm^2 (b) 5 A/dm^2 (c) 10 A/dm^2

Fig. 4.25 (a, b, & c) Grain structure in plated samples with DF 20% and PF 50 Hz

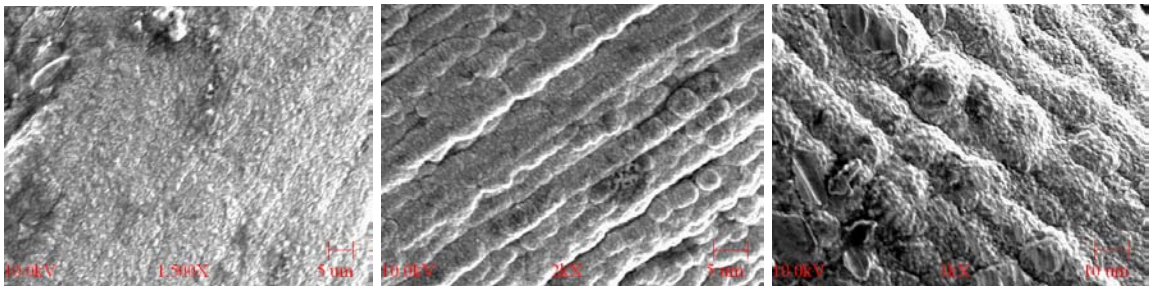

(a) 2.5 A/dm^2 (b) 5 A/dm^2 (c) 10 A/dm^2

Fig. 4.26 (a, b, & c) Grain structure in plated samples with DF 50% and PF 50 Hz

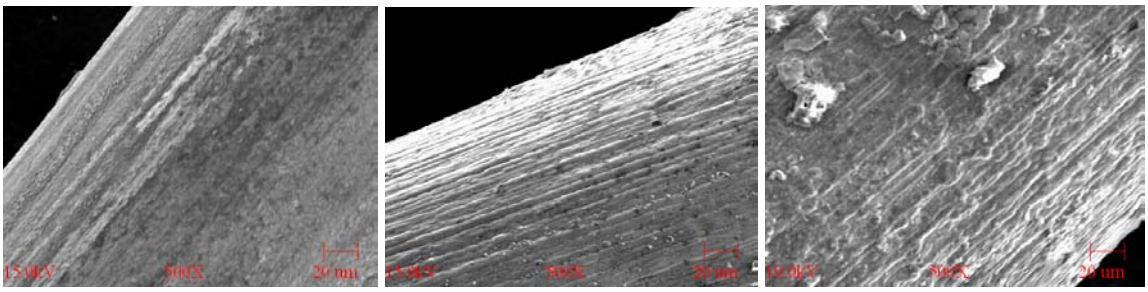

(a) 2.5 A/dm^2 (b) 5 A/dm^2 (c) 10 A/dm^2

Fig. 4.27 (a, b, & c) Grain structure in plated samples with DF 80% and PF 50 Hz

4.7 COMPARISON OF PULSE AND CONTINUOUS CURRENT (DC) PLATING

Considering the findings of this experimentation, the best parametric combinations were a short on time (duty factor 50% at pulse frequency 100Hz) and a current density of 5 A/dm^2. Comparing the coating achieved with this condition with that of a DC plated one at the same current density plated for 5 minutes, it was seen that the pulseplated sample had lower roughness (33.408 nm) than its DC counterpart (68.717 nm) and grain size was also finer in the pulse plated one. Therefore the surface morphology of the coated samples was superior when coated with pulseplating. The improved coating surface quality in pulseplated specimen can be well differentiated in the Fig. 4.28 (a, b, c, &d).

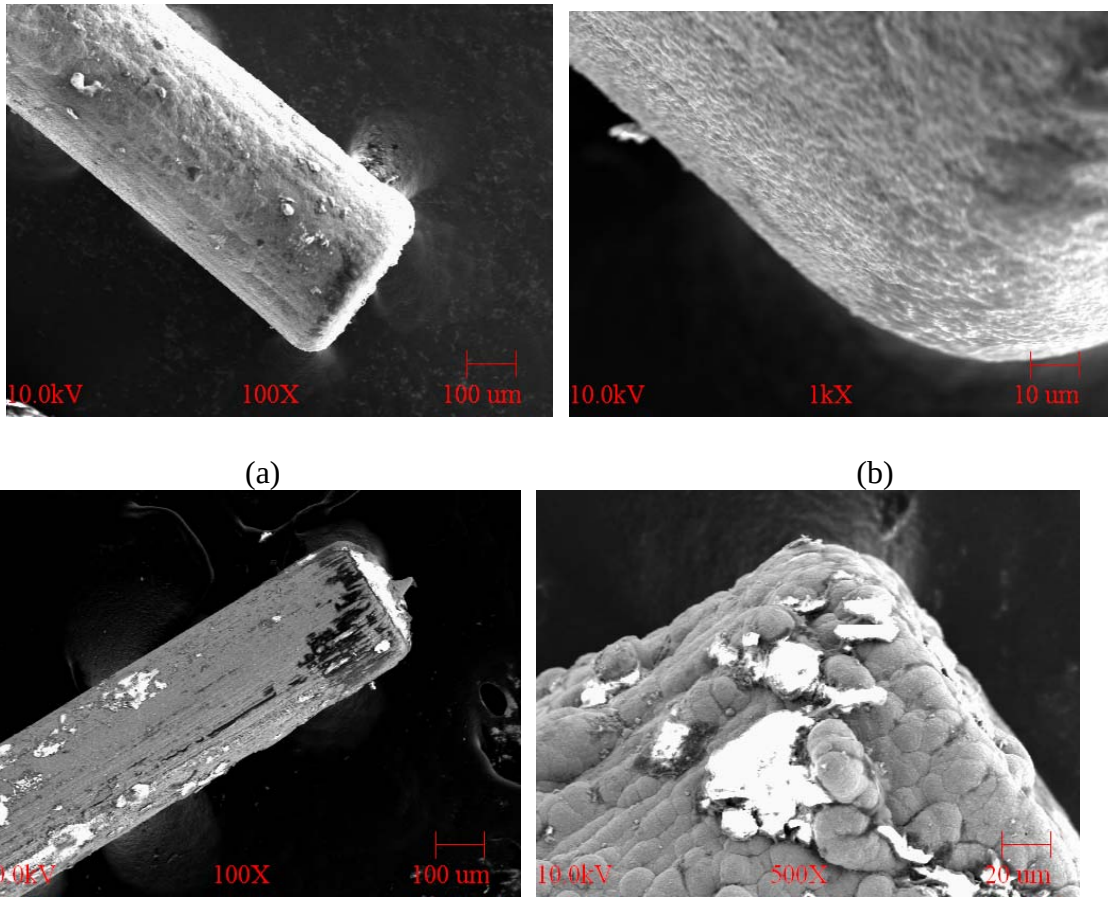

(a) (b)

(c) (d)

Fig. 4.28 Pulseplated sample (a) and (b), and DC plated sample (c) and (d)

4.8 SUMMARY

The objective of the experiments conducted in this study was to prepare the nickelcoated tungsten microtools to be used in electrochemical machining applications. It was also essential to study the effect of various controlled parameters on the coating quality in the DC and pulseplated nickel plated tungsten microelectrodes. The results of these analyses are summarized as follows.

- Pulseplated specimens were found to have better surface quality in terms of lower roughness value.
- The grain size in samples plated with pulse current was smaller in comparison with their DC counterpart and exhibited more uniformity in deposit characteristics.
- The overall thickness of coating and the percentage concentration of nickel in the deposit layer were superior in case of pulseplated coatings.
- The lowest grain size achieved was in the order of 220 nm using the additive free Watt’s bath.

CHAPTER 5

PERFORMANCE EVALUATION OF COATED MICROTOOLS

5.1 INTRODUCTION

Machining performance of ECM depends primarily on applied voltage and current, temperature, pressure, pH, conductivity, and flow rate of electrolyte, inter electrode gap, tool feed rate, and tool type, geometry, and configuration. All these parameters are closely interrelated. One of the objectives of this work was to study the behavior of the nickel coated tungsten micro electrode on few ECM process performance measures such as material removal rate and shape accuracy in terms of side machining gap of the machined surface. This chapter presents the results and analyses of the experimental data to illustrate the feasibility of use of coated tool in micro electrochemical machining. The behavior of the coated and the uncoated tool in a corrosive environment similar to an ECM operation has also been comparatively analyzed.

5.2 EXPERIMENTAL SYSTEM

The experimental system consisted of an electrochemical cell, a pulse generator, and X–Y–Z stage movement control with 0.1 μm resolution for the tool electrode and a holding device for the workpiece. The power supply in the setup was the same as the one used for plating experiments. The equipment setup for ECM experiments is shown in Fig. 5.1. Since pulse frequency is very high, pulse shape is easily affected by cable length, the

resistance between the tool electrode and the workpiece, etc. To make better rectangular pulse shape, the cable length was kept as short as possible.

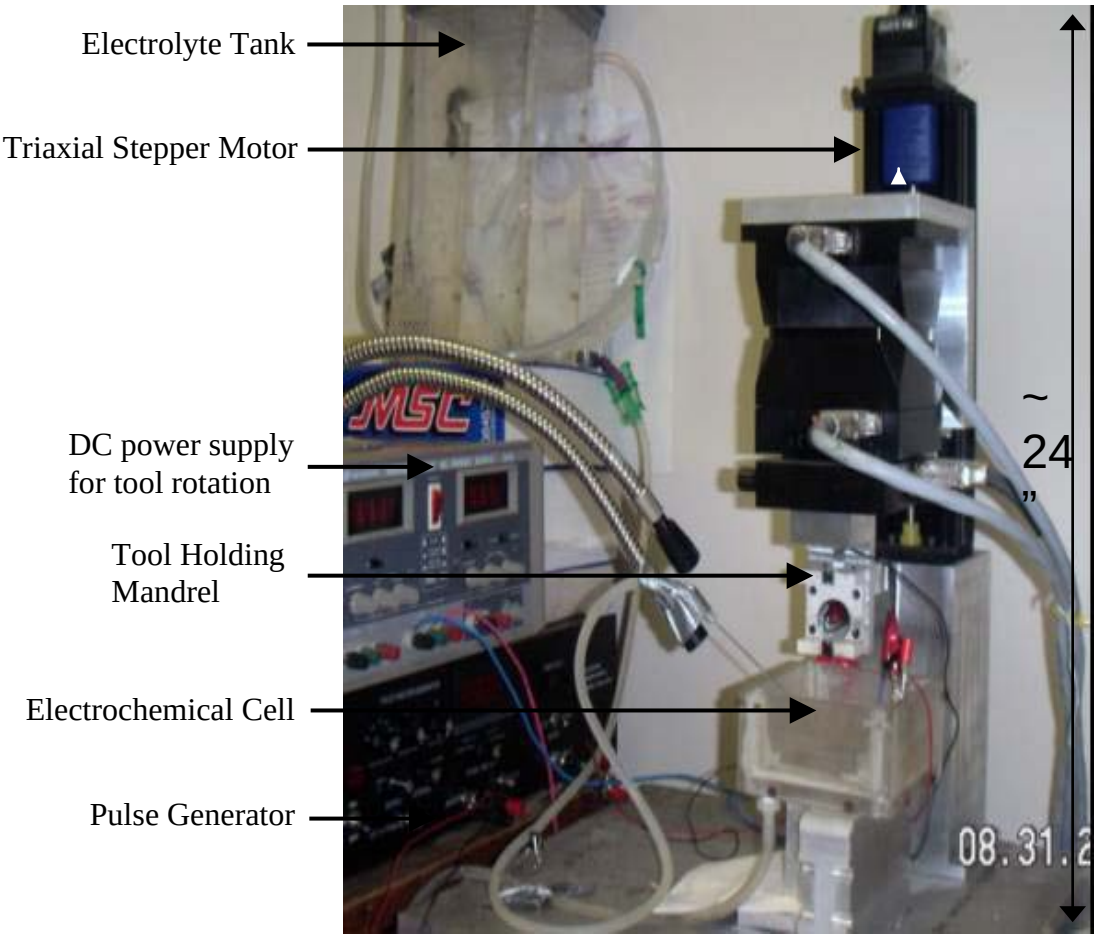

Fig. 5.1 Experimental set up for micro ECM experiments

5.3 ELECTROLYTE

Selecting the correct electrolyte is an important consideration in ECM. In conventional ECM, highly concentrated sodium chloride (NaCl) electrolyte has been used for fast machining of stainless steel [86]. In micro ECM, however, electrolyte and concentration should be chosen to consider the machining resolution, the prevention of an

oxide layer and the surface quality. ECM electrolyte is generally categorized as passivating electrolyte containing oxidizing anions such as sodium nitrate and sodium chlorate, and non-passivating electrolyte containing relatively aggressive anions such as sodium chloride. Passivating electrolytes are known to give better machining precision due to their ability to form oxide films and evolve oxygen in the stray current region. In most of the past investigations, researchers recommended sodium chlorate ($NaClo_3$), sodium nitrate ($NaNO_3$), and sodium chloride (NaCl) solution with different concentrations for microECM [87]. The metal removal rate (MRR) increases with increase in electrolyte concentration.

5.4 WORKPIECE AND TOOL

In this work, AISI stainless steel 303 (SS-303) was used as workpiece material. SS-303 is one of the most widely used stainless steels with excellent mechanical strength and corrosion resistance. The detailed composition of the workpiece material used is given in Table 5.1. The corrosion resistance of all stainless steels rests on the common factor of high chromium content (16-20%). The passivating property of a surface film also affects the corrosion resistance of stainless steels. General corrosion is not suffered in SS 303, except in cases of catastrophic oxidation, catastrophic sulfidation, or dissolution in nitric-hydrofluoric acid solutions.

Table 5.1 Workpiece (SS303) composition

MATRIAL	PERCENTAGE
Carbon	0.15
Chromium	17-19
Nickel	8-10
Silicon	1.0
Manganese	2.0
Phosphorous	0.2
Sulphur	0.03
Iron	Rest

The nickel coated tungsten microelectrodes prepared by pulse electrodeposition (described in the previous chapter) were used as tools for ECM experiments. Also for comparison, the uncoated tungsten electrode of 300 microns diameter was used in some of the experiments.

5.5 CONTROLLING INTERELECTRODE GAP

Machining accuracy and dimensional control are greatly influenced by the gap between microtool and workpiece. The smallest possible gap should be maintained for best results. However, factors such as stiffness of the machines, electrolyte boiling, process instability, and tool positioning errors limit the minimum gap size [88]. Other methods attempted to achieve better accuracy include: insulating parts (side walls) of the tool-electrode, using passivating electrolytes, using pulsed power, and lowering

electrolyte concentration. Pulsed ECM enables the recovery of the gap conditions during pulse-off times giving improved dissolution efficiency [89]. Use of inter-electrode gaps (<50μm) have resulted in improved dimensional accuracy of the order of 0.05 mm without the risk of electrolyte boiling [90]. In ECM, the pulse condition, one of the factors that determines the machining gap, is dependent on the pulse voltage, pulse on-time, and machining time [Butler–Volmer equation].

The workpiece in this work was held in a clamping device that can hold samples of about 15 mm x 15 mm in size. The tool electrode was fixed inside a mandrel similar to that in WEDG. The tool mandrel rested on V-shape bearing was rotated by a DC motor. The relative positions of the microtool electrode and the clamped workpiece were determined through contact sensing function of the experimental equipment for microECM, and then tool electrode was withdrawn about 10μm to form a reasonable machining gap. To detect a short circuit in the process, a digital continuity device similar to a multimeter was used. During the process, the tool electrode was given the feed movement while the workpiece was stationary. Tool feed rate, the velocity of tool traveling toward the workpiece, was decided by prior experience and judgment and machining speed was set in advance through numerically controlled (NC) system. Uniform machining speed was maintained throughout a single machining process. In case of a short circuit, when the tool electrode touched the workpiece surface or the distance between tool electrode and workpiece was only several microns, the machining current would jump up instantly and so would the voltage of the sampling resistance. At such incidence, the pulsed power was switched off immediately and the tool electrode was retracted several micrometers promptly to avoid short circuit damage. When the tool

electrode was gradually moved away from the workpice, there was a sudden drop in current in around a gap width of 10 μm. Adopting this sudden current variance signal gap control strategy, the interelectrode gap could be controlled in about 10 μm. The scheme of the experiment is shown in Fig. 5.2 along with the gap control strategy.

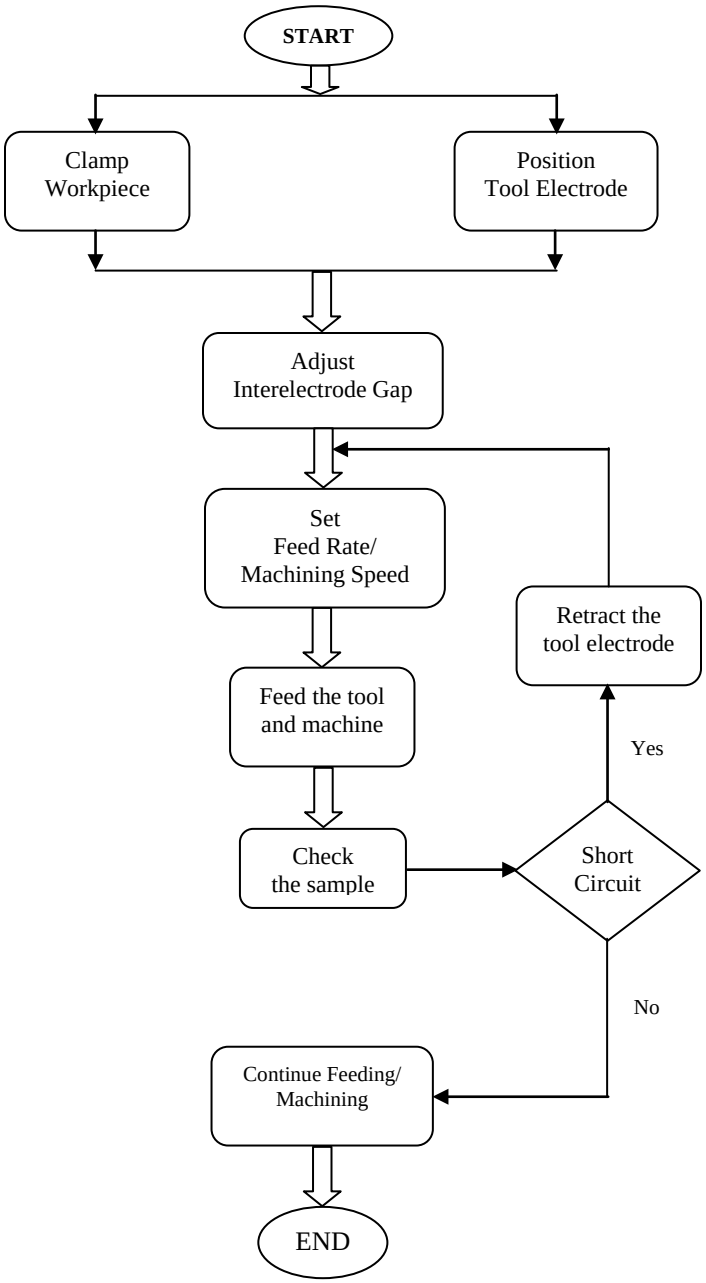

Fig. 5.2 Scheme of experiment and gap control strategy

5.6 EXPERIMENTAL CONDITIONS

Table 5.2 lists all the conditions set for the experiments in this work.

Table 5.2 Experimental conditions

FACTORS	TYPE	CONDITIONS/SIZE
Electrolyte	Sodium chloride	0.5 M
Workpiece	Stainless Steel (SS303)	15 mm X 15mm X 1.5 mm
Tool	Nickel coated tungsten	Dia 310 µm
	Uncoated tungsten	Dia 300 µm
Pulse Parameters	Voltage	3, 5, 7, 10 Volts
	Duty Factor	20% (on-time 20 ns, off-time 80 ns)
	Pulse Frequency	10 KHz
Feed Rate	Numerically controlled	0.1, 0.5, 1.0 µm/sec

5.7 RESULTS AND DISCUSSION

In electrochemical machining with high frequency short-pulse current, the major factors influencing the machining accuracy are applied voltage, feed rate, and electrolyte concentration [89]. The material removal rate and shape accuracy of the machined surface by both coated and the uncoated electrode were analyzed. The effects of supplied voltage and tool feed rate on the process output using both type of tools were also studied. The coated tool behavior was studied in the experimental conditions and compared with that of the uncoated tool in terms of electrochemical stability and corrosion resistance.

5.7.1 MATERIAL REMOVAL RATE (MRR)

As per Faraday's law, the material removal rate increased with the increased current density. An increase in supply voltage led to an increase in electrical conductivity of electrolyte which resulted in more current density. This phenomenon was observed in all our experiments; MRR went on rising with rise in the supply voltage for both types of tools. However, the material removed by the nickel coated tungsten tool was noticed to be higher at almost all supply voltages (Fig. 5.3). Although this phenomenon is not clearly understood, it could be explained by the corroded surface of the uncoated tungsten tool during the machining process which might have increased its electrical resistance and led to a net decrease in the amount of current flowing through the electrochemical cell. The surfaces of both tools were compared before and after machining. It was seen that the some kind of deposition and pitting corrosion has taken place on bare (uncoated) tungsten tool (W) (Fig. 5.4) where as the texture of the nickelcoated tungsten tool (Ni-W) has undergone very little change (Fig. 5.5).

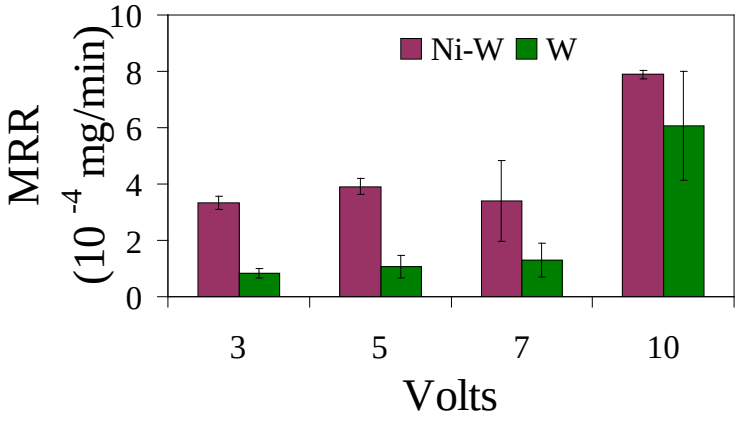

Fig. 5.3 Material Removal Rate (MRR) Vs Applied Voltage

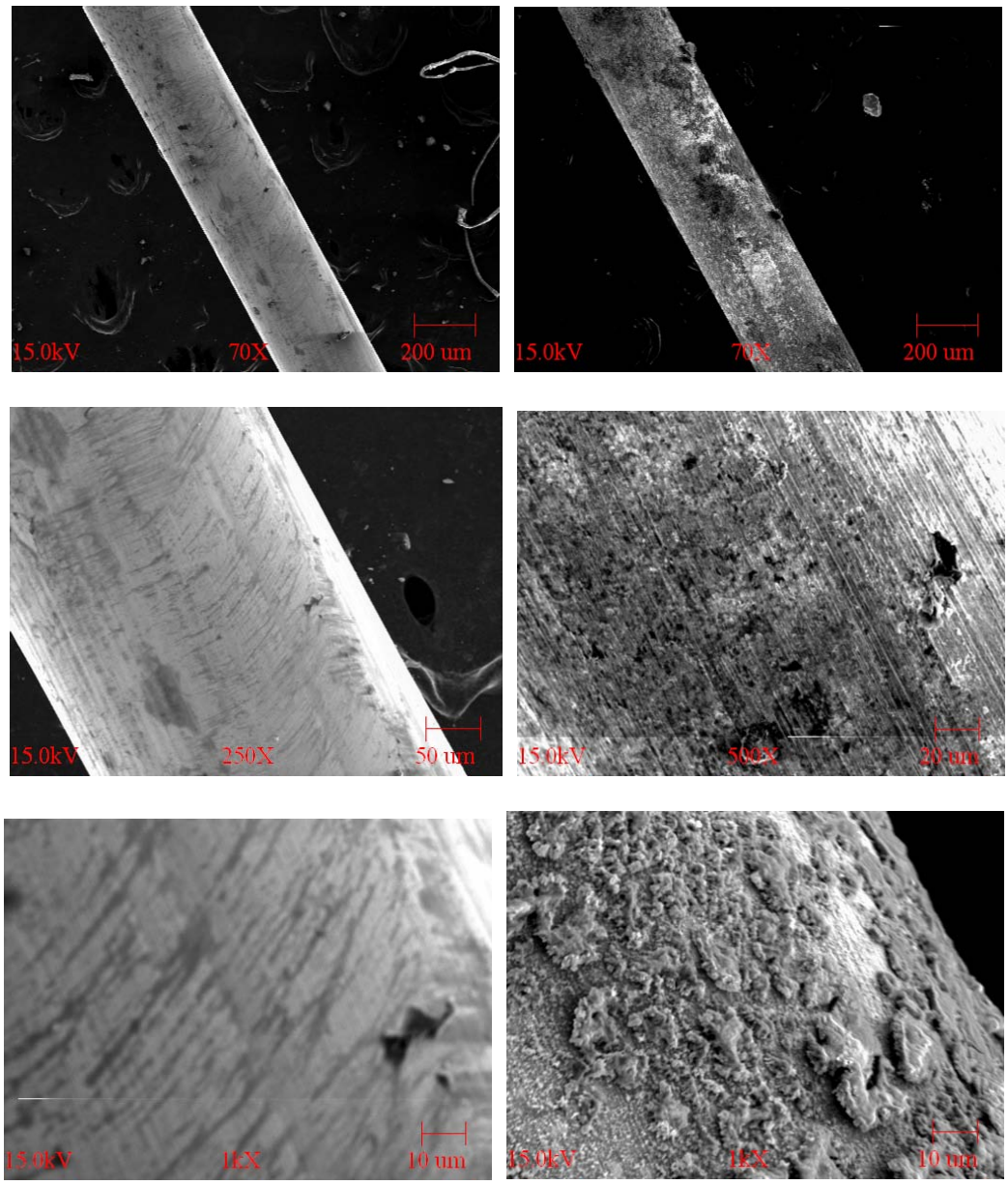

Fig. 5.4 Surface of the uncoated tool before (left) and after machining (right) at different magnifications

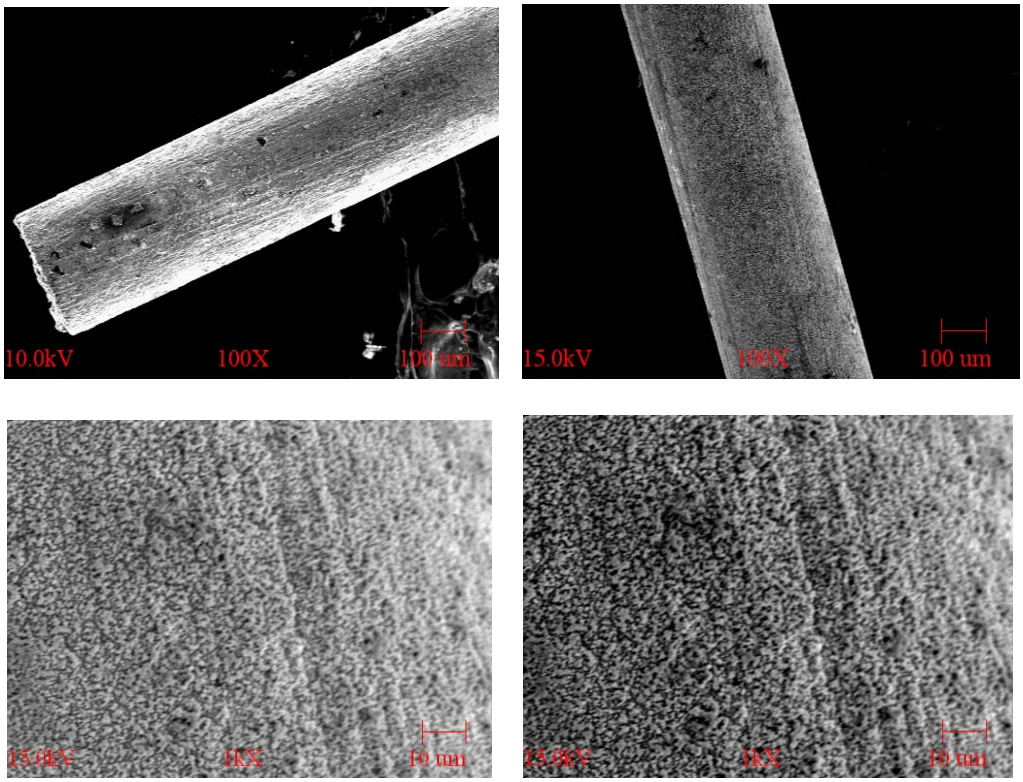

Fig. 5.5 Surface of the coated tool before (left) and after machining (right)

5.7.2 SIDE MACHINING GAP OR OVERCUT

Side machining gap or overcut is defined as the gap produced on both sides of the tool while machining and is measured as half the difference in width of the cut and the diameter of the tool. It increases with the rise in applied voltage and leads to poor machining quality. As material removal rate increases with the increase in current density, the capacity of localized dissolution is reduced leading to an increase in removal of material in the stray current region. For both type of tools used for the experiments, the side machining gap went on increasing with rise in supply voltage and the gap was found to be slightly more in case of the uncoated tool (Fig. 5.6).

Tool feed rate, defined as the velocity of the tool traveling towards the workpiece, has a significant impact on the machined surface quality. At lower feed rates, machining time is more and that results in a larger over cut and thereby poor surface quality. If feed rate was too high, material removal rate increased and interelectrode gap had to be too small and micro spark and short-circuit were frequent. Micro-sparking could cause uncontrolled material removal and possibly lead to larger overcut, relatively poor profile accuracy and tool damage. It was observed that at different tool feed rates, the over cuts generated by coated tool were comparatively smaller than overcut by the uncoated tool (Fig. 5.7). The SEM pictures of machined surface generated by both the tools are shown in Fig. 5.8. It can be easily marked that the coated tool has produced a better cut in terms of shape accuracy than the uncoated tool.

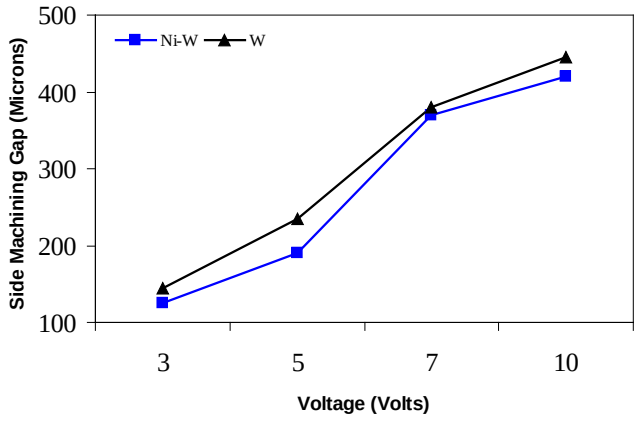

Fig. 5.6 Supply voltage vs. side machining gap

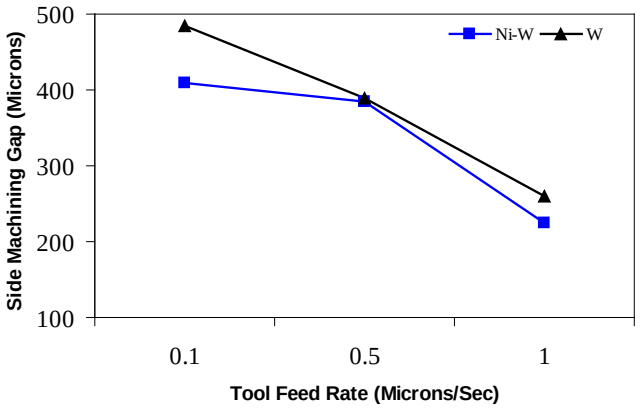

Fig. 5.7 Tool feed rate vs. side machining gap

Machined surface by coated tool **Machined surface by uncoated tool**

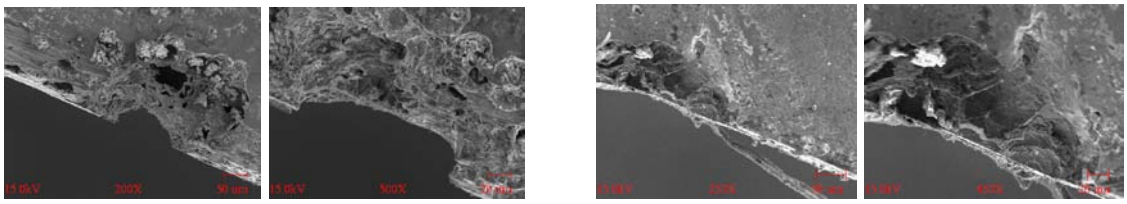

Voltage: 5 V, Feed Rate: 1 µm/s, and Pulse on/off: 20/80 ns

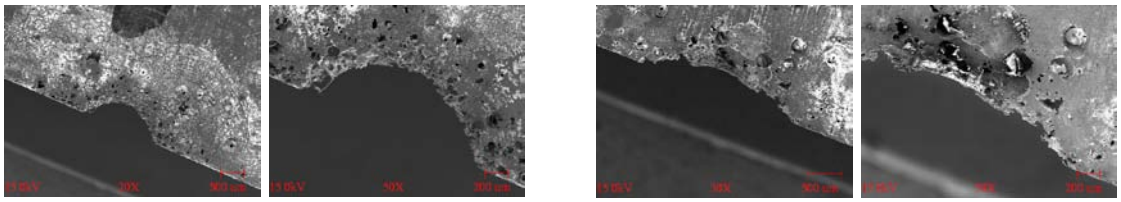

Voltage: 7 V, Feed Rate: 1 µm/s, and Pulse on/off: 20/80 ns

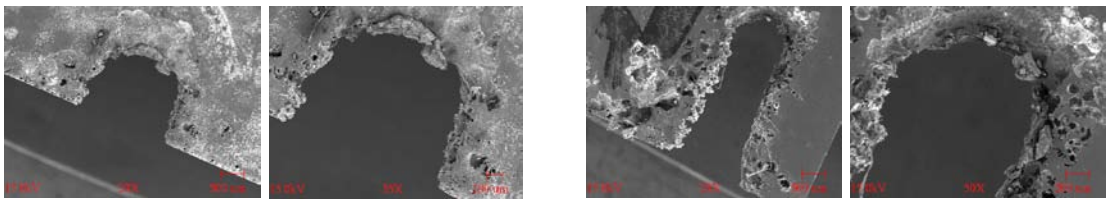

Voltage: 10 V, Feed Rate: 1 µm/s, and Pulse on/off: 20/80 ns

Fig. 5.8 SEM pictures of the machined surfaces using both types of tools

5.7.3 SURFACE ROUGHNESS

The uncoated tungsten tool generated a surface with lower roughness than the coated tool at the beginning of the machining process, but after a couple machining activities, the surface quality started to deteriorate with the uncoated tool. Initially, because of the good surface quality of the uncoated tungsten microtool, the surface generated was good, but as some kind of deposition and pitting took place on the uncoated tool surface, making the tool surface rougher, the produced machined surface quality worsened with subsequent machining trials. However, the roughness of the surface machined by the nickel coated tungsten microtool was somewhat consistent as evident from the SEM pictures (Fig. 5.9).

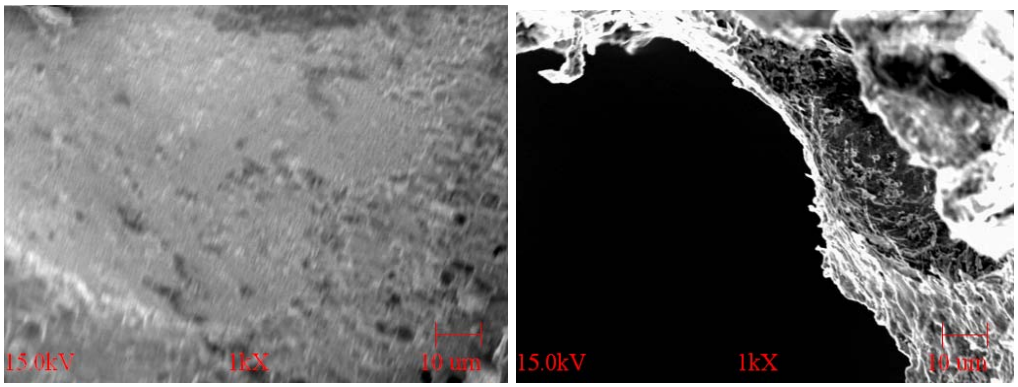

Fig. 5.9 Surface generated by Ni coated tungsten (left) and
by uncoated tool after a couple of machining operations (right)

5.7.4 CORROSION TEST

Sodium Chloride (NaCl) has been found to be an appropriate electrolyte for ECM and microECM applications and the tool used in such a solution is prone to attack such as pitting. It has been found that tungsten is more prone to corrosion when deionized water, chloride ions, or both are present. The chloride ions have particularly a significant role in

the corrosion and pitting of tungsten [91]. So it is logical to test the corrosion performance of the nickel coated tungsten tool against the uncoated tungsten microtool.

The corrosion resistance of the nickel coatings was investigated by the normal salt test by an in-house testing apparatus. The normal salt testing as per ASTM B117 conditions subjects the test samples to conditions that are actually more corrosive than actual machining conditions. The test uses sodium chloride in deionized water and usually lacks the moderating effects of other dissolved salts such as those containing calcium and magnesium, which tend to be somewhat protective. The duration of the test can typically range from 8 to over 3000 hours. In this work, testing was carried out over 16 hours. A 5% sodium chloride solution containing than 200 parts per million (ppm) total solids and with a pH of 6.5 was used. The temperature of the salt spray chamber was maintained at 35^{o}C [92].

The corrosion resistance of pulseplated nickel coatings and the uncoated tungsten sample was assessed in the salt environment. The surfaces of both types of samples after the test are shown in the SEM pictures below. It can be seen that the uncoated specimen was attacked more by the corrosive solution than the coated microtool. Severe pitting was found to have taken place on the bare specimen and along with some rust formation (Fig. 5.10 a). The pulseplated samples were not completely unaffected, but showed enough resilience to the corrosive environment and their surface were lot better than that of the uncoated specimen (Fig. 5.10 b).

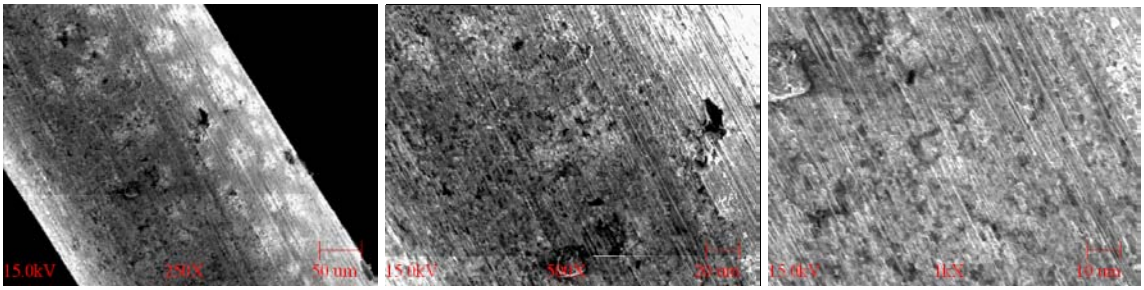

Fig. 5.10 (a) Surface of the uncoated tungsten microtool after the corrosion test

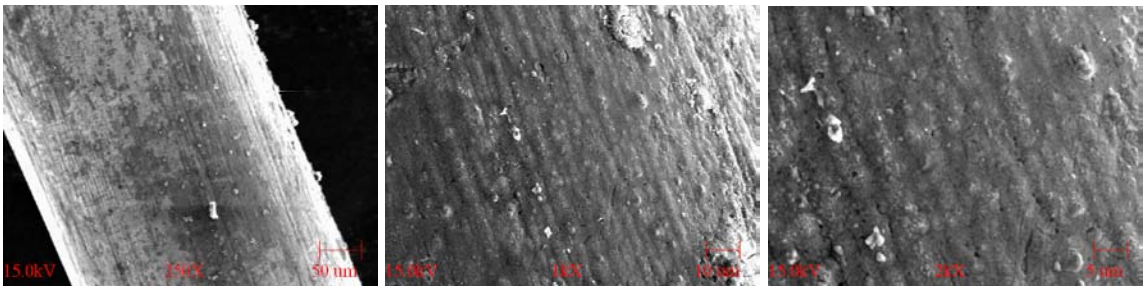

Fig. 5.10 (b) Surface of the nickel coated tungsten microtool after the corrosion test

5.8 DIFFICULTIES

The following is a summary of experimental challenges.

- The electrolyte can be easily boiled by the high current density in the inter- electrode gap. Sometimes the residue produced during machining process adhered to the workpiece surface and that made the machining difficult to continue. Using suitable pulse voltage with high pulse off-time this problem could be overcome.
- Although supply voltage of 3V and 5V were high enough for uniform dissolution, the machining rate was too slow and the electrodes often came into contact leading to short-circuiting. At higher tool feed rates with short pulse on-time, higher voltage was required for uniform dissolution.

- The pH of the electrolyte was difficult to control during the machining process and continuous measurement of conductivity of the solution was also problematic. It is apprehended that the variations in MRR readings could be for of this reason.
- It was extremely difficult to determine the appropriate interelectrode gap due to lack of automatic gap detection system and was managed by judgment and manual adjustment.

5.9 CONCLUSION

The chapter presented the comparative performance of the nickel coated tungsten microtool with that of the uncoated tool. It was observed that in terms of MRR, shape accuracy, and corrosion resistance, the coated tool exhibited better performance than its counterpart.

CHAPTER 6

SUMMARY, FINDINGS, AND RECOMMENDATIONS

This chapter summarizes the results of the experimental work relating to development of coated microtool for pulse electrochemical machining applications, parametric optimization, and lists out some of the keys findings. Few recommendations for future research in this direction are also presented here.

6.1 SUMMARY OF THIS WORK

The goal of this research was to explore the feasibility of using nickel coated tungsten electrode in pulse electrochemical machining and to evaluate the performance of the coated tool in terms of the process output. The main objectives were:

- To prepare nickelcoated tungsten microtool by electrodeposition for electrochemical machining applications
- To evaluate the performance of coated microtool in pulse electrochemical machining (PECM)

The specific tasks included, designing and developing an in-house electroplating setup for preparing the nickel coated tungsten microelectrode, conducting plating trials, and determining the optimum plating parameters for best coating quality. Another important task was to conduct pulse electrochemical machining experiments and compare the coated microtool performance with that of an uncoated tungsten electrode. As a part of the second objective, a comparative analysis of the behavior of the coated tool in an

environment similar to that of an ECM by a corrosion test was also conducted and presented.

For preparation of coated microelectrodes, an electroplating setup was developed by in-house resources. The tungsten microtool was nickelcoated by pulse and DC electroplating. The effects of different controlled parameters on the coating characteristics were studied. The components of the plating set up were again used for building the pulse electrochemical machining experimental setup. The developed system met the basic experimental requirements of micromachining.

6.2 FINDINGS

Some of the key findings of this investigation are listed here.

- Ni coating of thickness in the range of 2.6 - 8.6 µm and 2.1 - 11.9 µm was applied to the tungsten microelectrode by DC and pulse plating respectively. Most of the coatings obtained were thick, dense, and adhered well to the substrate. The combination of 5 A/dm^2, DF 80%, and PF 100Hz could plate the thickest coating in the trials (11.9 µm).
- Under the conditions used in this study, pulse electroplating produced more uniform and fine grained nickel deposits with grain size down to about 220 nm.
- Plating at lower mean current densities (2.5 A/dm^2) and DF 50% was found to produce smallest grain size in the range of 220 - 310 nm. PF of 100Hz at DF 50% produced the lowest grain sized coating for all the three mean current densities tried in this work.
- The lowest roughness achieved in DC plated samples was about 41 nm and the maximum was 110 nm; whereas the range of roughness readings were 13 -128 nm

for the pulseplated samples. The best of the parametric combinations tried for repeatable lowest roughness were 5 A/dm^2, DF 50%, and PF 100Hz.

- Pulseplating resulted in smoother and homogeneous coatings of lower porosity than the coatings produced by DC plating. The variation in composition of coatings at DF 50% with all mean current density and pulse frequency combinations was lowest (>99%-100).
- Based on the coating characterization, the optimum conditions for producing best nickel coating in terms of coating thickness, uniformity, grain fineness, and surface roughness, with the deposition conditions chosen in this work, could be proposed as: a mean current density 5 A/dm^2, DF 50%, and PF 100Hz.
- The nickel coated microelectrode was found to be capable of removing more material (about 28%) than the uncoated tungsten microelectrode. The difference in MRR of two types of tools decreased with increased supplied voltage.
- The dimensional and shape accuracy of machined surface (slot in this work) was better when the coated microtool was used as compared to that of the uncoated tungsten microelectrode. This was evident from the lower side machining gap of the generated surface.
- The nickel coated tungsten microtool exhibited higher electrochemical stability and almost retained its original surface topography during the machining process, where as the surface of the uncoated Tungsten microtool had some kind of deposition similar to corrosion that might have affected its machining performance.

- In the corrosion test for both type of tools, the nickel coated microelectrode showed higher chemical resistance than the bare uncoated tungsten tool.

6.3 CONCLUSIONS

- Considering the above findings, it could be concluded that nickel coated tungsten microelectrode can be prepared *in situ* with the optimized parameters mentioned above.
- The results presented here suggest a definite, consistent relationship between the input process parameters and the characteristics of the nickel coating on tungsten microelectrode. Detailed understanding of this relationship can be applied to improve and tailor properties of coated microelectrodes.
- Different coating materials with desirable ECM tool properties can widen the range of ECM tool materials that are currently in use.
- The coated tool could have higher material removal rate and produce better shape accuracy in ECM applications. More importantly, the nickelcoated tungsten microtool because of its higher electrochemical stability and greater corrosion resistance could be used as an effective microECM tool for a longer period in an ECM environment. That might result in reduced tool cost and improved reliability of the ECM system and process output.

6.4 RECOMMENDATIONS

- In this work nickel was used as coating material for improving the electrochemical stability of the tungsten microtool. Other materials of superior

electrochemical properties can be tried as coating. Also materials other than tungsten can be experimented as base materials.

- It has been reported that the grain size of the coating is affected by change in the bath temperature and bath agitation. All the plating trials in this work were conducted at room temperature without agitation because of hardware limitations and hence effects of these factors on the coating quality could not be studied. Future works may focus on studying this effect.
- The bath used in this work did not use any additives which could have improved the grain fineness of the nickel coating. Any subsequent work may include use of suitable additives to achieve better effects.
- The plating experiments were based on a 3X3 full factorial design with two replicates. However, it is felt that more electrochemical experiments are still required to reveal the exact dependence of grain size of the coating on various experimental conditions and details of the mechanisms that leads to unusual results (outliers).
- To limit the scope of this work, pulse reverse plating was not considered. However, this can be considered for continuation of this research.
- A theoretical approach is needed to predict the dimensional, grain size, and composition of the coating on the microelectrode.
- The coating method in this work was chosen to be electroplating because of its convenience and the apparatus proximity. Any other suitable, inexpensive method may be explored depending on the coating and substrate material.

- The pulse electrochemical machining set up used in this work lacked the facility of auto detection system of short circuiting and on-line assessment of machining status. For efficient use of the equipment and time, further investigation in terms of machine configuration is utterly desired.
- Due to hardware limitations, a duty factor below 20% could not be chosen. In recent works, as small as a duty factor of 1-2% is being used to produce features of very small dimensions (5 microns). This issue may be addressed in any subsequent PECM work.

REFERENCES

1. B. Bhattacharyya, J. Munda, and M. Malapati, 2004, Advancement in electrochemical micro-machining, Int. J. Machine Tools and Manufacture, 44: 1577–1589

2. M. Dutta, R. V. Shenoy, and L. T. Romonkiw, 1996, Recent advances in the study of electro-chemical micromachining. J Eng Ind, 118: 29-36

3. S. Sharif and E.A. Rahim, 2007, Performance of coated- and uncoated-carbide tools when drilling titanium alloy—Ti–6Al4V, Journal of material processing tech., 185, Issues 1-3: 72-76

4. S.S. Hong, H.K. Bo, N.C. Chong, 2008, Analysis of the side gap resulting from micro electrochemical machining with a tungsten wire and ultrashort voltage pulses, Journal of Micromechanics and Microengineering, 18: 1-6

5. P. Gyftou, M. Stroumbouli, E.A. Pavlatou, P. Asimidis, and N. Spyrellis, 2005, Tribological study of Ni matrix composite coatings containing nano and micro SiC particles, Electrochimica Acta, 50: 4544–4550

6. M.E. Bahrololoom, and R. Sani, 2005, The influence of pulse plating parameters on the hardness and wear resistance of nickel–alumina composite coatings, Surface & Coatings Technology, 192: 154–163

7. S.T. Aruna, G.V.K. William, and K.S. Rajam, 2009, Ni-based electrodeposited composite coating exhibiting improved microhardness, corrosion and wear resistance properties, Journal of Alloys and Compounds, 468: 546-552

8. L. Xue-Song, O. Jia-Hu, L. Yu-Feng, and W. Ya-Ming, 2009, Electrodeposition and tribological properties of Ni–SrSO4 composite coatings, Applied Surface Science, 255: 4316–4321

9. J. Spector, C. Jacobsen, and D. Tennant, 1997, Journal of Vacuum Science Technology B, 15: 2872

10. Y.F. Shen, W.Y. Xue, Y.D. Wang, Z.Y. Liu, and L. Zuo, 2008, Mechanical properties of nanocrystalline nickel films deposited by pulse plating, Surface & Coatings Technology, 202: 5140–5145

11. E.A. Pavlatou and N. Spyrellis, 2008, Influence of Pulse Plating Conditions on the Structure and Properties of Pure and Composite Nickel Nanocrystalline Coatings, Russian Journal of Electrochemistry, 44: 745–754

12. X. Yuan, Y. Wang, D. Sun, and H. Yu, 2008, Influence of pulse parameters on the microstructure and microhardness of nickel electrodeposits, Surface & Coatings Technology, 202:1895-190

13. G. Semon, 1975, A Practical Guide to Electro-Discharge Machining, 2nd ed., Atelier De Charmilles, Geneva

14. A.D. Davydov, V.M. Volgin, and V.V. Lyubimov, 2004, Electrochemical Machining of Metals: Fundamentals of Electrochemical Shaping, Russian Journal of Electrochemistry, 40: 1230–1265. Translated from Elektrokhimiya, 40/12: 1438–1480

15. D. Landolt, P.-F. Chauvy, and O. Zinger, 2003, Electrochemical micromachining, polishing and surface structuring of metals: fundamental aspects and new developments, Electrochimica Acta, 48: 3185-3201

16. S.K. Sorkhel and B. Bhattacharyya, 1989, Computer aided design of tools in ECM for accurate job machining, Proceedings of the ISEM-9: 240–243

17. S.H. Ahn, S.H. Ryu, D.K. Choi, and C.N. Chu, 2004, Electrochemical microdrilling using ultra short pulses, Precision Engineering, 28/2: 129–134

18. K.P. Rajurkar, D. Zhu, J.A. McGeough, J. Kozak, and A. De Silva, 1999, New developments in electrochemical machining, Annals of the CIRP, 48/2: 567–579

19. V.K. Jain and K.P. Rajurkar, 1991, An integrated approach for tool design in electrochemical micromachining, Precision Engineering, 13/2: 111–124

20. Y. Zhoo and J.J. Derby, 1995, The cathode design problem in ECM, Chemical Engineering Science, 50/17: 2679–2689

21. Y.M. Lim and S.H. Kim, 2001, An electrochemical fabrication method for extremely thin cylindrical micropin, International Journal of Machine Tools and Manufacture, 41:2287–2296

22. A.K.M. De Silva, H.S.J. Altena, and J.A. McGeough, 2000, Precision ECM by process characteristic modeling, Annals of the CIRP 49/1: 151–156

23. H. Ohmori, K. Katahira, Y. Vehara, Y. Watanabe, and W. Liu, 2003, Improvement of mechanical strength of microtools by controlling surface characteristics, Annals of the CIRP, 52/1:467–470

24. B. Bhattacharyya, B. Doloi, and P. S. Sridhar, 2001, Electrochemical micro-machining: new possibilities for micro-manufacturing, Journal of Materials Processing Technology, 113/1-3: 301-305

25. John. F. Wilson, 1971, Practice and theory of ECM, John Wiley and sons, New York

26. J. Bannard, 1977, Elecetrochemical machining, Journal of Applied Electrochemistry, 7: 1-29

27. A.D. Davydov, A.N. Kamkin, S.V.Klopova, and V.D.Kashcheev, 1973, Electro. Obrabot. Mat., 6/28

28. H. Bommer, 1998, Magnesium Alloys and their Applications , Proc. of the Conf. on Magnesium Alloys and their Applications, Werkstoff-infomationsgesellschaft, 79.

29. R.F. Bunsah, 1994, Handbook of deposition technologies for films and coatings, second edition, Noyes publications, Park Ridge, New Jersey

30. G. Erkens, 2005, A survey of advanced coatings as key element of modern cutting tools and functional components, Conference proceedings, The coatings: 53-65

31. Bewilogua et al., 2009, Annals of the CIRP, 58/2

32. R.F. Bunshah, 1982, Deposition technologies for films and coatings, developments, and applications, Noyes publications, Park Ridge, New Jersey

33. R. Foerster, A. Schoth, and W. Menz, 2005, Micro ECM for production of Microsystems with a high aspect ratio, Microsystem Technologies, 11: 246-249

34. L. Staemmler, K. Hofmann, and H. Kueck, 2005, ECF- An innovative Technique for Micro Mould Fabrication. Proceedings of first 4M Conference: 375-377

35. R.P. Van Kessel, P.A. Rensing, F.H.M. Sanders, and C.G. Visser, 1998, Electrode for electrochemical machining. Patent US 5,759,362

36. B. Bhattacharyya, S. Mitra, and A.K. Boro, 2002 Electrochemical machining: new possibilities for micromachining, Robot. Comput. Integr. Manuf., 18: 283–289

37. Min-Seop Han, Byung-Kwon Min and Sang Jo Lee, 2008, Modeling gas film formation in electrochemical discharge machining processes using a side-insulated electrode, J. Micromech. Microeng., 18/4: 1-8

38. Chan Hee Jo, Bo Hyun Kim, and Chong Nam Chu, 2009, Micro electrochemical machining for complex internal micro features, CIRP Annals-Manufacturing Technology, 58: 181–184

39. B.J. Park, B.H. Kim, and C.N. Chu, 2006, The effects of tool electrode size on characteristics of micro electrochemical machining. Annals of the CIRP 55/1: 197–200

40. Alan Richter, 2009, Lab coatings, micromanufacturing, Summer issue

41. F. Klocke and T. Krieg, 1999, Coated Tools for Metal Cutting — Features and Applications, Annals of the CIRP, **48/** 2: 1–11.
42. J.I. Duffy, 1981, Electroplating technology: Recent developments, Noyes Data Corporation, Park Ridge, New Jersey

43. J.W. Dini, 1992, Electrodeposition, the material Science of coatings and substrates. Noyes Publication, Park Ridge, New Jersey

44. Peter T. Tang, 2008, Utilizing Electrochemical Deposition for Micro Manufacturing, Proceedings of the 4th international conference on Multi-Material Micro Manufacture, September 9-11, Cardiff, UK

45. R.J. ContoUni, S.T. Mayer, R.T. Graff", L. Tarte, and A.F. Bernhardt, 1997, Electrochemical planarization of ULSI copper. Solid State Technology, 10: 155–161

46. R.K. Pandey, S.N. Sahu, and S. Chandra, 1996, Handbook of Semiconductor Electrodeposition Marcel Dekker, Inc., New York

47. ASM Metals Handbook, 1994, Surface Engineering, 5: 742-765

48. D. Landolt, 1986, Theory and Practice of Pulseplating, AESF: 189-199

49. U. Erb, K.T. Aust, and G. Palumbo, 2002, Nanostructured materials processing, Properties and potential applications, ed C C Koch (Noyes: Williams Andrew Publishing): 179-215

50. S. Tao and D.Y. Li, 2006, Tribological, mechanical, and electrochemical properties of nanocrystalline copper deposits produced by electrodeposition, Nanotechnology, 17: 65-78

51. H. Natter and R. Hampelmann, 1996, J. Phys. Chem., 100:19525-32

52. E.S.Chen and F.K. Sautter, 1976, The effects of pulse current plating on the mechanical properties of cobalt and cobaltAl_2O_3. Plating and Surface Finishing, 5: 28-32

53. R.T.C. Choo, A.M. El-Sherik, and U. Erb, 1995, Mass transfer and electrocrystallization analyses of nanocrystalline nickel production by pulse plating. Journal of Applied Electrochemistry, 25: 384-403

54. H. Natter and R. Hempelmann, 1996, Nanocrystalline palladium by pulsed electrodeposition. Ber. Bunsenges. Phys. Hem., 100/1: 55-64

55. D.F. Susan and A.R. Marder, 1997, Electrodeposited Ni-Al particle composite coatings. Thin Solid Films, 307: 133-140

56. E.J. Podlaha and D. Landolt, 1997, Pulse-Reverse plating of Nanocomposite Thin Films. Journal of the Electrochemical Society, 144/7: 200-202

57. C.H. Seah, and L.H. Chan, 1999, Fabrication of D.C.-plated nanocrystalline copper electrodeposits. Journal of materials Processing Technology, 89-90: 432-436

58. J.L. Stojak and J.B. Talbot, 1999, Investigation of electrocodeposition using a rotating cylinder electrode. Journal of the Electrochemical Society, 146/12: 4504-4513

59. A.B. Vidrine and E.J. Podlaha, 2001, Composite electrodeposition of ultrafine gamma-aluminaparticles in nickel matrices Part I: citrate and chloride electrolytes. Journal of Applied electrochemistry, 31/4: 461-468

60. Nasser Kanani, 2004, Electroplating-Basic Principles, Processes and Practice, Elsevier Science

61. E.B. Saubestre, 1958, Plating, 45: 927

62. A. Watson, 1998. Nickel electroplating solutions. App. Note, Nickel Development Institute, Toronto, Ontario, Canada

63. A.H. Du Rose, 1977, Plating and surface finishing, 64/2: 48-52

64. J.P. Hoare, 1989, J. Electrochem soc., 134/12: 3102

65. Standard no. BS 558, 1970, Nickel anodes for electroplating

66. T. Rodgers, 1959, Handbook of practical electroplating, The Macmillan Co., New York

67. A.M. El-Sherik, U. Erb, and J. Page, 1996, Microstructural evolution in pulse plated nickel electrodeposits, Surface and coating technology, 88: 70-78

68. E. Valles, R. Pollina, and E.Gomez, 1993, J. Appl. Electrochem., 23: 508

69. V.S. Abdulin and V.I. Chernenko, 1982, Prot. Metals, 18: 777

70. H.D. Merchant, in H.D. Merchant (Ed.), 1995, Defect Structure, Morphology and Properties of Deposits', TMS Publication, Warrendale, PA: 1

71. P.Q. Dai, Hui Yu, and Q. Li, 2004, Trans. Mater. Heat Treatment, 25:1283

72. F. Ebrahimi and Z. Ahmed, 2003, The effect of current density on properties of electrodeposited nanocrystalline nickel, Journal of Applied Electrochemistry 33: 733–739

73. K.L. Morgan, Z. Ahmed, and F. Ebrahimi, 2001, MRS Proc., 634: B3.11.1

74. S.T. Aruna, S. Diwakar, A. Jain, and K.S. Rajam, 2005, Surf. Eng., 21: 209

75. A. Cziraki, B. Fogarassy, I. GerÄocs, E. Toth-Kadar, and I. Bakonyi, 1994, J. Mater. Sci., 29: 4771

76. J.W. Dini, 1988, Plat. Surf. Finish., 75: 11

77. A.M. El-Sherik and U. Erb, 1995, J. Mater. Sci., 30: 5743

78. K. Haug and T. Jenkins, 2000, J. Phys. Chem. B, 104, 10017

79. A.M. Rashidi and A. Amadeh, 2008, Surf. Coat. Technol., 202: 3772

80. C. Kollia, N. Spyrellis, J. Amblard, M. Froment, and G.J. Maurin, 1990, Appl. Electrochem., 20: 1025

81. D. I. Rehrig, H. Leidheiser, Jr., and M. R. Notis, 1977, Plat. Surf. Finish., 64: 40

82. S. Yoshimura, S. Chida, and E. Sato, 1986, Met. Finish., 84**:** 39

83. J.Cl. Puippe and N. Ibl, 1980, Plating Surface finishing, 67/6: 68

84. W. Schmickler, 1996, Interfacial Electrochemistry, OUP-Oxford: 129

85. A. Czira´ ki, B.F. Fogarassy, I. Gero¨ cs, E. To¨ th-Ka´ da´ r, and I. Bakonyi, 1994, J. Mater. Sci., 29: 4771

86. L. Cagnon, V. Kirchner, M. Kock, R. Schuster, G. Ertl, W.T. Gmelin, and H. K¨uck, 2003 Electrochemical micromachining of stainless steel by ultrashort voltage pulses, Z. Phys. Chem., 217**:** 299–313

87. B. Bhattacharya, B. Doloi, and P.S. Sridhar, 2001, Electrochemical micromachining-new possibilities for micromachining, J. of materials processing technology, 113: 301-305

88. C. de. Regt, 1986, ECM for the Production of High Precision Components, Proc. of ISEM VIII: 120-128

89. K.P. Rajurkar, J. Kozak, B. Wei, and J.A. McGeough, 1993, Study of pulse electrochemical machining characteristics, Annals of the CIRP, 4211: 231-234

90. K.P. Rajurkar, B. Wei, J. Kozak, and J.A. McGeough, 1995, Modeling and monitoring inter-electrode gap in pulse electrochemical Machining, Annals of the CIRP, 4411: 177-180

91. F. Di Quarto, S. Piazza, and C. Sunseri, 1988, Electrical breakdown and pitting in anodic films on tungsten in halogen ion-containing solutions. J. Electroanal. Chem., 248: 117
92. http://www.astm.org/Standards/G85.htm

93. R. Polini, 2006, Chemically vapor deposited diamond coatings on cemented tungsten carbides: Substrate pretreatments, adhesion and cutting performance, Thin Solid Films 515: 4 – 13

94. W. Schintlmeister, W. Wallgram, J. Kanz, and K. Gigl, 1984, Cutting tool ,materials coated by chemical vapor deposition, Wear, 100: 153-169

95. C.H. Che Haron, J.A. Ghani, and G.A. Ibrahim, 2007, Surface integrity of AISI D2 when turned using coated and uncoated carbide tools, Int. J. Precision Technology, 1/1: 109-114

96. M. Nalbant, H. Gokkaya, I. Toktas, and G. Sur, 2009, The experimental investigation of the effects of uncoated, PVD- and CVD-coated cemented carbide inserts and cutting parameters on surface roughness in CNC cutting and its prediction using artificial neural networks, Robotics and Computer-Integrated Manufacturing, 25: 211-213

97. H. Gokkaya and M. Nalbant, 2006, The effects of cutting tool coating on the surface roughness of AISI 1015 steel depending on cutting parameters, Turkish J. Eng. Env. Sci., 30: 307 – 316

98. A. Aramcharoen, P.T. Mativenga, and S. Yang, 2007, The Effect of AlCrTiN Coatings on Product Quality in Micro-milling of 45 HRC Hardened H13 Die Steel, 35th International Matador Conference. 18- July

99. J.C. Aurich, J. Engmann, G.M. Schueler, and R. Haberland, 2009, Micro grinding tool for manufacture of complex structures in brittle materials, CIRP Annals - Manufacturing Technology 58: 311–314

100. Min-Seop Han, Byung-Kwon Min, and Sang Jo Lee, 2009, Geometric improvement of electrochemical discharge micro-drilling using an ultrasonic-vibrated electrolyte, J. Micromech. Microeng., 19: 065004

101. Zhiyong Li and Guangming Yuan, 2008, Experimental Investigation of Micro -holes in Electrochemical Machining Using Pulse Current, Proceedings of the 3rd IEEE Int. Conf. on Nano/Micro Engineered and Molecular Systems January 6-9, Sanya, China